USE OF CONCRETE GRINDING RESIDUE AS A SOIL AMENDMENT

By

Patrick E. B. Bollinger

A THESIS

Submitted to
Michigan State University
in partial fulfillment of the requirements
for the degree of

Civil Engineering - Master of Science

2021

ABSTRACT

USE OF CONCRETE GRINDING RESIDUE AS A SOIL AMENDMENT

By

Patrick E. B. Bollinger

Discarded or landfilled construction debris (specifically from roadway projects) may have untapped recycling potential to help stabilize different types of soil. However, blending some types of debris may not produce the desired results in all soils. Concrete diamond-grinding on pavement projects generates a non-hazardous waste byproduct called concrete grinding residue (CGR). CGR has known cementitious characteristics that suggest a latent use as a soil-stabilizing amendment, especially for poor and problematic soils. In Phase 1 of this study, Western Iowa loess soil was amended with CGR and subjected to indoor rainfall simulations to measure soil erodibility. In Phase 2, lab-based wind erosion simulations were performed on CGR-amended soils to measure the erodibility due to "wind whip" from passing vehicles. Phase 1 include the review of different methods for collecting CGR discharge; discussed design, construction, and use of a uniform compaction apparatus; and analyzed stormwater runoff. Post-rainfall analysis included pH, water quality (turbidity) and total suspended-solids (TSS) tests. Lab tests on rainwater runoff samples from CGR-amended loess exhibited dramatically higher turbidity with an increase in TSS from 1.8 to 4.7 times that of untreated loess. In Phase 2, soil loss due to wind erosion was measured for CGR-amended loess and Class A-1 highway shoulder soils. Results showed that erosion was reduced in more granular shoulder material, decreasing -2.2 T/mi. (-25%) to -5.3 T/mi. (-58%), respectively. Conversely, for shoulder material containing more organics, soil erosion increased from 0.9 T/mi. (25%) to 1.9 T/mi. (50%) on average with the 20% and 40% CGR dosages, respectively.

This thesis is dedicated to God, my beautiful wife Brooke, my dear, dear parents and 3 fun-loving sisters, extended family, Dunkin' Donuts coffee, Starbucks coffee, Sparty's coffee, in fact, anyone's coffee (and donuts), ibuprofen, ear buds, a comfortable office chair, my big external monitor, and my dependable Dell. I think the world needs more of these honest dedications. And naps. Lots of naps.

I would also like to Walt Disney World in advance for the long-awaited graduation trip that my wife and I will surely plan and take very soon.

ACKNOWLEDGEMENT

Thank you to my advisor Dr. Bora Cetin, for his time, experience, and expertise on this project and my committee members, Dr. Neeraj Buch and Dr. M. Emin Kutay for volunteering their tutelage in the classroom and for their time and commitment to my academic success at Michigan State University. Thank you to the Iowa Highway Research Board (IHRB), the Iowa Department of Transportation (Iowa DOT), and the Recycled Materials Resource Center (RMRC) of Madison, Wisconsin for the generous grant that funded this research. This thank you extends to the gracious volunteer work of my Technical Action Committee (TAC) which includes:

Todd Hanson, P.E. - Iowa DOT, John Hart, P.E. - Iowa DOT, Todd Kinney, P.E. - Clinton County, IA, Melissa Serio, P.E. - Iowa DOT, Brian Moore, P.E. - Iowa County Engineers Service Bureau, Jacob Thorius, P.E. - Washington County, IA, Bob Younie, P.E. - Iowa DOT and Vanessa Goetz, P.E. - Iowa DOT

To Jacob Thorius and Todd Kinney especially, thank you for providing the manpower and equipment to excavate the shoulder materials for the five roadway projects in your counties. This donation of time and expense for your crew, materials, and equipment was greatly appreciated.

I would also like to extend a heartfelt thank you to Dr Halil Ceylan with Iowa State, Dr Michael Perez with Auburn University, Dr. Mustafa Hatipoglu with Istanbul Technical University, Dr. Sinan Coban with Michigan State, and Dr. Masrur Mahedi with Iowa State, and Dr. Bo Yang with Iowa State. Your time and ideas used on this project were invaluable.

I would like to acknowledge and thank the faculty and staff of the Department of Civil, Construction and Environmental Engineering and the Department of Agricultural and

Biosystems Engineering (ABE) at Iowa State University as well as the Department of Civil and Environmental Engineering at Michigan State University for their generous contributions of lab space, equipment, help and support toward the execution of this project.

At Iowa State, my sincerest thank you to Dr. Matt Helmers and to Dr. Steven Mickelson for their generous donation of time and use of the ISU rainfall simulator and to Carl Pederson for without whose mechanical expertise and initial training on the rainfall simulator, the rainfall study would not have been possible. Special thanks for Chaitanya Dokala, Nathan Miner, Jamie Schussler, Declan Costello, and James McGonegle for your generous help in the labs.

At Michigan State, thank you to Sia Ravanbakhsh, Chuck Meddaugh, and Joseph Nguyen for brainstorming sessions, guidance, hands-on work, and mentoring. To my dear friend and colleague Ceren Aydin for her tireless help in the lab and to my dear friends Hamad Muslim, Mahdi Ghazavi, Mumtahin Hasnat, Remi Gonety for their gracious help in the labs, ideas, sense of humors, and wonderful friendships.

Finally, I want to thank my dedicated wife Brooke who has the patience of a saint, my parents, Ed and Chris Bollinger, my wonderful sisters Sandra, Natalie, and Marjorie, my 3 terrific brother in-laws, especially David, for his construction ideas during this project and for their collective encouragement in my pursuit of this degree. Thank you for your loving support. God bless you.

TABLE OF CONTENTS

LIST OF TABLES

LIST OF FIGURES

CHAPTER 1 INTRODUCTION

1.1 Background

The first concrete road in the United States (U.S.) was installed in Bellefontaine, Ohio in 1891 [1,2,3]. The first concrete highway however would not be installed for another 22-years, where a 24 mile, 9 foot wide, 5" thick stretch of roadway called "Dollarway Road" (its namesake from the dollar per mile cost at the time) was installed in Pine Bluff, Arkansas in 1913 [4,5]. Today there are 4.13 million miles of roads in the United States, 2.91 million miles classified as paved [6,7]. Like any manmade structure, eventual maintenance is required to extend the life of this extensive network of paved roadways. One of these maintenance methods is concrete diamond grinding to roadway surfaces. Different from concrete tining, where either transverse or longitudinal groves at dragged through the wet concrete mix, concrete diamond grinding is performed on hardened concrete pavements. While the main purpose for tining is to provide drainage channels to improve skid resistance, longitudinal tining and concrete diamond grinding are both useful methods for reducing noise emissions from traffic over concrete pavements [8,9,10,11]. In addition to reducing noise, concrete diamond grinding has the added benefit of improving macrotexture and correcting irregularities due to faults, cracks, warping, and overall roughness issues of the concrete driving surface [12,13,14].

Concrete grinding on roadway surfaces was first experimented with in the late 1940s [15]. By 1972, the International Grooving and Grinding Association (IGGA) was formed to support the concrete and concrete grinding industries. Since then, the need for grinding and grooving concrete of roadway surfaces has grown and the practice of grinding and grooving roadway surfaces has developed into an industry standard worldwide [16,17,18,19]. Today IGGA and the American Concrete Pavement Association (ACPA) both promote best management practices

(BMPs) for concrete pavements and concrete grinding and grooving for new portland cement concrete (PCC) roadway, concrete pavement preservation (CPP), and concrete pavement restoration (CPR) projects [20]. The greatest fear authorities have is environmental concerns with the disposal of CGR, primarily discharge directly onto adjacent roadway shoulders and on the surrounding landscape, and to a lesser degree disposal of CGR into landfills [21,22,23]. Chief among the concerns for disposal along roadsides is the chemistry and mineral composition of the CGR and the caustic nature of this highly alkaline waste biproduct [14,21,24,25].

The crux of the argument from an environmental and health perspective is the effect of CGR discharge (or slurry) spread onto sensitive areas, including roadside vegetation, soil, or nearby streams and bodies of water [26]. The United States Environmental Protection Agency (U.S. EPA) classifies hazardous waste as a substance that is ignitable, corrosive, reactive, or toxic [27]. Although not ignitable or reactive, the question of the corrosiveness and the toxicity of CGR has been the source of consternation, because of the known high pH and high alkalinity of the wastewater and solids in a typical CGR slurry. As a result, many States have developed regulations and standards limiting or prohibiting discharge of CGR onto roadway shoulders, medians, or embankments [23]. Two additional environmental concerns revolve around the question of trace metals and potential leachate concerns with CGR when in contact with water and soil [14,24]. Kluge et al. [24] and Yang et al. [23] also found that State regulations varied greatly by region with 41 out of 50 States having regulations regarding CGR [24] and 19 States requiring "continuous removal" of CGR [23] from roadway surfaces during concrete grinding operations.

In 1990, a failed roadway overlay on a large-scale (and very public) PCC pavement project resulted in an environmental firestorm which led to significant changes in the way the Federal

Highway Administration (FHWA) and State Departments of Transportation (DOTs) still view and handle the treatment and disposal of CGR on roadway projects today. On this Utah project, an experimental thin bonded portland cement (PC) overlay on a 12-mile stretch of Utah's I-15 failed after 1 month, with 15% delamination reported after only 4 months [28]. This initiated a large-scale concrete diamond grinding project, with direct disposal of CGR discharge onto the roadway shoulders and median swales [28] which was consistent with Utah's current CGR disposal regulations at the time. Grab samples taken from the initial CGR discharge from this remediation project revealed a highly caustic CGR discharge with a pH of 12.0 (above regulation limits) which promptly caused the project to be halted to address this environmental problem and modify the disposal procedures for this project. The unique aspect of this project was that the PC overlay was thick, with an average depth of 3/4" being removed. It was later determined that this project generated 891,000-gallons of alkaline wastewater and 3,200 cubic yards of alkali solids [28] which at the time was an environmental nightmare for the Utah Division of Environmental Health and the Utah DOT at the time due to the unknown long term effects of CGR on soil and vegetation. PCC overlays are not new and both unbonded overlays (PC over PC) and bonded overlays (PC over asphalt concrete) and have been installed successfully over aging roads for decades [29]. Additionally, concrete diamond grinding has also been around this long, dating back to at least 1965 when the purported first large scale concrete diamond grinding project was performed on the San Bernardino Freeway (I-10) in southern California to eliminate excessive faulting between PCC roadway slabs [13,30]. Through the years similar removal and disposal challenges have undoubtedly been faced by State DOTs as their roads have required similar concrete pavement preservation or restoration.

The pH of CGR has been studied vigorously since the initial 1965 San Bernardino project, with high pH values above pH of 11.0 reported in many studies [31,32,33,34]. In addition to high pH values, Holmes and Narver [31] also found high cation and anion concentrations of aluminum, iron, and sulfate above California drinking water standards, and DeSutter et al. [33,35] also found concerning but not toxic levels of various minerals including arsenic, chromium, and lead in CGR samples tested. The high pH in CGR is the result of hydroxide ions formed from the metal oxides present in the CGR discharge, with the lime (CaO) and magnesium oxide (MgO) contributing to both the high pH and high alkalinity of the CGR discharge [14]. The high metals content in CGR (including chromium and iron) is attributed to the use of portland cement replacement pozzolans like fly ash and steel slag used in cement production and concrete mix preparation [23]. In addition to pH, numerous studies have classified CGR as a non-hazardous material by EPA standards [14,24,31,36]. The 1997 study by Holmes and Narver [31] also concluded that the effects of CGR on fish were minimal with a reported 100% survival rate for fish tested with both solid and slurry filtrate samples of CGR, concluding that CGR was compliant with California Title 22 wastewater treatment standards.

Additional research on CGR has also focused on environmental effects from CGR on soils and plants. With respect the effects of CGR on soil and existing vegetation, several recent studies have affirmed CGR having a positive impact on plant growth [14,21,22,25,33,34]. Mamo et al. [14], in particular, studied the effects of CGR on established vegetation on roadway foreslopes, with research focused on how existing vegetation, soil chemistry, and water quality from stormwater runoff might be affected by CGR. This important study concluded that CGR did not have an adverse effect on existing vegetation, soil chemistry, or water runoff volume or soil chemistry. The arduous debate on any long-term environmental effect from CGR discharge onto

soils on vegetation were largely put to rest by 2 environmental studies by Mamo et al. [14] and Ceylan et al. [21] which both concluded that CGR did not cause any long term negative affects to existing vegetation or soil chemistry. Additionally, Ceylan et. al [21], Yang et al. [34], and Luo et al. [22,25] studied vegetated test plots with various dosages of CGR with results from these 3 studies finding only short term increases in pH and no long term detrimental effect to the soil and vegetation, including changes in infiltration and plant biomass with the addition of CGR to the soil.

Studies have also been performed on CGR as an additive in various applications. In a 2017 study, CGR was used as a mortar amendment with results finding that an increase in CGR as a replacement for portland cement, generally decreased the compressive strength of the mortar with an increase in CGR [24]. However, one CGR sample with finer gradation (and an average particle size of 27um) at 5% portland cement replacement, outperformed the control mortar with no CGR replacement [24]. With respect to CGR used as a soil amendment, DeSutter et al. [33] amended a silty clay and a fine sandy loam with CGR and found no appreciable change in the infiltration for these two soils. Yonge and Shanmugam [32] studied the pH neutralization and soil metal concentration changes when CGR was mixed with organic composts. Results from this study concluded that compost did help reduce the pH levels of the CGR but changes in metal concentrations were negligible. Yang et al. [34] further tested the chemical changes (including pH, electroconductivity (EC), alkalinity, metal concentrations, and cation exchange) with CGR added in different dosages to a sandy loam (clayey sand). Results found that CGR showed no long term detrimental effects to the soils amended with CGR [34].

Research into CGR as a soil amendment for the purpose of soil stabilization is currently minimal. In 2019, Yang et al. [23] added CGR to 2 different soils, a clayey sand, and a sandy silt. Two

strength tests including unconfined compressive strength (UCS) and California Bearing Ratio (CBR) were performed with dosages of CGR ranging from 0% to 40% (amended to these two soils). Results showed increases in UCS and CBR with the addition of CGR, with the highest improvement exhibited by the soils with 20% CGR dosages [23]. No other research was found where strength tests were performed where CGR was used as a soil amendment. Additionally, no soil erosion studies were found with CGR used as a soil amendment. Furthermore, no research was found on CGR as a soil stabilizing amendment with other types of soils too. Since testing soil amendments with a wide range of soils and testing soil amendments for both strength and erosivity are important measures for soil stabilizing amendments, the purpose of the study in this thesis, was to evaluate the effects of CGR on several different soils. Soil erosivity in particular was the primary focus of the research in this dissertation. By evaluating erosion by both wind and rain, this study looked at aspects not previously studied with CGR and adds to the mechanical characteristics already known about CGR from the Yang et al. [23] study.

The research performed in this study involved both a rainfall erosion study and a wind erosion study. In the rainfall erosion study, Western Iowa loess was tested with 2 different CGRs with 20% CGR dosages. Total Suspended Solids (TSS), water quality (turbidity), and pH tests were performed in this first study. In the second wind erosion study, tests were performed on the same rainfall erosion CGR amended soil mixtures along with additional tests to 5 Iowa shoulder aggregates combined with 2 different CGRs at 2 different CGR dosages (20% and 40%). The wind erosion test consisted of 3 phases with soil loss measurements taken for each phase of the wind erosion cycle.

1.2 Concrete Diamond Grinding

Thousands of roadway construction projects are completed each year. On portland cement concrete (PCC) roadway projects where surface repairs are required, concrete diamond grinding is commonly included in the scope of work. While CGR generated from these projects is often discharged onto adjacent roadway embankments, current environmental concerns have pushed 29 states to restrict roadside disposal in favor of offsite CGR disposal [23]. This is because many environmental authorities including the U.S. EPA, State Departments of Natural Resources (DNR), and State Departments of Public Health (DPH) view CGR solely as a pernicious waste byproduct [21,23,37]. The purpose of this research, therefore, is to further evaluate the potential of recycling uses for CGR, namely the stabilization of roadway embankments, underlying soils, and/or subgrades, as suggested in previous studies by Yang et al. [23] and Kluge et al [24]. Pavements rely on subgrades and confining slopes. Permeability and drainage are important/key factors for subgrades [38,39], while strength and stiffness are primary critical design criteria for embankments [40,41]. Side-slope erosion and long-term infiltration are also important design factors with embankments [42,43], and exposed embankments with little or no vegetation are particularly vulnerable to erosion from wind and rain [44,45]. Such erosion, whether the result of new construction or due to exposure caused by natural elements like wind and rain, can lead to slope failures or structural confinement issues [41] while slopes comprised of collapsible soils (e.g., silts and loess deposits) are susceptible to failure due to sudden changes in volume when exposed to moisture [42]. While amending soils with lime or portland cement are two of the more common methods for combatting some of the more worrisome material characteristics of poor soils [46,47], exploring the use of waste byproducts for stabilizing soils would provide a more sustainable solution [48,49]. Venn diagrams are commonly used to show the wholistic

approach for sustainable design. The 3 R's (reduce, reuse, and recycle) when incorporated into an engineering design determine the extent that an engineering design or construction process is 'green' or sustainable [50]. Often referred to as the 'triple bottom line' approach, recycling responsibly looks at environmental and societal impacts not just the monetary cost of the project [50]. The use of recycled products like reclaimed asphalt pavement (RAP), reclaimed portland cement concrete (RPCC), high carbon fly ash (HCFA), and CGR are examples of waste products in abundance that if integrated into roadway projects, not only could reduce the bottom line costs of a project, but also significantly reduce the burden on landfills [50,52,53,54,55,56].

Concrete pavement restoration (CPR) projects that include diamond grinding vary significantly in size and scope, and although the selection of grinding equipment for a project is often based on the size of the grinding job, disposal procedures are often prescriptively dictated by county, state, and/or federal guidelines [23]. With only general regulations for project execution left at the discretion of the contractor, offsite disposal of CGR discharge remains somewhat arbitrary [36,57]. For example, on a project where the collection of CGR discharge is required, a ready-mix truck or tanker truck might be used for transport and offsite disposal to a third party's sedimentation pit.

CPR projects with diamond grinding to make roadway surface corrections (primarily remove roadway bumps) are generally referred to as "bump grinding" jobs. Smaller bump grinding jobs vary from simply correcting high spots in a single roadway intersection to leveling miles of multi-lane highway pavement sections. Diamond Products Limited out of St. Elyria, Ohio is one of the largest grinding equipment manufacturers in the concrete grinding industry. Included in Diamond Products (DP) commercial product line are their 1500 Series, 4500 Series, and 6000 Series [drivable] grooving and grinding equipment rigs. Their 1500 Series grinding rig has a 38

inch (~3-foot) grinding drum/head with a series of parallel grinding blades, while their larger 4500 and 6000 Series rigs each have 50 inch (~4-foot) grinding heads. Unless a project has space restrictions, Section 2532 of Iowa DOT's Standard Specification for Highway and Bridge Construction specifies that a 3-foot minimum grinding head is required on roadway projects [57]. Companies including Cedar Falls Construction, Manatt's Inc., and West Fork Grinding, for example, each specialize in smaller bump grinding projects. On the bump grinding jobs visited in Palo, IA (Cedar Falls Construction and CGR-1), in Des Moines, IA (Manatt's Inc. and CGR-2) and in Ruthven, IA (Cedar Falls Construction and CGR-3), smaller 1500 Series DP grinders were utilized.

Concrete diamond grinding on larger county, state, or interstate roadway projects, are commonly referred to as mainline surface repair projects (or simply "mainline" jobs). Mainline jobs typically utilize one (or more) larger concrete grinding rigs, each with 4-foot [grinding] heads, to perform the required roadway profile improvements. Mainline grinding jobs can be as short as a few miles on a smaller 2-lane rural road, to 10 to 20 miles on larger 4-lane (or wider) undivided and divided highways. National firms including Penhall, Interstate Improvement, and Diamond Surfacing, Inc., for example, each have multiple DP 6000 Series (or similar) mainline grinding rigs. These larger firms often deploy 3 larger grinding rigs [with 4-foot grinding heads] in series to grind the full surface across 12-foot driving lanes. This is accomplished by operating 3 machines in tandem with a small overlap of the edge of each successive grinding strip, which allow grinding of a full driving lane in a single pass with three trucks. It is not uncommon for several lane miles of grinding to be completed per workday in this manner. Larger mainline rigs can also be used on smaller bump grinding jobs when time is a factor to meet compressed project schedules. Smaller grinding rigs with 3-foot heads are typically used on smaller projects, while

larger mainline rigs [with 4-foot grinding heads] are used on larger highway projects. On a mainline grinding project in Muscatine, IA, for example, West Fork Grinding (CGR-4 detailed below) deployed a larger DP 6000 Series grinder to handle grinding along a multi-mile section of a 2 lane undivided highway completing surface corrections to several lane miles in a single workday.

1.3 Soil Conservation

Soil conservation practices took the national spotlight in the United States in the 1920's and 30's. Although created under President Lincoln's administration in 1862, the United States Department of Agriculture (USDA) gained prominence and took important strides to promote better farming and land management practices in the 1930s under the leadership of Hugh Hammond Bennett, the USDA's prominent Soil Scientist and Land surveyor [58]. National Historian Douglas Helms chronicled the pioneering work of Bennett and the USDA in the 1930s and 40s, much of which focused on the problem of severe soil erosion caused by drought and poor farming practices. A failure to apply appropriate dryland farming techniques combined with drought-stricken, over-plowed and exposed farmland led to the catastrophic dust storms and a National crisis commonly known as the Dust Bowl [59]. To study and address this serious problem, federal agencies including the Soil Erosion Service (1933) and the Soil Conservation Service (1935) were created, who then with Congress enacted critical environmental legislation including the National Industrial Recovery Act (1933), the Soil Conservation Act (1935), the Flood Control Act of 1936, the Cooperative Farm Forestry Act (1937), and the Flood Control Act of 1944. These laws led to funding for many of the United States' early soil surveying data and erosion studies, many performed by the USDA and Bennett himself [58, 60]. In 1991, USDA Conservation Agronomist M. Scott Argabright led a study using Bennett's data, where

erosion rates from both 1982 and 1992 of the Northern Mississippi Valley "Loess Hills" were compared to the 1930s [61]. The Loess Hills is one of the largest loess deposits in the country and extends up from Mississippi into Iowa along the Eastern edge of the Missouri River flood plain. Argabright's research team analyzed the 1930s soil loss data using the more modern Universal Soil Loss Equation (USLE) and estimated a staggering 14.9-tons per acre per year (TAY), plus or minus 6.7%, (or 1 ton per acre per year) of soil loss occurred in this region during the 1930s [61]. With this being consistent with the consensus of annual soil loss previously recorded between 13.9 and 15.9 TAY for this region, analysis was extended to the 1982 and 1992 data. USLE results estimated that 7.8 TAY and 6.9 TAY of soil loss for 1982 and 1992 respectively were still occurring in the Loess Hills [61]. While these numbers are alarming, this does not come as a complete surprise, due to the nature of loess, a highly friable, silty collapsible soil [62,63,64,65,66].

With respect to loess, the largest loess deposits in the world are located in China, with the most extensive areas in Northwest China, commonly referred to as the Chinese Loess Plateau [65]. The Chinese Loess Plateau spans some 243,000 mi2 [65], suffers from severe erosion and is the topic of ongoing soil erosion studies [67,68]. On the topic of loess in the United States, the Great Plains Loess Deposit spans approximately 115,000 mi2 [69], of which the loess hills region encompass an estimated area of 22,000 mi2 [70]. Loess deposits in the United States are included in the 3 maps in FIGURE 1 for reference [71]. A significant amount of research has been performed over the last century, mainly with loess sampled from the Loess Hills in Iowa, which is known for its two major erodible soils, loess, and glacial till.

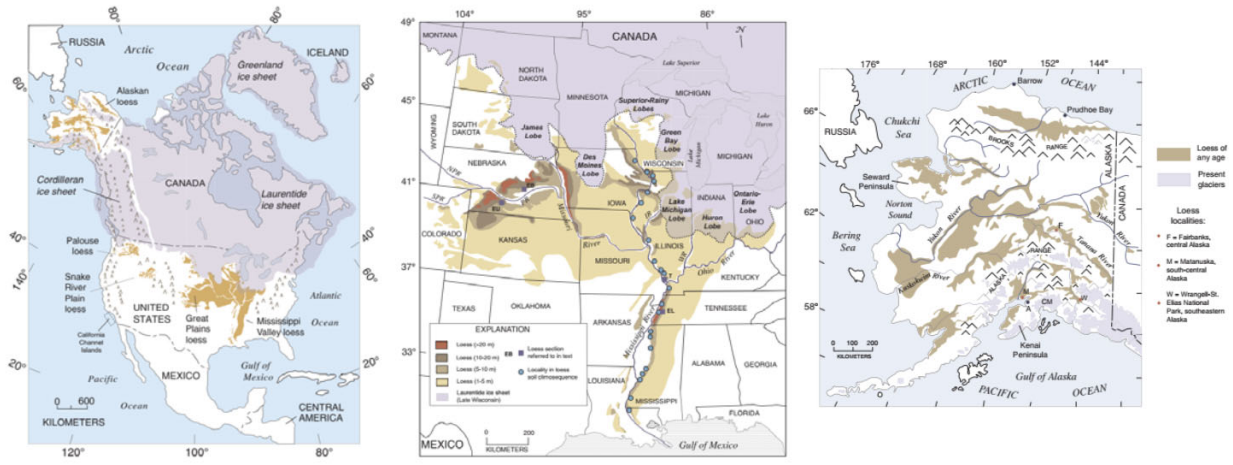

Figure 1: Loess Deposits in the United States [71]

A few noteworthy studies of loess include research on the geology of loess [63,64,72,73,74], slope-erosion relationships of loess soils [75,76], the structure of friable loess [62], erosion linkages to tillage practices [77,78,79], erosion as it relates to vegetative cover [80] erosion due to cut slopes and bare soils [81] and comparative studies of loess and soil erosion rates [60]. Each of these studies have continued to advance the understanding and characterization of loess and silty soils and its susceptibility to erosion. In addition to agricultural and farming industries, soil behavior and soil erosion studies are also important topics of research for the transportation industry. Federal agencies as well as State DOTs have also vested in soil erosion and soil characteristic research. A few noteworthy State DOT studies on the topic of loessial soil erosion and soil stabilization include research into loess cut slopes in Nebraska [81], a design manual for roadway cut slopes [82], soil characterization for improved roadway subgrades and subbases [42] and the repair of inundated roadways from loess erosion [41]. In each of these studies, an evaluation of the soil properties of loess was performed in an effort to better understand both this soil and to improve and better stabilize roadway embankments and subgrades. In the 2013 IHRB study referenced above [46], research was funded in part, in response to a 2011 Missouri River flood that buried a series of Iowa roads in eroded loessial silt from the Western Iowa Loess Hills.

When loess was collected from Crescent Quarry for this study late in 2018, the City of Council Bluffs, Iowa had closed sections of Interstate I-680 due to major flooding and soil erosion once again of the Missouri River [83]. The presence of this current flooding and more recent road closures show that soil erosion is still a problem and reinforces the continued need for research into new and improved soil stabilization methods to protect the Nation's roadway infrastructure.

1.4 Erosion

Rain erosion is simply defined as the detachment of soil particles due to the impact of raindrops on the soil, followed by the transport and deposition of these particles away from the source [84]. This erosion can be categorized into 4 types: splash erosion, sheet erosion, rill erosion, and gully erosion [85]. As raindrops impact the ground, inter-rill erosion starts as the drops strike the ground [86] which leads to sheet erosion (or overland flow) and concentrated flows in rivulets/small channels that lead to create grooves or rill erosion [86,87]. Conservative estimates of soil loss due to sheet and rill erosion in the United States are appraised at 3.4 billion T/yr. [88]. This is 3 times the annual erosion rates due to wind erosion in the United States, which accounts for an additional 1.2 billion T/yr. in transported soil from farmlands alone [88]. Erosion of sediment from local heavy rainstorms are dependent on a number of factors including rainfall characteristics, topography, soil type, and soil conservation practices [89]. In Iowa, average rainfall varies for a given 24-hour rainfall event but falls generally into a range of 0.5 in. to 3 in., with estimated average runoffs during this period around 2 in. [89]. However, climate modeling in the United States shows increases in heavy precipitation from 1958 to 2007 in all regions of the country, including a 15% increase in the Midwest (including Iowa) to as much as a 67% increase in the Northeast [90]. In more recent data, the 2015 Iowa Statewide Urban Design and Specifications (SUDAS) manual has divided the State into 9 climatic sections. Using data from

the National Oceanic and Atmospheric Administration (NOAA) for these 9 Iowa regions, average rainfall for a 24-hour storm event is 3.07 in. with a standard deviation of 0.09" across the state [91]. This confirmed the 2010 climate change estimates reported by the Iowa Climate Change Impacts Committee (ICCIC) in the State report to the Governor and the Iowa General Assembly at this time [90] which postulated that this increased rainfall would lead to continued erosion and soil loss to exposed and vulnerable lands despite current soil conservation practices. Dr. Richard Cruse, Professor of Agronomy, and the Director of the Iowa Water Center at ISU, estimated current sheet and rill erosion at 5.1 T/ac. annually for the state of Iowa [89]. This erosion rate is supported by the 2017 data from the National Resources Inventory (NRI) which estimated 5.6 tons/acre/year for the State of Iowa [92] or approximately 3600 T/sq. mi./yr. With an area of just over 56,000 sq. mi. in Iowa, this translates to an alarming 201 million tons of "rain eroded" soil per year for the State.

Wind erosion is a complex physical phenomenon that until the Dust Bowl of the 1930's was viewed primarily as a regional problem during periods of drought [93]. Some of the earliest research and quantifiable methods for predicting wind erosion was done by renowned USDA soil scientist Dr. William S. Chepil. Chepil developed a byzantine wind erosion equation, coined WEQ [94] in an effort to develop a method to predict wind erosion. The Chepil WEQ equation consisted of a step-by-step process of determining "11 concomitant soil and climate variables" [94] each determined through a series of complex nomographs, charts, tables, and maps [94,95]. The WEQ method was an empirical tool that served as the industry standard for over 30 years and is still largely used today to gauge the accuracy of newer software-based simulations, including the current Wind Erosion Prediction System (WEPS), a tool presently used by the USDA and NRCS [93,96]. Chepil's soils research, determined that the "most erodible discrete

soil particles" had diameters of approximately 0.1 mm and that "relatively few particles greater than 0.5 mm" (in diameter) were displaced by everyday winds events [97]. Saltation (movement and airborne spreading) of these small 0.1 to 0.5 mm airborne soil particles account for between 50% to 80% of erosion by wind erosion [84]. Since wind erosion involves soil particle detachment, transport, and deposition [95] this range of particle size is an important soil characteristic especially for loess and other silty soils, which have a median particle size of 0.01 mm [98] or $1/100^{th}$ of the most erodible 0.1 mm soil particle size most susceptible to wind erosion identified by Dr Chepil.

The median particle size for the Western Iowa loess used in the initial rainfall testing portion of this study was 0.03 mm with 99.9% of the particles in this soil measuring less than 0.5 mm [39]. The first batch of loess was from Monona County, IA, while the second batch of loess was collected from Crescent Quarry in nearby Pottawattamie, IA. A sieve analysis was not performed on this second batch of soil from Crescent Quarry but is believed to share the same soil properties and particle size distribution. Further analysis for the Monona County loess (and assumed similar for the Crescent Quarry, Pottawattamie County loess) classified the Western Iowa loess as an inorganic silt, with USCS soil classification ML and AASHTO soil classification A-4 [39]. This soil was further characterized to contain 0% gravel, 1% sand, 87% silt, and 12% clay-sized particles [39]. Based on particle size alone, Western Iowa loess is a highly erodible soil. The median particle size for the Clinton and Washington County, Iowa Class-A-1 shoulder aggregates used in this study was much larger at 4.5 mm and 3.7 mm respectively, with only 16.3% and 18.9% of the particles in this soil measuring less than 0.5 mm, respectively. This shows that the Class-A-1 shoulder aggregates have a much lower propensity to erode compared to the Western Iowa loess specimens. However, these percentages still translate

to significant amounts of erodible soil particles under 0.5 mm for these Class-A-1 shoulder aggregates. With the compacted wind erosion specimens discussed later in this dissertation weighing approximately 20 kg, each of these specimens tested would have approximately 3.3 kg to 3.8 kg of erodible particles under 0.5 mm (particles most susceptible to wind erosion). Unpaved, compacted, gravel shoulders also suffer from erosion from both wind and rain. Guidelines for the proper installation and maintenance of gravel roadways exist for every state as well as the Federal Highway Administration (FHWA). One of the more comprehensive unpaved gravel road manuals was created in 2000 by the South Dakota DOT [99] and sponsored by the FHWA. Adopted and updated by the FHWA in 2015, the Gravel Roads Construction and Maintenance Guide [100] is a well-known construction manual for the construction and maintenance of unpaved gravel roads across the country. This comprehensive and prescriptive guide, details some of the more common problems found in unpaved gravel roads and shoulders caused by both wind and rain erosion. The primary cause of erosion by wind is attributed to an effect called “whip off” [99,100] or “wind whip” referred to by Washington County, IA roadway officials and maintenance workers. Wind whip is the wind-scouring of shoulder soils due to larger trucks traveling at high speeds on unpaved roads or on paved roads with unpaved gravel shoulders. The lab-based wind erosion testing at MSU in the research in this thesis was geared at reproducing wind whip on a smaller scale. This was done to simulate and measure the wind erosion of different soils in a lab-controlled environment.

CHAPTER 2 RAIN EROSION STUDY

2.1 Materials

The soil used in the rainfall erosion portion of this dissertation were loess from the "Loess Hills" of Western Iowa. In addition to the loess, 5 CGRs were collected from active concrete diamond grinding projects located in Eastern, Western, Northern, Central, and South Central Iowa.

2.1.1 Western Iowa Loess

Western Iowa Loess soil [hereafter referred to as loess] was selected as the base soil (control) to amend with CGR for the Phase 1 portion of this study. Loess was chosen for evaluation with CGR due to its abundance, its poor compaction characteristics, and its high degree of erodibility. Two batches of loess were needed for this project. The first batch of loess was transported by Iowa State University's Department of Civil Engineering from a farm in the "Loess Hills" (in Monona County, IA) located in Western Iowa. No other details were available about the collection of this first truckload of loess.

Figure 2: Crescent Quarry (Pottawattamie County, IA), Photos by Patrick Bollinger

The second batch of loess was also sourced from the Loess Hills but was collected from Crescent Quarry located in the City of Crescent, Iowa (in Pottawattamie County), owned and operated by Schildberg Construction Company (FIGURE 2). During the mining process for aglime and

crushed aggregates, stockpiles of loess spoils are generated. Over time these stockpile deposits have grown into a mountain of unused loess surrounding the quarry. This soil is seeded to help mitigate erosion of this highly friable soil. The loess sampled from Crescent Quarry was excavated using a Caterpillar CAT 980B front-end loader with a 5 cubic yard bucket. The loader operator excavated the soil from a section of stockpiled loess, first scarifying the top 2 to 3 feet of soil from the stockpile to minimize any small roots and vegetation from getting into the desired soil. A total of (62) 5-gallon buckets (or approximately 1.8 tons of soil) was loaded and transported back to Iowa State University (ISU). While unloading the loess at the civil engineering lab, remaining visible small roots and vegetation were removed. No stones or rocks were found in the soil collected. The general appearance of the loess from both Monona County and Crescent Quarry had the same royal brown color with a soft, velvety composition, and appeared free from contamination from other soils or foreign matter, namely gravel, peat, and vegetation.

2.1.2 Concrete Diamond Grinding (CGR)

Five CGRs were collected for research and testing in this study. On each of the grinding projects where CGR was generated and collected, Diamond Products grinding rigs were exclusively used. The DP 1500 Series, DP 4500 Series, and DP 6000 Series grinding rigs on the projects visited were each operated by a single driver. These rigs have the versatility of "grinding" (or texturing) PCC roadway surfaces using closely spaced blades, or "grooving" the roadway surface (to improve traction) with blades spaced slightly further apart. Grinding (not grooving) was performed on the 5 grinding jobs visited on this project. Each of the grinding jobs visited had water trucks following the grinding rigs with pumps supplying up to 5 psi of pressurized water, at a rate of approximately 8-gallons per minute, to cool the blades on the grinding heads. As a

result, a wet discharge mixture of sediment laden water with concrete grindings (hereafter referred to as CGR discharge) was generated. CGR discharge collection was done by hand into 5-gallon buckets for each of the 5 CGRs collected. Results are shown in TABLE 1.

Table 1: Concrete Grinding Project Details

CGR	Discharge Method	Grinding Rig	Grinding Heads	Project Details
CGR-1	Ready-Mix Truck	DP 1500 Series	3-foot wide	50 ft. section, at traffic intersection
CGR-2	Ready-Mix Truck	DP 1500 Series	3-foot wide	250 ft. section, 4-lane undivided hwy.
CGR-3	Direct Discharge	DP 1500 Series	3-foot wide	2-3 mi. on 2-lane undivided rural rd.
CGR-4	Tanker Truck	DP 6000 Series	4-foot wide	2-3 mi. on 2-lane undivided hwy.
CGR-5	Direct Discharge	DP 4500 Series	4-foot wide	4-5 mi. on 4-lane undivided hwy.

2.1.3 CGR Discharge Collection Process

Five Iowa concrete grinding projects were visited starting with CGR-1 in May 2019 and ending with CGR-5 in October 2019. CGR discharge was collected into Lowe's standard 5-gallon PVC buckets with snap-on lids, which were then transported back to Iowa State University for processing and testing. The project sites sampled were selected initially based on 2 primary criteria: geography and the size of the grinding job. The goal in the selection process was to obtain CGRs from projects ranging in size from small concrete pavement "bump grinding" jobs to larger "mainline" highway projects. A list of grinding contractors was created by starting from a roster of contractors who attended the Iowa Concrete Paving Association (ICPA) concrete paving workshop held February 2019 in Des Moines, IA. In addition to this list, several Iowa DOT engineers recommended a few additional leads. From this list, (27) concrete grinding contractors were qualified and then contacted bi-monthly in search of future concrete grinding projects scheduled for the Spring and Summer 2019. A large net was initially cast, centered on Ames, IA and including a 350-mile radius from the center of Iowa State University's main campus. This range was based on realistic travel to-and-from grinding jobs with a roundtrip

distance that could be traveled in one to two days. However, after collecting the first three grinding projects within the State of Iowa, the project range was reduced to a 150-mile radius (or a search within the State of Iowa) for the last two grinding jobs. The last two grinding projects came from both the Eastern and Western borders of the state. Results are shown in TABLE 2.

Table 2: Concrete Diamond Grinding Sites

CGR	Date	Location	Contractor(s)	Job Type, Size
CGR-1	29-May-2019	Palo, IA	Croell / Cedar Falls Construction	Bump Grinding, Small
CGR-2	30-May-2019	Des Moines, IA	Manatt's, Inc.	Bump Grinding, Small
CGR-3	6-Jun-2019	Ruthven, IA	Croell / Cedar Falls Construction	Bump Grinding, Moderate
CGR-4	14-Jun-2019	Muscatine, IA	West Fork Grinding	Mainline, Small
CGR-5	21-Oct-2019	Sioux City, IA	Cedar Falls Construction	Mainline, Moderate

On each project, (30) 5-gallon buckets were collected by hand, with the exception of CGR-3, where (50) 5-gallon buckets were collected. Each bucket was filled with CGR discharge filled approximate to a 10” fill line (marked inside 14” tall 5-gallon buckets). This equated to filling each bucket to approximately 3.6-gallons, weighing (on average) 40 to 44-pounds per bucket. Fifty buckets were collected for CGR-3 as mentioned above because more water was expected in this CGR discharge due to the direct discharge collection method used on this job. A minimum of (30) 5-gallon buckets was chosen for this project based on CGR quantities obtained for MnDOT CGR research performed at Iowa State University and comparisons made to testing on this project compared to the compaction and rainfall and wind erosion testing required in this study [21].

2.1.4 CGRs Collected

CGR-1 from Palo, IA was generated and collected from a small bump grinding job at a roadway intersection on a 2-lane undivided PCC highway. Due to county restrictions, the CGR produced on this job was collected into a cement mixing (ready-mix) truck where it was hauled

offsite to a sedimentation basin owned by a third party. Collection of the CGR-1 samples involved manually holding 5-gallon buckets up to the end of the mixing truck discharge chute while the truck operator slowly rotated the mixing truck drum/barrel. The resulting CGR collected from this discharge method was a mix of buckets that contained both heavy and light CGR solids in the CGR discharge. Thirty 5-gallon buckets (weighing 1244 lb.) of CGR-1 discharge was collected from this job site. Results are shown in TABLE 3.

Table 3: Collection Method and CGR Discharge Comparison

CGR	Collection Method	Discharge, lb. (gal.)	Supernatant, lb. (gal.)	Cakes, lb. (gal.)
CGR-1	Ready-Mix Truck	1244 (111.5)	508 (60.9)	736 (40.9)
CGR-2	Ready-Mix Truck	1131 (93.6)	301 (36.1)	830 (46.5)
CGR-3*	Direct Discharge	1964 (193.7)	1094 (143.2)	937 (53.0)
CGR-4	Tanker Truck	1160 (95.8)	272 (32.6)	889 (52.7)
CGR-5	Direct Discharge	1445 (112.8)	332 (39.8)	1083 (67.0)

Cakes = Moist (saturated) CGR solids after decanting supernatant

* CGR-3 weights and volumes back-calculated from final slurry weight and volume

CGR-2 from Des Moines, IA likewise came on a small bump grinding job on a 250-foot long section of a 4-lane undivided PCC city highway recently replaced by Des Moines Water Works. Due to City disposal restrictions, the CGR produced on this job was also collected into ready-mix trucks and hauled offsite for disposal. Disposal was made into a formal sedimentation basin owned by Manatt's Inc.. Collection of CGR-2 samples similarly involved holding each empty bucket up to the end of the mixing truck discharge chute while the truck operator slowly rotated the mixing truck drum. Building on experience from collecting CGR-1 in this manner, the CGR-2 collected from this discharge method had slightly more CGR solids to water ratio collected. This discharge and collection method however produced a lot of splash and the amount of CGR solids to water was random with each bucket. Thirty 5-gallon buckets (weighing 1131 lb.) of CGR-2 discharge was collected from this job site.

CGR-3 from Ruthven, IA was generated on a bump grinding job with a moderate amount of grinding on a new two to three mile pavement section of a 2-lane undivided PCC rural road (FIGURE 3). On this grinding job, discharge onto the roadway embankment was allowed and there did not appear to be any CGR discharge restrictions. Since this project was a new road in the final stages of construction, the roadway embankments on this job site consisted of compacted soil with no established vegetation. As a result, the CGR discharged directly from the concrete grinding rig ran directly down the sloped embankment and soaked into the bare soil. CGR-3 discharge collection involved holding each bucket up to the grinding rig discharge pipe while the rig operator slowly advanced in his normal grinding operation. The resulting CGR discharge collected from this discharge method contained a lot more water than CGR material (by volume). With more water anticipated in the discharge, (50) 5-gallon buckets of CGR-3 was collected from this job site. No offsite impoundment was required by the contractor for the balance of CGR discharge produced. Approximately 2000 lb. (50 buckets x estimated 40 lb./bucket) of CGR-3 was collected from this job.

Figure 3: Direct Discharge CGR Collection (Site CGR-3 Shown), Photos by Patrick Bollinger

CGR-4 from Muscatine, IA (like CGR-3) was generated from grinding on a 2 to 3-mile section of 2-lane undivided PCC highway. However, with the CGR-4 job, substantially more PCC

grinding was required on this job. As a result, the contractor referred to this job as a mainline job and used a larger DP 6000 Series concrete grinding rig for this grinding work. Due to project restrictions, the CGR produced on this job was collected into a large 3-stage tanker/hopper truck and hauled offsite to a sedimentation basin owned by a third party. CGR-4 samples were collected from a discharge pipe from the undercarriage of the tanker truck. Collection of these samples involved holding each empty bucket up to the discharge pipe spigot while the truck operator slowly opened the discharge pipe spigot/valve. This discharge method was more controlled in comparison to the first 3 CGRs collected. In addition, because the CGR had settled slightly to the bottom of the tanker truck, the resulting CGR discharge from this collection method had a slightly higher percentage of CGR solids to water ratio. The tanker truck disposed of the balance of CGR discharge offsite into a large sedimentation basin owned by a third party. Thirty 5-gallon buckets (weighing 1160 lb.) of CGR-4 discharge was collected from this job site.

CGR-5 in Sioux City, IA was generated on a longer new 4 to 5-mile pavement section of a 4-lane undivided PCC highway project. This roadway was closed to thru traffic and only appeared to require moderate bump grinding throughout the job. Although this project required primarily bump grinding, it was classified as a mainline job, due in part to the harder rose quartzite aggregate used in the PCC pavement. The contractor selected a moderate size DP 4500 Series grinding rig for this work. On this project, like CGR-3, discharge onto the roadway embankment was allowed and there did not appear to be any CGR discharge restrictions. Since this project was in the final stages of construction too, the embankments on this job site consisted of compacted soil with minimal established vegetation. As a result, the CGR discharged directly from the concrete grinding rig ran directly down the sloped embankment and soaked into the bare soil. CGR-5 collection involved holding each empty bucket up to the grinding rig discharge

pipe while the grinding rig operator slowly advanced in his normal grinding operation. One notable difference between CGR-5 and the previous CGRs collected, was that rose quartzite aggregate was used in the mix design. With this known prior to visiting the site, only (30) 5-gallon buckets were needed for collecting samples compared to CGR-3 with the same direct discharge method. This was because the contractor shared that less water was typically used with concrete grinding work on PCC pavements with harder aggregates in the mix design to keep the blades hotter. The CGR discharge collected on this job contained less water (by volume) to previous CGRs collected. No offsite impoundment was required by the contractor for the balance of CGR discharge produced. Thirty 5-gallon buckets (weighing 1445 lb.) of CGR-5 discharge was collected from this job site.

Recall from earlier, for both CGR-1 and CGR-2, the CGR discharge was collected into ready-mix trucks and transported offsite for disposal. For these two jobs, CGR discharge was collected directly off of the discharge chute attached to the back of the ready-mix truck. The discharge collection rate for these 2 jobs was controlled by the truck operator, which generally allow for the collection of more solids to water (by volume) in each bucket compared to direct (road-side) CGR discharge collection on a smaller bump grinding job. On grinding jobs using ready-mix trucks, the inside of the truck mixing drum is outfitted with T-shaped blades (or fins) inside the truck mixing barrel/drum. As the drum is rotated, the end of the fins become visible as the barrel turns, which indicates that clumps of CGR solid can be anticipated slightly for collection. Although less water was collected in the CGR discharge for CGR-1 and CGR-2, each bucket collected still contained random amounts of CGR solids and discharge water. In comparison, CGR-3, CGR-4, and CGR-5 had roadside CGR discharge collection). For CGR-3 and CGR-5, CGR discharge was captured directly off of the grinding rig. With CGR-4 while technically the

CGR was collected along the job roadside, because CGR-4 was pumped into a tanker/hopper truck, CGR-4 more closely resembled CGR-1 and CGR-2. For CGR-4, samples were collected from a spigot under the tanker truck. This provided the most control, clean, and efficient means of CGR discharge collection. CGR-4 resulted in the least amount of supernatant collected (272-lb.) compared to the other 4 CGRs collected, ranging from 301 to 1071 lb. of supernatant collected.

Ultimately, the amount of CGR solids collected is the product of 3 primary factors. The type of grinding job (bump grinding verses mainline or full lane width grinding), the size of the grinding rig head (3-foot verses 4-foot widths), and the experience of the person(s) collecting the CGR discharge, contribute the most to the collection of more CGR solids. For CGR-5 (collected from a large mainline job), 852 lb. of oven dry CGR solids was collected compared to a range of 565 to 653 lb. from the other CGRs collected.

2.2. Methods/Testing

The methods and testing for the rainfall erosion portion of this dissertation involved the collection and preparation of the soils and CGRs as well as initial pH, EC, and compaction tests of both the untreated and treated (CGR-amended) soil specimens.

2.2.1 CGR Specimen Preparation

Early in this research, the idea of creating "pourable" (homogeneous) CGR slurries to blend with different soils was conceived. The main idea was to pour or spray CGR onto different soils similar to a hydromulch application and then test how well the CGR stabilized the soil. With this plan in mind, homogeneous CGR slurries were made with high amounts of water (and consequently high moisture contents). Little was known about CGRs and whether or not CGR discharge collected was a consistent material. It was known that each field collected CGR

discharge contained a significant amount of water. Originally it was believed that the CGR discharge collected directly from the concrete diamond grinder discharge pipe was homogeneous. This theory proved incorrect while decanting and mixing the first CGR selected (CGR-3) into a CGR slurry. Breaking-up the stiff CGR cakes in a surplus of supernatant water was difficult and the use of garden hoes, flat-nosed shovels, and metal scoopers was required. Since too much water was kept in the mix with the first 10-buckets with CGR-3, the next 20-buckets were partially decanted, leaving one to two inches of supernatant in each bucket in with the solids before adding them to the large mixing bin. The CGR-3 solids from these buckets were not chopped-up prior to adding them to the large Rubbermaid trough. This was a mistake and later all CGR cakes were broken-up after decanting prior to adding any mixing water back into the solids. The final 20-buckets of CGR-3 were fully decanted, but too much water from the first 30-buckets had already determined that the CGR-3 slurry would be too watery. The mixing of CGR-3 into a homogeneous CGR slurry took approximately 10 hours to mix.

An early assumption was that a significant amount of supernatant would need to be retained (to add back in with decanted solids) in order to produce a homogeneous CGR slurry. However, this assumption also proved wrong after processing the CGR-3 slurry. After producing the homogeneous CGR-3 slurry, a new mixing procedure was created. This procedure was created after struggling to break-up the stiff and cohesive CGR-3 cakes. By observing the settling of the particles for the next CGR collected more closely, it was found that 12 to 24 hours provided sufficient time for the CGR solids to settle in each bucket (but not making the solids too consolidated to break-up by hand). Conversely with CGR-3, the solids had settled for seven days prior to mixing. After seven days, the CGR-3 solids had consolidated and coagulated into a semi-solid state in the bottom of each 5-gallon bucket. The congealed CGR solids showed significant

cohesive properties and proved quite difficult to remove from the buckets and break-up using garden tools and a handheld mixer.

All homogeneous CGR mixes were blended in a new clean 150-gallon heavy-duty plastic Rubbermaid bin. CGR-3 was selected first for processing because this CGR discharge contained the most water of the five CGRs samples collected. CGR-3 was also expected to be more workable compared the other CGRs for the same reason. Mixing began by dumping the contents of the first 10 (of 50) buckets of settled CGR-3 solids as well as all of the supernatant from these buckets into a large Rubbermaid bin. Each CGR cake consisted (visually) of both sand-sized particles (that had settled first to the bottom of the buckets) and a few inches of a putty-like cohesive surface comprised of consolidated silt-size particles that had settled last. FIGURE 4 shows particles taken from a typical settled, decanted, and broken-up CGR cake.

Figure 4: Consistency of Typical Settled CGR Solids (After Decanting), Photo by Patrick Bollinger

The amount of CGR solids in each 5-gallon bucket varied from as little as two to three inches, to as much as eight to nine inches deep. This was how it was determined that the CGR discharge buckets were non-homogeneous in comparison to each other, which became a deciding factor for choosing to mix the buckets for each CGR in a large mixing bin.

Figure 5: Typical CGR Cakes and CGR Slurry Mixing Process, Photos by Patrick Bollinger

After discovering the cohesive characteristics of the settled CGR-3 cakes and how well CGR solids consolidated at the bottom of each bucket, the mixing methods were reexamined. Although a "pourable" CGR slurry was desired for each mix, the final CGR-3 slurry had too much water in it. As a result, a new mixing strategy and methodology was employed for the remaining mixes. FIGURE 5 shows the CGR solids before and after breaking-up the CGR cakes (left) and the power mixing into a homogeneous CGR slurry (right).

For each of the remaining 4 CGRs processed, the following five steps were developed and followed for producing homogeneous CGR slurries. In Step 1, a visual observation was made to determine if sufficient time had been allowed for the CGR solids to settle. Buckets judged acceptable for decanting had clear supernatant on top of the CGR solids that had settled to the bottom of each bucket. The surplus supernatant that separated from the CGR solids was virtually clear, containing only a thin white film on the surface of the water. The supernatant water had a soapy feel to it, which was expected and attributed to the high alkalinity of the water. In Step 2, each bucket was weighed before and after decanting, with surplus supernatant kept and temporarily stored in clean 5-gallon buckets for reuse. In Step 3, the decanted CGR cakes were transferred to metal mixing trays and broken-down using garden hoes, flat-nosed shovels,

trowels, and metal scoopers to break up the cakes into particles smaller than one to two inches. This process was repeated for all 30-buckets with each separate CGR mix. In Step 4, a small amount of decanted supernatant water was added to the mix starting with 2-gallons. In Step 5, additional water was added to the mix. Added water was recorded during the mixing process and water was added only as needed to produce a moderately wet (pourable) homogeneous slurry similar in consistency to a sandy masonry grout. A Brutus 21665Q 120-Volt 2-Speed handheld power mixer with a mortar mixing paddle (used for thinset grout and mortar mixes) was chosen to mix the initially stiff CGR clumps and added water. The supernatant water added back into the CGR cakes for CGR-1, CGR-2, CGR-4, and CGR-5 was 3.5, 2, 8, and 8-gallons, respectively. Supernatant water was not tracked with the first CGR mix (CGR-3) but was later estimated at 16-gallons. Mixing (excluding CGR-3) ranged from two to three hours to produce a homogenous CGR slurry. After mixing, the slurries were poured back into clean 5-gallon buckets for storage and future testing. CGR slurry weights were determined by adding the initial weight of the decanted CGR cakes with the supernatant water mixed-in during the homogeneous mixing process. The weight of the supernatant water was estimated at 8.34 lb./gal. Five homogeneous slurries ranging from 752.2 lb. (42.9 gal.) to 1179.9 lb. (75 gal.) were produced for this study. The least amount of slurry was produced with CGR-1, and the most amount of slurry was produced with CGR-5. A summary of weights recorded is shown in TABLE 4.

Table 4: Homogeneous CGR Slurry and CGR Cakes Comparison

CGR	Slurry (lb.)	Slurry, gal. (pcf)	Cakes (lb.)	Cakes, gal. (pcf)
CGR-1	752.2	42.9 (131.3)	735.5	40.9 (134.8)
CGR-2	859.2	50.0 (128.5)	830.0	46.5 (133.5)
CGR-3*	1053.6	67.0 (117.7)	936.8	53.0 (132.3)
CGR-4	954.9	60.7 (117.7)	888.2	52.7 (126.2)
CGR-5	1180.0	75.0 (114.7)	1113.2	67.0 (120.9)

Slurry = Homogeneous CGR slurry and decanting and remixing

Cakes = Moist (saturated) CGR solids after decanting supernatant

* CGR-3 cake weight and volume back-calculated from final slurry weight and volume

In addition to the weights of the CGR cakes and homogeneous slurries produced, since the volume of the final CGR slurries and the volume of the added mixing water was known, unit weights for both the slurries and the CGR cakes for each CGR site was calculated. The unit weights for the CGR cakes ranged from 120.9-pcf to 134.8-pcf. This range in unit weights is attributed to different sand and aggregate PCC constituents as well as the range in degree of saturation of the CGR cakes.

2.2.2 CGR (Solids) Collection Efficiency

The following index was created to measure the weight of water and solids collected from a concrete grinding project. This index is important, as it could help a contractor estimate costs for transporting and disposing of CGR discharge (CGR laden water) produced on a given project. Each CGR discharge consists of CGR solids and water. The volume of the CGR moist solids (or cakes) can be measured against the total gallons of CGR produced on a project. An example of how a contractor could use this index is included in APPENDIX.

The Collection EFF is an important measure for CGR collection as the CGR solids collected (not the surplus supernatant) is the material that is currently landfilled in many states. CGR discharge collected from a grinding project consists of discarded cooling water and CGR solids. The total water and solids collected in a given CGR discharge can vary significantly based on the duration

and type of grinding job. Smaller bump grinding jobs with sporadic bump grinding like CGR-1 and CGR-3 averaged 30% Collection EFF, while larger mainline jobs like CGR-4 and CGR-5 averages around 55% Collection EFF. Results measured for the 5 CGR slurries produced in tabulated in TABLE 5. The higher the discharge water content, the lower the Collection EFF, meaning more water is expended on these projects during grinding operations.

Table 5: CGR Discharge Solids Collection Efficiencies

CGR	Discharge (gal.)	Slurry (gal.)	Cakes (gal.)	Collection EFF
CGR-1	111.5	42.9	40.9	37%
CGR-2	93.6	50.0	46.5	50%
CGR-3*	193.7	67.0	53.0	27%
CGR-4	95.8	60.7	52.7	55%
CGR-5	112.8	75.0	67.0	59%

Cakes = Moist (saturated) CGR solids after decanting supernatant

* CGR-3 discharge and cake volumes back-calculated from final slurry volume

2.2.3 CGR Solids Ratio

An alternate index was also created in this research to measure the weight of the "dry CGR solids" produced on a given concrete diamond grinding project. In a recent Minnesota DOT (MnDOT) study, CGR was found to enhance plant growth in certain plants with minerals such as calcium and magnesium, providing nutritive benefits to the soil [21, 22,25]. Based on the potential use of CGR as a fertilizer, calculating the dry CGR solids produced on a given CGR project, could be important for a contractor. Knowing the Solids Ratios for different types of CGR projects, would allow a contractor to determine the available solids on a particular project and estimate the amounts of dry CGR solids that would be produced on a grinding project. The Solids Ratio is the ratio of the oven dry (OD) CGR solids to the total water in the CGR discharge (cake water + decanted supernatant). For the five CGRs in this study, the Solids Ratio ranged from 0.30 to 0.60. CGR projects with high water (low solids) discharge like CGR-3 will produce

the lowest Solids Ratios. In comparison, projects with less water (high solids) in the CGR discharge like CGR-5 will produce the highest Solids Ratios. Results measured for the five CGR slurries produced are summarized in TABLE 6.

Table 6: CGR Discharge Solids Ratios

CGR	Discharge (lb.)	OD Solids (lb.)	Water (lb.)	Solids Ratio
CGR-1	1243.6	565 (45%)	679 (55%)	0.45
CGR-2	1130.5	632 (56%)	499 (44%)	0.56
CGR-3*	2130.9	638 (30%)	1493 (70%)	0.30
CGR-4	1160.2	653 (56%)	508 (44%)	0.56
CGR-5	1445.1	852 (59%)	563 (41%)	0.60

OD = Oven dry

* CGR-3 discharge constituent weights back-calculated from final slurry weight and post mixing measurements

Both Collection EFFs and Solids Ratio are important because the total weight and volume of the CGR discharge on a project directly effects the transport costs of the CGR on the project. These measures are also important because the weight of the aggregates used in PCC mixes can result in much heavier CGR cakes, also affecting transport costs, while not necessarily having larger volumes, since less water is used to grind PCC roadways with harder aggregates (like rose quartzite and granite) when used in the mix design.

2.2.4 CGR Slurries

The final moisture contents of each CGR slurry produced were recorded, and a method for creating a pourable CGR for future CGR slurries was created. FIGURE 6 shows part of the mixing process where water was added back into the decanted moist CGR solids (left) and the consistency of a typical homogeneous CGR slurry produced (right). The weight of the CGR slurries and moisture contents were also measured and recorded in TABLE 7. The Standard Test Method for Laboratory Determination of Water (Moisture) Content of Soil and Rock by Mass

(ASTM D2216) was followed for oven drying of CGR slurry samples to test for moisture content. All CGRs dried were also dried at 60-degrees Celsius to help avoid changing the chemical composition of the CGR.

Figure 6: Moisture Contents of Homogeneous CGR Slurries, Photos by Patrick Bollinger

Table 7: Collected CGR Discharge Solids and Water Breakdown Comparisons

CGR	Discharge (lb.)	OD Solids (lb.)	Net Cake Water (lb.)	Supernatant (lb.)
CGR-1	1243.6	565 (45%)	171 (14%)	508 (41%)
CGR-2	1130.5	632 (56%)	198 (17%)	301 (27%)
CGR-3*	2130.9	638 (30%)	299 (14%)	1194 (56%)
CGR-4	1160.2	653 (56%)	236 (20%)	272 (24%)
CGR-5	1445.1	852 (59%)	231 (17%)	332 (24%)

Net Cake Water = Water decanted from CGR cakes excluded supernatant added back into the mix

OD = Oven dry

* CGR-3 discharge weight back-calculated from oven dried values and additional post mixing measurements

CGR-3 was the initial CGR slurry created, but the process for making an ideal pourable CGR slurry was not fully determined when the CGR-3 slurry was being mixed. As a result, this first extremely watery CGR slurry created had roughly four times the amount of water needed for an ideal, pourable CGR slurry, and had the highest moisture content at 65.2%. For the remaining four CGR slurries produced, a more controlled mixing process was used. This process involved

first decanting the CGR buckets then reintroducing measured amounts of water into the moist CGR solids (or CGR cakes) during the homogeneous slurry mixing in the larger 150-gallon mixing trough.

In addition to measuring the moisture contents of the CGR slurries produced, moisture contents were also measured for the two loess soil batches, again following ASTM standard D2216. The first batch of loess (stored inside of the soil mechanics lab at Iowa State University) had moisture contents ranging from 4.3% to 5.3% with an average of 4.8%. The second batch of loess (collected from Crescent Quarry) had much higher in-situ moisture contents that ranged from 14.1% to 18.3%. This was due to the excavation and collection of this soil following a strong week of rain in the region. Due to the high variability of moisture contents found in both loess batches, moisture contents of loess specimens to be used were always tested before use to ensure moisture content was known ahead of any compaction tests.

2.2.5 Soil Mixtures and CGR Dosages

In choosing a CGR dosage for amending Iowa loess, unconfined compressive strength (UCS) of CGR-amended soils was the primary selection criterion. A secondary measure was how the plasticity index (PI) of a soil was affected with the addition of CGR. In a 2019 TRR study, Yang et al. analyzed the feasibility of four different CGR dosages (10%, 20%, 30% and 40% CGR by weight) as a soil stabilizing amendment for two common Iowa soils [23]. These soils included a coarse sand (SC) and a silty clay (CL-ML). Yang et al. found that all 4 CGR dosages showed improved UCS, while the PI reduced with increasing CGR dosages and concluded that a 20% CGR dosage resulted in the highest USC gains. As a result, 20% CGR (by weight) was added to loess [23].

2.2.6 pH (CGR)

The testing of pH for the solids (loess and CGR dry solids) in this study was performed in accordance with the Standard Test Methods for pH of Soils (ASTM D4972-19). Similarly, the testing of pH for water samples in this study was performed in accordance with the Standard Test Methods for pH of Water (ASTM D1293-18). pH was measured for the soil, soil amendments, and soil mixtures (untreated loess, CGRs, and CGR-amended soils) as well as for the rainwater runoff samples collected for rainfall simulations on the Loess and CGR-1 amended and CGR-2 amended mixes.

With respect to the pH levels of the untreated loess, both batches of loess (control) had an average pH of 7.10, while the pH in dry CGR solids had a range between 11.13 and 11.83. Amending loess with 20% CGR increased the alkalinity of the amended soil, ranging from a pH of 9.59 to a pH of 10.87. Results are shown in FIGURE 7.

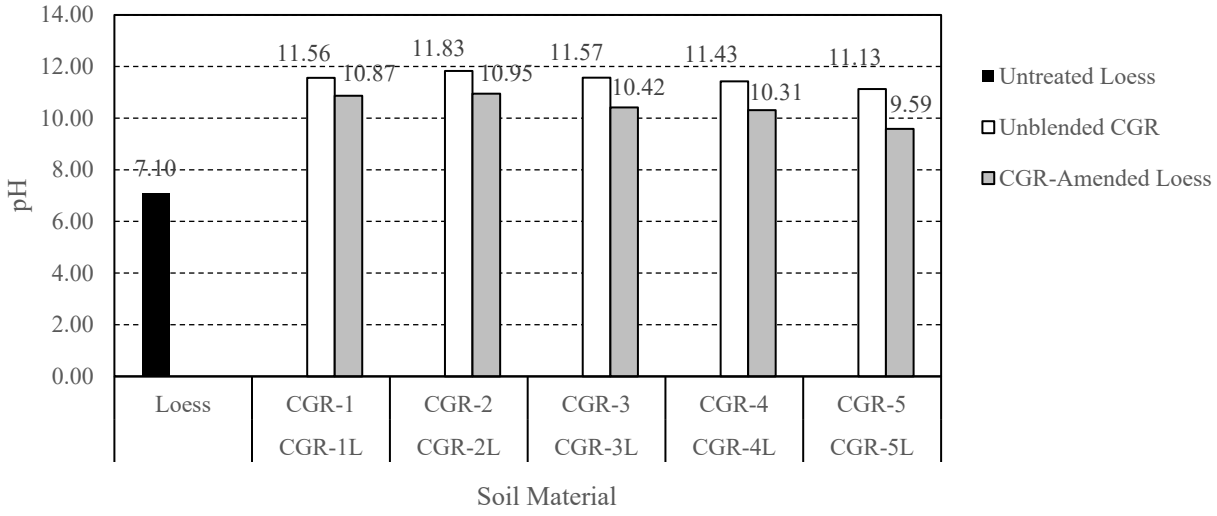

Figure 7: pH of Untreated Loess, Oven Dried CGR's, and CGR-Amended Loess Mixtures

The pH of the runoff water was also measured for each rainfall simulation at each of the 3 rainfall intensities (storms) in each of the simulated rainfall trials. The building water (supplied to the building by the City of Ames) was also tested for pH as well. Both the simulation water

and the runoff water from the loess during the final (6 in./hr.) storm of the simulation had similar slightly basic pH values of 8.01 and 8.19, respectively. For each of the simulation with CGR-amended loess (CGR-1L and CGR-2L) the pH levels gradually increased through the course of the 60-minute simulations. For CGR-1L the pH increased 5% over the course of the simulation, while CGR-2L the pH increased 14%. Results are shown in FIGURE 8.

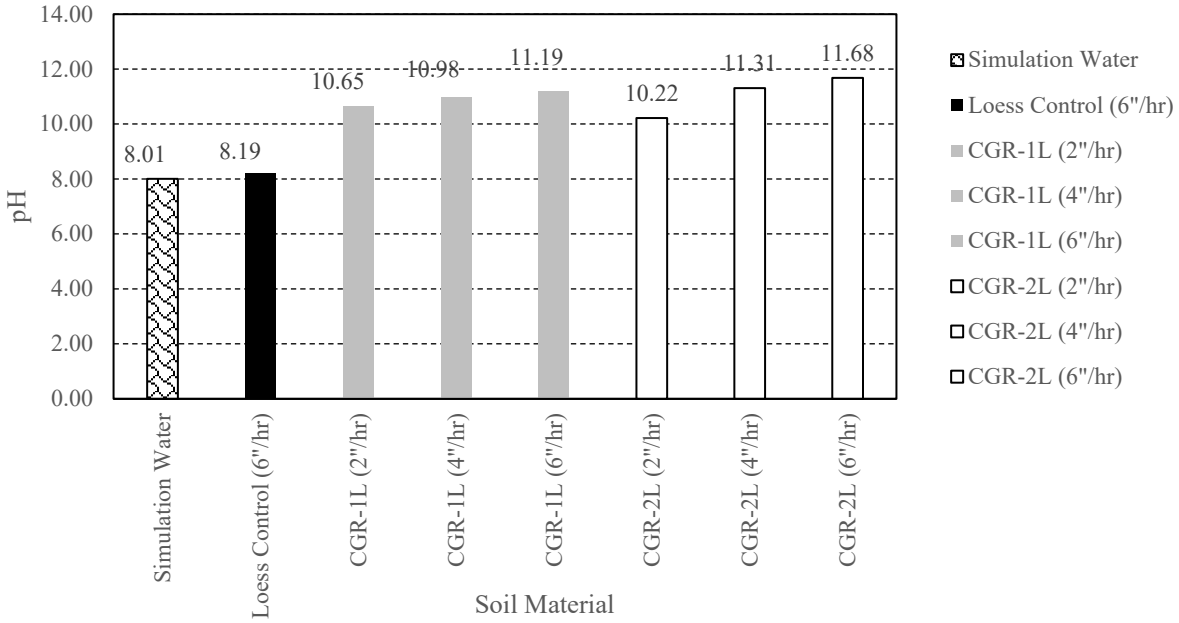

Figure 8: Post-Rainfall pH of Untreated Loess and CGR-Amended Loess (by Storm Intensity)

2.2.7 Standard Proctor

Initial Standard Proctor tests (ASTM D698-12) were performed on the untreated loess (control) as well as on CGR-1 and CGR-2 amended loess (hereafter referred to as CGR-1L and CGR-2L). The loess/control had an OMC of 16.8% and a MDD of 105.6-pcf. CGR-amended soil produced mixed results. With CGR-1L, OMC decreased 1% to 15.8% with a virtually unchanged MDD of 105.5-pcf. The OMC for CGR-2L on the other hand increased 0.5% to 17.3% with a slightly improved MDD of 106.8-pcf. The average OMC for the loess/control and both CGR-amended

soils was 16.6% with an average MDD of 106.0-pcf, with a standard deviation of 0.76% and 0.72-pcf for OMC and MDD measured values. Results are shown in FIGURE 9.

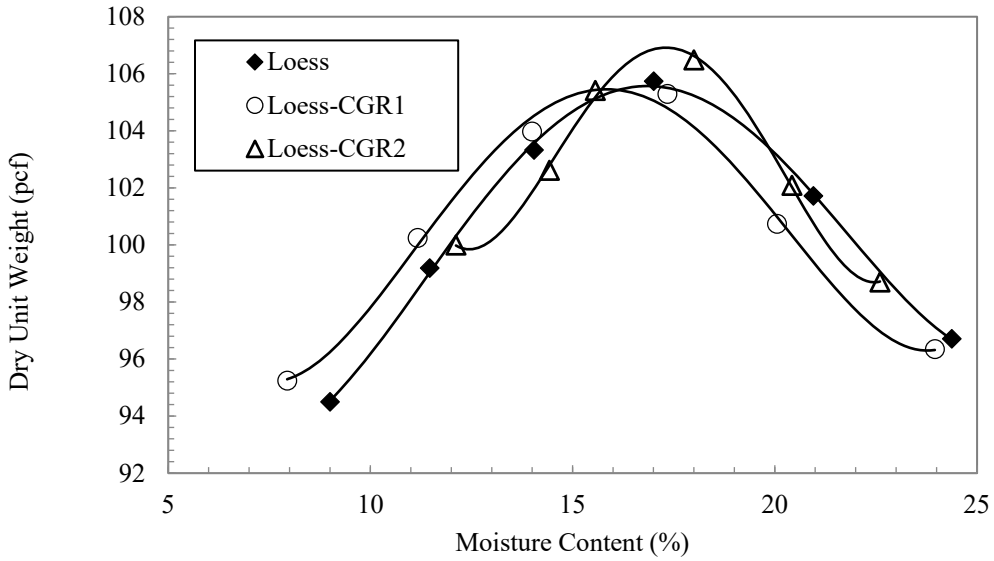

Figure 9: Standard Proctor Results for Loess and CGR-Amended Loess

2.3. Compaction

Compaction of the soil specimens in this rainfall erosion study required the design and construction of soil forms with drainage funnels and supporting racks as well as design, construction, testing, and calibration of a uniform compaction (tamping) apparatus. Lastly, a method of tamping was required for compacting the soil forms tested in this study.

2.3.1 Rainfall Racks and Soil Forms

In order to perform rainfall simulations and erosion testing, the design and fabrication of soil forms, supporting racks, and compaction methods were each required. Soil forms specifically for this use have been made in the past using many different configurations and soil depths. For this study, the soil media being tested included both loess (soil) and CGR-amended loess mixes. Due to the high alkalinity of the CGR there was a high potential for corrosion using metal forms. For this reason, combined with the significant weight and cost of materials, metal forms were

eliminated from consideration. Plastic forms were considered as well, but wood was ultimately selected due to its durability, low cost, and feasibility for building a custom sized soil form. Soil forms with inside dimensions of 24” (wide) x 48” (long) x 3-1/2” (deep) was selected, with the size modeled after soil forms built by Shoemaker and later by Wilson in their respective master’s theses research at Auburn University [101,102]. The choice of this size allowed for a comparison of CGR-amended soils to other erosion mitigating materials.

In both Wilson’s and Shoemaker’s research, rainfall simulations were also performed on compacted soil forms, however in these studies, the focus was in testing the erosivity of different surface treated products over exposed soils. Wilson’s research tested 4 types of hydromulch against two conventional straw mulch products, while Shoemaker’s research tested effectiveness of different applications of anionic polyacrylamide (PAM), a well-known chemical soil stabilizer and flocculating agent. In comparison, this study looked at the viability of amending soils with CGR to potentially stabilize the soil and reduce soil erosivity. The design of the soil forms and tamping methods used by both Shoemaker and Wilson were also improved upon in this study. Construction photos of the soil forms and supporting rack is shown in FIGURE 10.

Figure 10: Construction of Wooden Rainfall Racks and Soil Form, Photos by Patrick Bollinger

Like Wilson's soil forms, new wooden soil forms were built with 2x4's (1-1/2" x 3-1/2" lumber) for the end rails and 2x6's (1-1/2" x 5-1/2" lumber) for the side rails and 1/2" plywood for the soil form bases. The increased height of the side rails was made to avoid wash-out and soil loss over the side rails during rainfall simulations.

To protect the untreated plywood and lumber, the interior of each soil form was treated (sealed) with a durable waterproof coating. Three waterproof sealers were evaluated along with outdoor acrylic and latex-based paints. The three waterproof sealers reviewed included Swift Response's Flex Seal (a rubberized sealer), Henry's white roofing sealant (an elastomeric roof coating), and Gardner Coating's Leak Stopper (an asphalt-based sealer). Although each product had merit, Flex Seal was chosen for this project. Key features of Flex Seal include its waterproofing properties, ease of application (no prime coat needed), low volatile organic compounds (VOCs) and off-gassing during application, durability, and moderately low cost. Since only water resistance was needed on the outside of the wood forms, 2-coats of KILZ-2, a water-based, mildew-resistant primer, was used. In lieu of stacked blocks and saw-horses used in Shoemaker's and Wilson's research, a more substantial, braced wooden rack was required for this project. A conceptual wooden rack was envisioned next and then turned into a conceptual design with the help of Iowa State University structural engineering graduate student, Nathan Miner [103] (FIGURE 11). This final structural rack design included 2x4 diagonal bracing in both the X and Y axes as well as removable lateral all-thread rods to provide lateral stability to prevent failure under loading.

Figure 11: Concept Design Sketch and Completed (Built) Version of Rainfall Test Apparatus, Photo and sketch by Patrick Bollinger

In order to design a structural wooden rack capable of supporting heavy forms (filled with wet compacted soil) the MDD of the compacted loess soil at OMC was required. A MDD of 16.7-kN/m3 (107-pcf) was determined for a similar Western Iowa loess in research performed by Coban and by Mahedi at Iowa State University [39,104]. Multiplying 107-pcf times an 8-sf soil form with a depth of 3-1/2", adding in the weight of the empty 40 lb. soil form, and applying a safety factor of 1.2 produced an estimated 350 lb. weight requirement for each compacted soil form. This design concept was then finalized and built using 2x4 lumber and heavy-duty, corrosion-resistant, exterior deck screws. A fixed 3:1 slope (18.4-degrees) was built into the wooden racks for this study (FIGURE 11). This slope was selected based on typical embankment foreslopes shown in Iowa DOT roadway design drawings and detailed in Section 2107 for embankments in Iowa DOT's Standard Specification for Highway and Bridge Construction [105].

The top edge of each rack was built with a height of 22" to allow for a 6" clearance from the metal funnel to the top of a typical 5-gallon bucket. The drainage of each soil form was also engineered and improved upon in this project. The rainwater collection gutter used by

Shoemaker as well as the metal flume used by Wilson (installed at the base of each soil form) both appeared to successfully collect the rainwater samples; however, each did not appear to be very easy to clean or reset after a rainfall event. Moreover, the fine-grained loess and CGR soil particles on this project required an improved method of collection and handling. Shoemaker utilized a PVC gutter and downspout and the end of his soil forms, while Wilson chose a metal flume [101,102]. These gutters and flumes were secured directly to the wood soil forms, which then required extra handling and care with removal, cleaning, and reattachment after each rainfall simulation. With the prospect of significant test repetitions, a more durable, "detachable funnel" was designed to address these product limitations. A new funnel design was modeled and dimensioned in AutoCAD and then given to Drexel Metals, Inc. who fabricated a prototype. The main features of this new funnel were that it allowed for easy removal and cleaning and provided a more seamless way to direct and capture rainwater runoff samples.

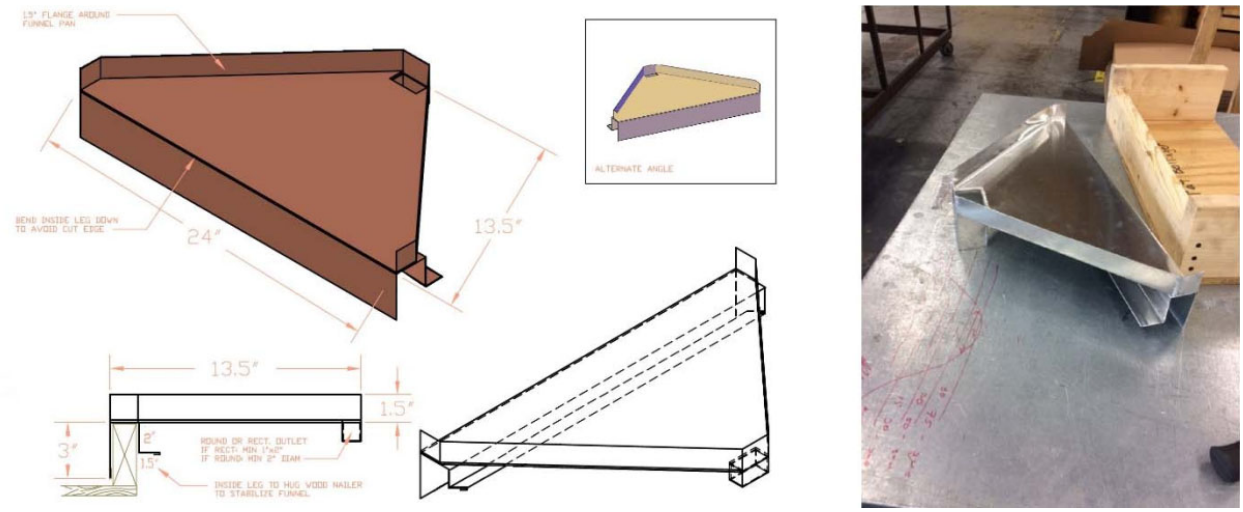

Figure 12: CAD Drawing and Actual Aluminum Soil Form Funnel, Photo and CAD Drawing by Patrick Bollinger

The final design included a welded (not pop riveted) aluminum funnel with a U-shaped back (that snuggly fit over the bottom end rail), a triangular-shaped design with 1-1/2" high side walls,

a rectangular drainage outlet, and an open top (to provide visibility during testing for addressing any clogs that might occur) (FIGURE 12).

Testing of the funnel prototype involved outfitting a soil form with a plexiglass cover and then running a maximum 6”/hour maximum rainfall simulation to check for leakage and/or any overflow issues. The results of the test found no functional issues with the prototype. After this rainfall test, an easier attachment method was added to the transparent plexiglass covers fitted over the funnels. The exposed wood on the racks were also primed with 2-coats of KILZ 2 primer to better protect them from water penetration as well.

2.3.2 Uniform Tamping Apparatus (UTA)

With the soil forms, supporting racks, and collection funnels designed and fabricated, focus turned to the design of a uniform tamping device/apparatus. Both Shoemaker and Wilson shared the same tamping methods, which involved lifting and dropping a hand-tamper a series of drops to achieve 95% compaction. The hand tamper used appeared to be an effective soil compaction tool in both of these studies. Wilson and Shoemaker each achieved the desired compactions of similar Alabama sandy clay loams with 80-drops and 90-drops (per square foot) respectively. Both researchers also determined optimum drop counts for each of their projects through regression analyses of the drops, graphing the unit weights achieved through compaction using a smaller 12”x 12” (1-sf) test form. Shoemaker and Wilson each manually tamped their smaller test forms in trials consisting of 10, 20, 30, 50, and 60 drops, to determine the optimum number of drops [101,102].

The challenge with any manual drop compaction method is ensuring that the energy from each drop is both uniform and repeatable. Important drop factors including drop height, drop angle, and landing position of the tamper/weight, each need to be kept reasonably constant for each

drop to deliver the same amount of compaction energy to the soil. The tamper also needs to be gravity-dropped (not thrust down) so the impact delivered to the soil does not dramatically very with each drop sequence. In addition to drop factors, the maneuverability of the tamper and/or soil form is another important design consideration. With a larger 8-sf soil form footprint, compared to 10”x 10” (0.69-sf) or 12”x 12” (1-sf) tamper footprints for example, repositioning of the form and/or the tamper is required during compaction. An automated compaction apparatus could better account for this repositioning in the design. These important design considerations were incorporated into the design and construction of a uniform tamping apparatus (UTA) created for this study (FIGURE 13).

Figure 13: Wooden Uniform Tamping Apparatus (UTA), Photos by Patrick Bollinger

Like the soil forms, the UTA frame was fabricated primarily from 2x4 nominal wood lumber. Borrowing from Shoemaker’s and Wilson’s process, a 13.05 lb. hand tamper with a 10”x 10” square footprint was also incorporated into the UTA. A fixed drop height of 12” above the top of the soil surface was built into the UTA frame and a 24” (wide) x 48” (long) rolling platform with 8 heavy-duty casters was built to allow the soil forms to be repositioned easily on the floor.

Horizontal casters were added to the UTA frame to restrict movement of the rolling soil forms in the longitudinal (8-foot) direction .

With respect to the tamping angle, a PVC pipe sleeve was integrated into the UTA frame to confine the tamper to a fixed, vertical/plumb position. A horizontal slot was added for horizontal movement of the tamper, with removable check blocks added to hold the tamper (horizontally) in one of two positions in the slot during tamping. This still allowed for free tamping in variable horizontal positions if needed. Vertically, the PVC pipe containing the tamper, also served as a "limiter" to fix the maximum drop height to 12" from a fully raised (set) position of the tamper down to the top surface of the soil. Lastly, a hole was drilled in the metal tamper handle for safety. A removeable carriage pin was installed in the hole to hold/lock the tamper (safely) in a raised position. This pin was used when the soil form was repositioned during compaction.

2.3.3 Uniform Compaction

Uniform compaction, that was easily replicated, was required for the soil forms used in the rainfall trials in this research. Creating the UTA discussed above, provided the equipment to achieve uniform compaction, but determining a repeatable Uniform Tamping Method (UTA Method) to compact the soil forms was also required. To test the UTAs compaction capability to produce uniform compaction over a series of test trials, a smaller 12"x 12" (x3- ½" deep) wood test form was built. This small 1-sf test form was also waterproofed with Flex Seal to simulate a scaled-down version of the full size 8-sf rectangular soil form. The purpose of the UTA compaction trials was to determine the degree of compaction from an increasing amount of compaction effort. Compaction trials were performed with 50, 75, 100, 125, and 150 (gravity) drops per 1-sf form with the 13.05 lb.-ft. tamper built into the UTA. This tamper was raised and then dropped (not thrust down) for each tamp (or drop) (FIGURE 14).

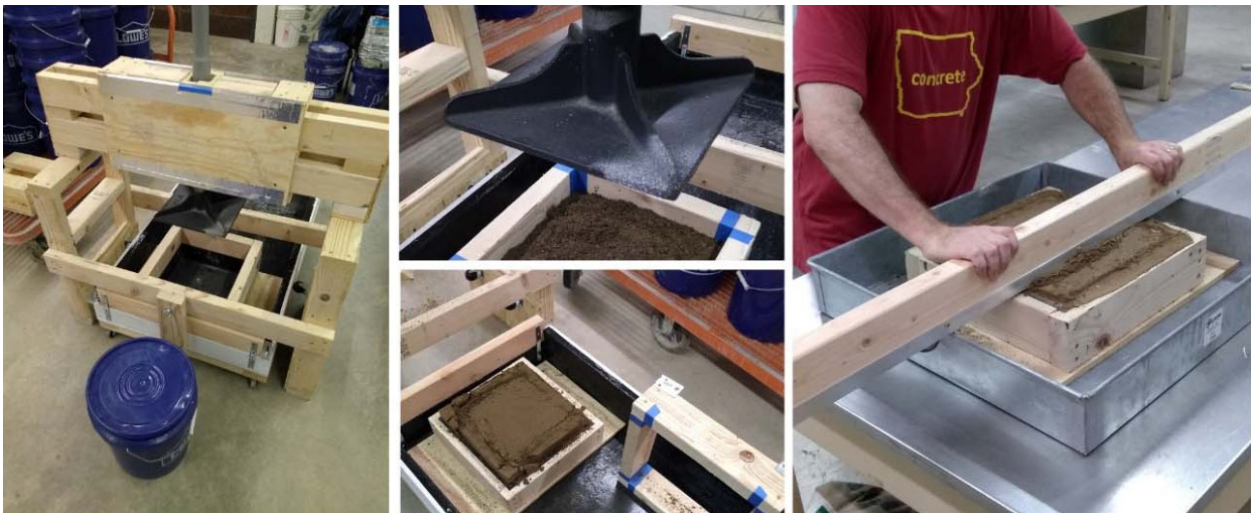

Figure 14: Calibration Test Trials of UTA, Photos by Patrick Bollinger

The UTA compaction trials were performed on loess samples prepared with an 11.5% (-5.3% OMC) constant moisture content. This moisture content (on the dry side of optimum) was chosen to help ensure no excess pore water pressure would adversely affect compaction, while still providing enough moisture to achieve good [soil] compaction. Using the data from the UTA compaction trials and linear regression, a linear relationship with a high degree of confidence (R^2=93.3%) was found between the drop trials and the dry unit weights measured for all five test trials (50, 75, 100, 125 and 150 drops). Extrapolating from this data, a theoretical number of drops to achieve 90% and 95% compaction is 175 and 240 drops per 1-sf form, respectively. The theoretical drops required to reach a theoretical 100% or maximum compaction was determined at 305 drops/sf. Multiplied by 8 (for an 8-sf soil form, to achieve 90%, 95%, and (a theoretical) or 100% compaction would require 1400, 1920, and 2440 drops, respectively, for these degrees of compaction at OMC. Since this number of drops per soil form would be extremely difficult to achieve for dozens of soil forms, the prospect of compacting the soil forms required a lower more manageable number of drops.

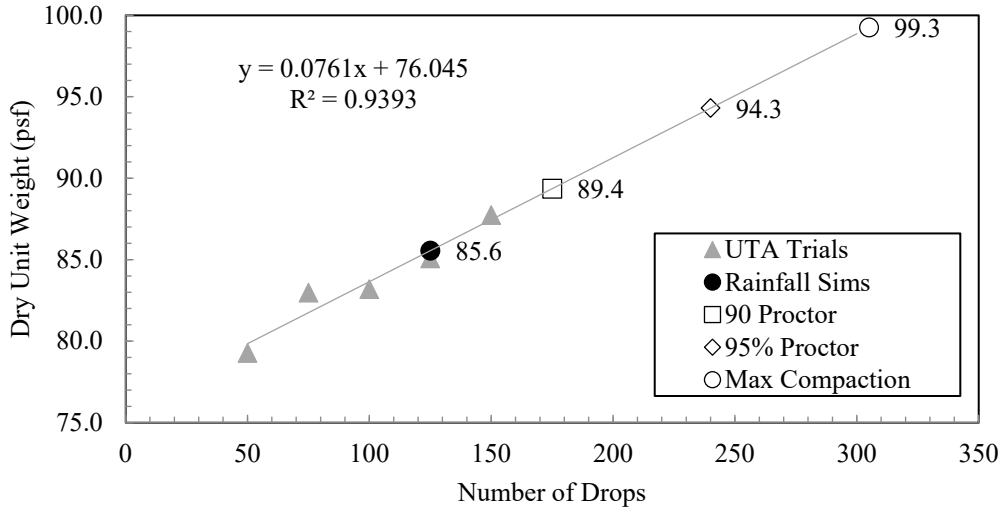

Figure 15: UTA Test Trial Data (Degree of Compaction per Numbers of Drops)

Included in the test trials were 150-drops/sf (1200 drops per soil form) and 125-drops/sf (1000 drops per soil form). The drops in these 2 trials achieve 88% and 86% compaction, respectively (FIGURE 15). Although 90% compaction was desired for these trials, 125-drops/sf (1000 drops per soil form) was selected for the compaction standard for the rainfall trials. This reduced number of drops was believed to still provide adequate compaction of the soil forms for erosion testing. In hindsight, changing from 1 lift of soil to 2 lifts of soil (theoretically) with 125 drops/sf would have produced sufficient compaction energy to achieve 90% compaction at this same number of drops.

2.3.4 Tamping Pattern

During the selection of the number of drops/sf, a choice of eight drop locations 125-drops/sf x 8 drop locations in the soil form was assumed. Initially the soil form was divided into a grid of 15 overlapping drop locations. However, if the drop locations in the soil form was increased to 15, the total number of drops would increase to 1875 total drops (15 locations x 125/location). Based on this dramatic increase in the total number of total drops required, eight drop locations were kept, and a serpentine pattern (shown in pattern “C” in FIGURE 16 was adopted to provide an

alternating pattern to the tamping and minimize the amount of time the soil form needed to be shifted longitudinally under the UTA tamper.

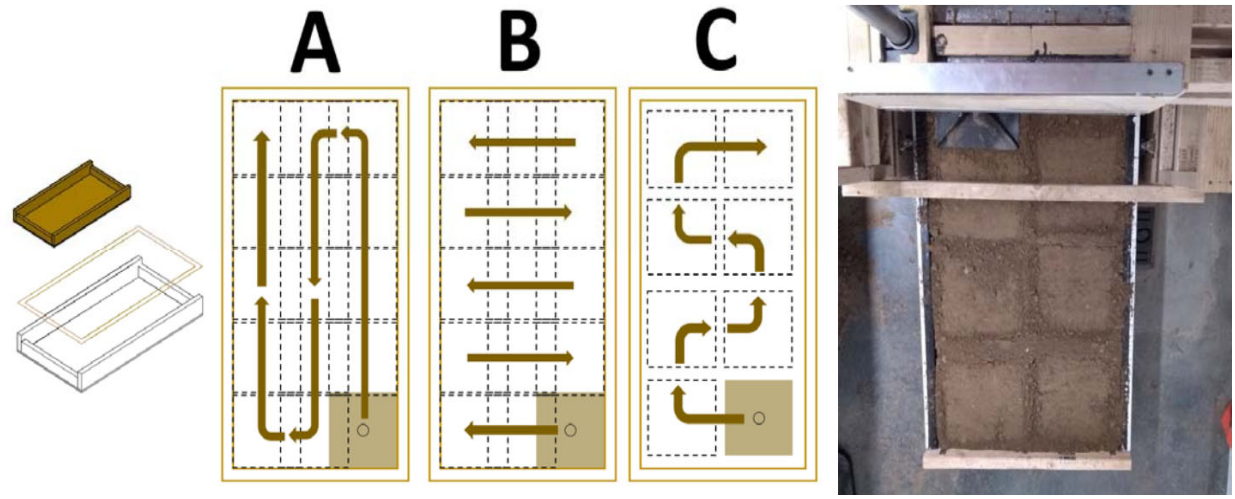

Figure 16: Rainfall Soil Form Tamping Patterns. Pattern C (Right) Chosen, Photo and sketch by Patrick Bollinger

2.4 Rainfall Erosion Simulation

With respect to the Iowa State University rainfall simulator used in this study, an understanding of the simulator system of devices and mechanisms as well as calibration and testing of this equipment were required prior to performing the rainfall erosion testing. The calibration and testing of this equipment did not exist. As a result, processes were developed to accomplish this work.

2.4.1 Rainfall Simulator (ISU)

An indoor, ceiling-mounted, 3-bay, 9-nozzle, Purdue-type, rainfall simulator located in the Biorenewables Research Laboratory at Iowa State University (ISU) was used for this study. It employed a total of 9 VeeJet Model 80100 flat-spray nozzles (3-per bay), each with laminar flow fittings, to produce a fine rainfall spray with an 80-degree fan spread (FIGURE 17). The drainage area with metal grates area under the rainfall simulator was 11 ft wide (left-to-right) by

15 ft deep (front to back), with a maximum potential rainfall zone of approximately 9 ft wide by 11 ft deep beneath the rainfall simulator.

Four independently controlled winches were connected to the simulator corners to control its height, that ranged from approximately 1.2 m (4 ft) to 4.6 m (15 ft), measured from the ground to the bottom of the metal simulator troughs. An optimal height of between 2.3 m (7.5 ft) to 3 m (9.8 ft) was determined by the late distinguished USDA Agricultural Engineer, Dr. L. Donald Meyer for use in rainfall simulators using the same VeeJet 80100 nozzles with 41 kPa (5.9 psi) spray pressure [106]. Two previous nitrate leachate soils studies were performed at Iowa State University that appeared to use the same rainfall simulator, and the height of the simulator was placed at 3.05m (10 ft) above the soil specimens tested in these studies [107,108].

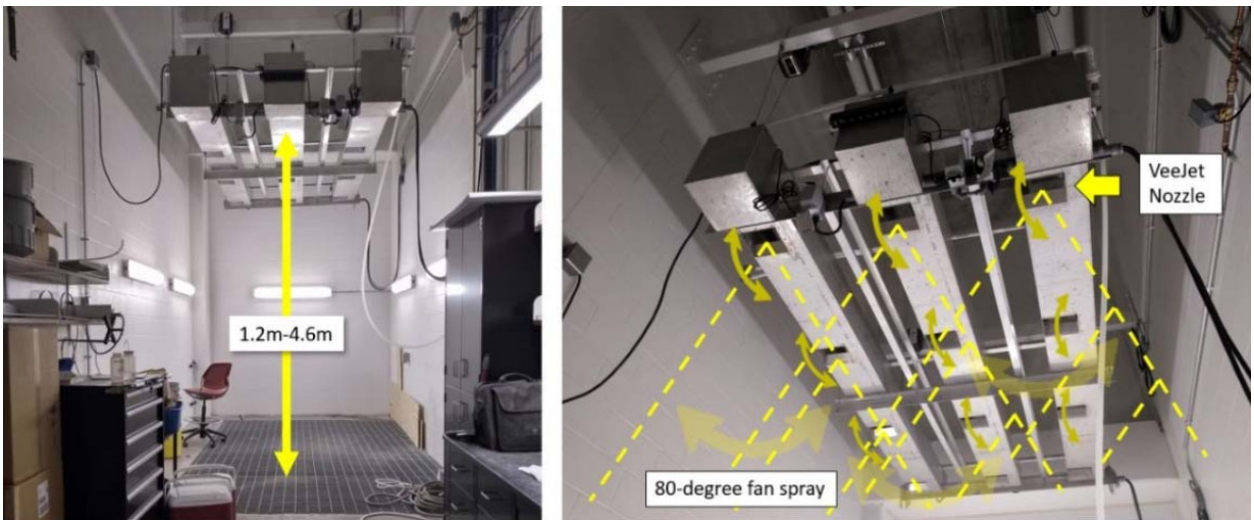

Figure 17: Iowa State University (ISU) Ceiling Mounted, Purdue-Type, Rainfall Simulator, Photos by Patrick Bollinger

Since the same VetJet 80100 nozzles and similar water pressures were used in the ISU simulator, a working height of 2.4 m (8 ft) – selected within the Meyer range – was chosen for this study. Each bay could be turned on or off with rainfall produced by 1 bay or a combination of two of three bays. All three bays were used for the rainfall simulations in this study.

To accommodate the variable height of the simulator, 1” flexible plastic tubing supplied water to the three bays in lieu of rigid pipe. This tubing transitions to rigid PVC pipe at a valve and spigot mounted to each bay. Potable water from the City of Ames (Iowa) was controlled in the simulator with ballcocks (floats) attached to lever arms that opened and closed supply valves to regulate the amount of water supplied to reservoir tanks in each metal bay/trough. A small 1/3 horsepower submersible (recirculating) pump was located in the bottom of each reservoir tank. Additional PVC piping with adjustable 15-psi in-line pressure gauges extended up from the pumps to the nozzles. The metal troughs had tapered cut-outs with raised edges at each nozzle. This prevented any extra discharge water from flowing out of the trough between nozzle oscillations. The far end of the simulator frame was raised 2” higher in the back, which allowed extra water retained in the troughs to flow back to the reservoir tanks with the submersible pumps. Each pump continuously recycled water from the reservoir tanks to the nozzles. Rainfall was created by VeeJet Model 80100 flat-spray nozzles with laminar flow fittings which produced a fine rainfall spray with an 80-degree fan spread.

Each bay contained 3-nozzles connected to a coupling bar which was driven by a small motor at the back end (high side) of the troughs. This configuration produced an oscillating (or sweeping) motion in the nozzles (similar to a windshield wiper on a car). Again, the rainfall footprint generated by the simulator was approximately 11 feet wide by 15 feet deep (front to back) with a workable (uniform rainfall) area of approximately 9 feet wide by 11 feet deep. Because of the overlap of rainfall spray between the bays, rainfall under the center bay is generally higher than the outside bays. However, lowering the pressure gauge to the center bay effectively lowered the rainfall intensity for this bay during calibration.

2.4.2 Rainfall Simulator Calibration

Rainfall simulations and testing for this study were modeled after Standard Test Method for Determination of Rolled Erosion Control Product (RECP) Performance in Protecting Hillslopes from Rainfall-Induced Erosion (ASTM D6459-15). Raindrop size distribution and the Christiansen uniformity coefficient (Cu) detailed in this standard were calculated for each rainfall intensity in this study.

Rainfall intensities were set through a combination of adjustments to (3) 15 psi pressure gauges (1-per bay) and a central GraLab Model 451 electronic timer (FIGURE 18). By changing water pressure and timing calibration settings, rainfall intensities ranging from approximately 1"/hour to 8"/hour could be generated. The GraLab timer controlled the nozzle sweep timing for each bay. This sweep timing consisted of two settings, a sweeping motion (M1) and a pause time (M2). These settings together determined the oscillation frequency of the nozzles, and changes to these two settings combined with adjustments to the three in-line water pressure gauges made up a "calibration set" for a single rainfall intensity (storm) event. Three calibration sets were needed to create the required 60-minute, three storm rainfall simulation, however, only one rainfall intensity could be set at one time. This meant that in order to transition between the three storm events, manual changes to the GraLab (nozzle) timer were required real-time during a running rainfall simulation (assuming the water pressure could be kept constant for all three storms).

Figure 18: Iowa State University Rainfall Simulator Apparatus, Timer, and Controls, Photos by Patrick Bollinger

To determine the water pressure and nozzle settings required for each storm, a series of rainfall intensity trials (RI trials) were required. To measure the rainfall at different points within the rainfall simulation room, a set of graduated one quart containers were placed in a grid on the floor under the simulator to serve as rain gauges. After each RI trial, the containers were dried on the outside, weighed, and the water depths were recorded. The goal for each RI trial was to attempt to match one of three targeted rainfall intensities within a 10% margin of error. Two patterns were used in the RI trials, a full pattern, and a reduced, staggered pattern. The reduced pattern consisted of a staggered 6x7 grid that consisted of 21-containers, 24 in. on center, with seven rows and six columns covering a uniform rainfall area of 42-square feet (the estimated area for three compacted soil forms). The full pattern consisted of a 11x9 grid of 99-containers, spaced 12 in. on center, with 11-rows and 9-columns covering the full (non-uniform) rainfall area of 99-square feet. The full pattern (99-containers) was used to first determine the most uniform rainfall section within the full rainfall area. The reduced pattern (21-containers) was then used to determine the water pressures and nozzle timer settings required to produce the three required rainfall intensities (2 in., 4 in., and 6 in./hr. storms).

After a series of 28-RI test trials, three calibrations sets were selected that most closely matched the desired 60-minute, 3-storm rainfall simulation with a 2 in., 4 in., 6 in./hr. increasing rainfall storm sequence (three successive 20-minute storms). The best RI trials for both the 2 in./hr. and 4 in./hr. rainfall intensities had great results, with margins of error in the volume of water collected in each of the 21-containers calculated at 1.08% and 0.94%, respectively.

Table 8: Initial and Selected Rainfall Intensity Trial Calibration Sets

Trial ID	Timing Settings	Pressure Settings	Bay1 (in./hr.)	Bay2 (in./hr.)	Bay3 (in./hr.)	Total (in./hr.)	Target (in./hr.)	% Error
1	Manual (max rainfall)	N/A - Not tracked	6.69	9.94	7.38	8.00	-	-
2	Manual (max rainfall)	L: 12.5 psi, C: 12.5 psi, R: 12.5 psi	5.04	4.61	5.10	4.92	-	-
3	Manual (max rainfall)	L: 12.5 psi, C: 8 psi, R: 12.5 psi	7.25	5.83	6.92	6.67	-	-
7 *	M1 (0.5s), M2 (0.8s)	L: 12.5 psi, C: 6 psi, R: 12.5 psi	1.85	2.24	1.97	2.02	2.00	1.08%
18 *	M1 (0.7s), M2 (0.1s)	L: 12 psi, C: 7 psi, R: 12 psi	3.64	4.48	3.99	4.04	4.00	0.94%
22 *	M1 (0.4s), M2 (0.1s)	L: 12 psi, C: 7 psi, R: 12 psi	6.16	7.13	6.22	6.50	6.00	8.36%

* Settings selected for the 3 rainfall intensities (2"/hour, 4"/hour, and 6"/hour)

The best RI trial for the 6 in./hr. storm produced a higher (but still acceptable) margin of error at 8.36% from the targeted rainfall intensity volume desired. TABLE 8 shows the calibration sets for the first three RI trials as well as the three (best) selected RI trials from the 28-RI trials. FIGURE 19 shows a spatial graph of the rainfall depths recorded for the grid 99-containers measured for the 4”/hour rainfall intensity (storm) facing the simulator. The X-axis represents the width of the rainfall simulation room from 1-foot to 9-foot.

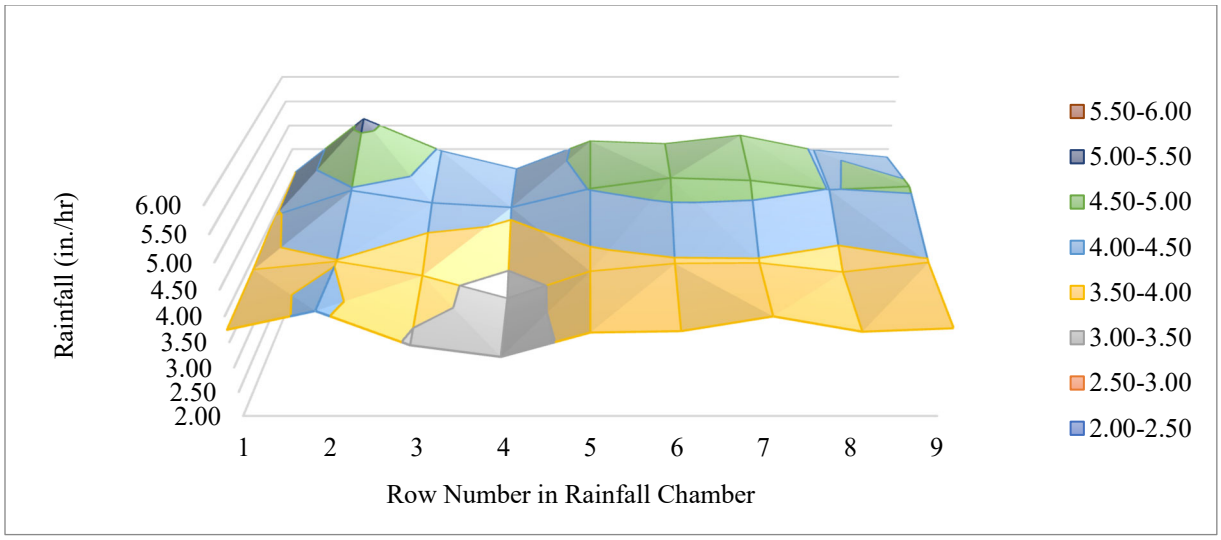

Figure 19: Rainfall Uniformity Data for 4"/hr. Rainfall Intensity

With the three best calibration sets selected, a final rainfall simulation at each rainfall intensity (2 in., 4 in., and 6 in./hr. storms) was run with the full pattern (99-containers). Using data from these 3 full pattern simulations, the final placement of the soil forms in the "most uniform" rainfall area within the simulator room was performed. In addition, the rainfall data from these simulations allowed the Christiansen Uniformity Coefficients for the 2 in., 4 in., and 6 in./hr. storms to be calculated.

The Christiansen Uniformity Coefficient (Cu) is a commonly used measure for assessing the uniformity of water distribution from a sprinkler or irrigation system. This procedure was used for each rainfall intensity produced by the rainfall simulator on this project. These coefficients were determined from the rainfall depths measured during the full pattern (99 container) RI trials performed after choosing the final simulator timing and pressure settings (calibration sets) for the three desired storm events. Cu was calculated as 88.1%, 82.44%, and 57.41% for the 2 in., 4 in., and 6 in./hr. storms, respectively. The Cu's for the 2 in. and 4 in./hr. storms produced a high degree of uniform rainfall distribution, while the Cu for the 6 in./hr. storm was deemed moderate to low uniformity. This disparity in uniformity for the 6 in./hr. storm is attributed to equipment

limitations in being able to produce this last heavy storm event. However, since the simulator was able to produce the required volume of rainfall with a low margin of error with the volumetric rainfall test (detailed next below) the 6 in./hr. storm calibration set was deemed satisfactory for the purposes of this study.

A volumetric rainfall test was created to calculate the volume of water landing on the surface of the targeted 8-sf compacted soil forms. For this test, a 20-minute rainfall simulation was performed for each of the 3 rainfall intensities (using the calibration sets selected for each storm). During each volumetric test rainfall simulation, a soil form was fitted with a plexiglass cover that allowed the total rainwater runoff from one 8-sf soil form to be collected and weighed. Rainfall volumes for each simulated storm (2 in., 4 in., and 6 in./hr.) were then calculated. Results found a margin of error of less than +/- 5% error for each simulation as well, under the 10% maximum margin of error desired. A summary of volumetric test results is shown in TABLE 9.

Table 9: Calibration Rainfall Intensity (Storm) Volumetric Test Results

Rainfall Intensity	Trails, Wt. (Vol.)	Total, Wt. (Vol.)	Error, Wt. (Vol.)	% Error
2"/hour	10569 g (3.28 gal.)	10569 g (3.28 gal.)	-154 g (-0.04 gal.)	-1.43%
4"/hour	22403g (6.95 gal.)	21447g (6.65 gal.)	956g (0.30 gal.)	4.46%
6"hour	31733 g (9.84 gal.)	32170 g (9.97 gal.)	-437 g (-0.13 gal.)	-1.36%

A raindrop gradation (or flour test) was also performed to measure the raindrop particle size distribution of the rainfall generated by the rainfall simulator. This test was performed for each of the three rainfall intensities (2 in., 4 in., and 6 in./hr.) in this study. For this test three 8 in. aluminum pie pans were filled and screeded flush with the top of the pie pans. The pans were then covered with aluminum foil and staggered inside of the rainfall room (FIGURE 20). The rainfall simulator was then started and each of the flour pans were uncovered for a brief three to four second period and then recovered. This allowed the raindrops to impinge into the flour.

Nine pans total were tested, three pans per storm intensity, resetting the rainfall simulator between each test.

Figure 20: Raindrop Particle Size Distribution Test (Flour Test), Photos by Patrick Bollinger

The flour was air dried for 12-hours before gently screening off the dry pellets that formed from the raindrops. These pellets were then oven-dried at 110 degrees C for two hours before sieving the drop pellets with a fine grain set of 8 in. diameter sieves. The sieve sizes used included #4, #8, #10, #20, #30, #40, #60, #80, #100, #200 and a pan. According to the American Meteorological Society (AMS), the average raindrop has a diameter between 1 to 2 mm [109]. AMS also describes drizzles drop sizes which are smaller drops ranging from 0.2 to 0.5 mm.

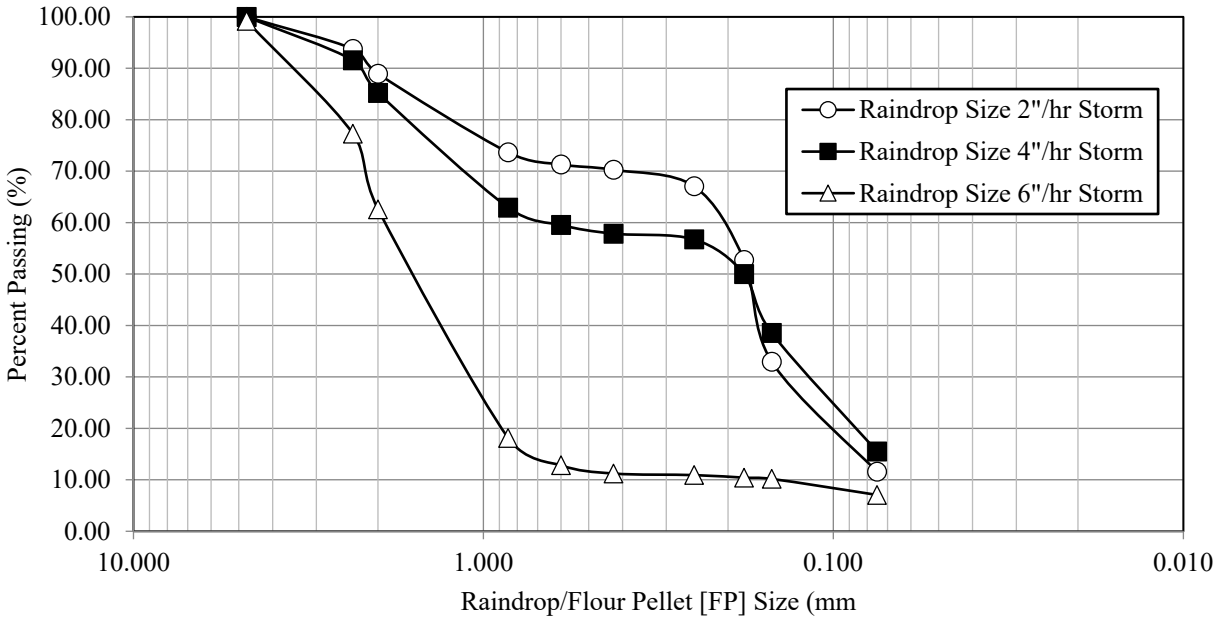

Figure 21: Raindrop Gradation Curves for Each Rainfall Intensity (Storm)

The rainfall simulator used for this study produced uniquely different sized raindrops and drizzle drops in each of the three rainfall intensities tested. If 1 mm is used as the distinction between raindrops and drizzle drops, the 6 in./hr. storm produced the greatest raindrops (79%) compared to the 2 in./hr. storm (24%) and the 4 in./hr. storm (34%). On the other hand, the 2 in./hr. storm produced the most drizzle drops (76%) compared to the 4 in./hr. storm (66%) and the 6 in./hr. storm (21%) (FIGURE 21).

2.4.3 Rain Erosion Test Procedure

The test procedure for each rainfall simulation involved stepping through a series of manual settings to the timer and rainfall intensities settings to produce a real-time, 3-storm, 1-hour rainfall event while also collecting turbidity and total suspended solids (TSS) samples at fixed increments for 3-soil forms tested at the same time in the rainfall simulation room (FIGURE 22). Setup for each new rainfall test, involved first lifting the three compacted soil forms up on to the structural wood racks located inside the rainfall room. Plastic sheeting was placed over the three

racks and soil forms to prevent contamination while setting up and pre-testing the rainfall simulator.

The purpose for pre-testing (or priming) the simulator was to ensure the water pressure gauges, pumps, and rainfall intensity and timing equipment were all set to the proper settings and functioning properly. This usually involved running the rainfall simulator through a quick 1 minute rainfall simulation. After verification, the rainfall was turned off and the plastic sheeting was removed. Buckets were then placed under the drainage funnels to each soil form and a stopwatch was reset. It took three people dawned with rain ponchos to properly collect the turbidity samples every 3-minutes and exchange the 5-gallon buckets at the transition between each of the (3) 20-minute storm events. The entire sequence for a single rainfall test takes 60 minutes.

Figure 22: Typical Rainfall Simulation and Captured Sediment-Laden Water Runoff, Photos by Patrick Bollinger

During this time pressure gauges must also be monitored along with the level arms to the submersible pumps in each of the three rainfall simulator trough to ensure a successful test. Care was taken to ensure both the turbidity grab samples and 5-gallon buckets were collected, capped, and sealed to avoid cross contamination during the test. A completed rainfall test captures

approximately (15) 5-gallon buckets and (60) 50-ml grab samples of sediment laden water for future testing. Each grab sample and bucket were labeled prior to performing the rainfall test to prevent any mix-up of the samples after the rainfall simulation was completed.

Water Quality (ss. turbidity) testing was performed in accordance with the Standard Test Method for Determination of Turbidity in Static Mode (ASTM D7315 2017). Turbidity tests were performed on sediment-laden runoff water collected during four indoor rainfall simulations, with turbidity (grab) samples collected at 3-minute intervals (from three separate soil forms) over the duration of a 60-minute rainfall simulation. A HACH 2100Q portable turbidimeter was used to test turbidity readings for each grab sample with results reported in nephelometric turbidity units (NTUs). The 2100Q unit was calibrated using 10ml sealed cells (comprised of 0, 10, 100, and 800 NTU specimens). The maximum range for the turbidimeter was 1000 NTUs, so dilution was required (as much as 40 times) for each grab sample using filtered water retrieved from an ELKAY drinking water station. Water quality measurements (12 in total) were randomly taken of the ELKAY dilution water used to ensure clean dilution water was being used for testing. Low turbidity values ranging from 0.39 to 1.97 NTUs were measured across all 12 dilution water samples, with only 2 values greater than 1 NTU and an average of 0.78 NTUs across the samples. These low NTU values for the ELKAY dilution water are consistent with the EPA's National Secondary Drinking Water Regulations (NSDWR) for turbidity, wherein potable water should not exceed 5 NTUs and filtration systems with a turbidity no higher than 1 NTU [110].

In total, 60 grab samples per simulation (20 samples from each soil form) were collected into 50-ml clear plastic centrifuge tubes with screw-top caps. The remaining stormwater runoff flowing-off the surface of each soil form was also collected into 5-gallon buckets (separated by rainfall intensity) for the duration the simulation. Three 20-minute rainfall (storm) events were run back-

to-back with continuous rain throughout the simulation. Each 20-minute storm progressed in intensity, beginning with a 2 in./hr. storm, proceeding to a 4 in./hr. storm, and finishing with a 6 in./hr. storm. Buckets were changed at the transition point between each storm event. Extra empty buckets were also used (when needed) to ensure none of the 5-gallon buckets overflowed during each simulation. Snap-on lids were used to seal each bucket to prevent cross contamination and protect against evaporation prior to testing. Buckets stored for an extended period of time were also sealed with packing tape.

2.5. Results

All rainfall trials were performed in triplicate using three identical compacted rainfall soil forms. The first three compacted soil forms tested in the rainfall simulator were of loess with a moisture content of 11.5% (Control-1). The soil forms were covered with plastic (after compaction) to provide a 24-hour rest/curing period for the soil prior to rainfall testing. A second loess control (Control-2) with a moisture content of 16.5% was tested second, with three compacted soil forms also covered with plastic for 24-hours prior to testing. The last two rainfall simulations for CGR1 and CGR2 amended loess (CGR-1L and CGR-2L) were prepared with moisture contents of 16.5%. For these two tests, the compacted soil forms were also covered for a 24-hour curing period, prior to testing. An average OMC of 16.5% was chosen for the last 3 simulations (Control-2, CGR-1L, and CGR-2L) to simplify soil and CGR-amended soil preparation since the OMC for loess and CGR-amended soils (CGR-1L and CGR-2L) shared similar OMCs to untreated loess at OMC (Control-2) falling within 1% of the OMC for the loess.

Turbidity testing of the grab samples collected for the loess at 11.5% MC (Control-1) did not show consistent water runoff between the 3 soil forms tested in the first loess control trial. The compacted soil forms in Control-1 absorbed virtually all of the rainwater runoff during the first

10-minutes of the simulation, which led to a saturated, loosely-compacted soil and erratic turbidity results across the three soil forms throughout the simulation. A second test was performed with loess with a 16.5% MC (Control-2). The compacted soil forms in Control-2 at a moisture content close to OMC produced much more consistent water quality samples between the 3 soil forms tested. A side by side comparison of both controls, Control-1 (top) and Control-2 (bottom) are shown in FIGURE 23.

With respect to Control-2, the short spike in turbidity for the first 2 readings (3-minutes and 6-minutes) is attributed to loose fines initially washing off the surface of the soil at the beginning of the rainfall simulation. The turbidity values for Control-2 leveled-off starting at the 12 to 15-minute mark of the simulation, indicating relatively uniform erosion throughout the simulation. Control-2 ended with a consistent (average) turbidity value of 8500-NTUs as the simulation finished.

Conversely, CGR-1L showed high turbidity values throughout the test with multiple peaks crossing 39000-NTUs throughout the duration of the simulation. CGR-1L also leveled-off at 38400-NTUs from just after the middle of the simulation to the end. CGR-2L had behavior similar to the turbidity trends for both Control-2 and CGR-1L, but to a lesser degree. A side by side comparison of both CGR-amended soils, CGR-1L (top) and CGR-2L (bottom) are shown in FIGURE 24. CGR-2L peaked at 18400-NTUs at the 9-minute mark and then gradually decreased in turbidity for the remainder of the simulation, plateauing at 14400-NTUs from 30 to 48-minutes before decreasing to its lowest value of 11400-NTUs at the end of the trial. The turbidity results in general showed that the untreated loess at OMC (Control-2) produced much lower water quality samples compared to both CGR-amended soils (CGR-1L and CGR-2L).

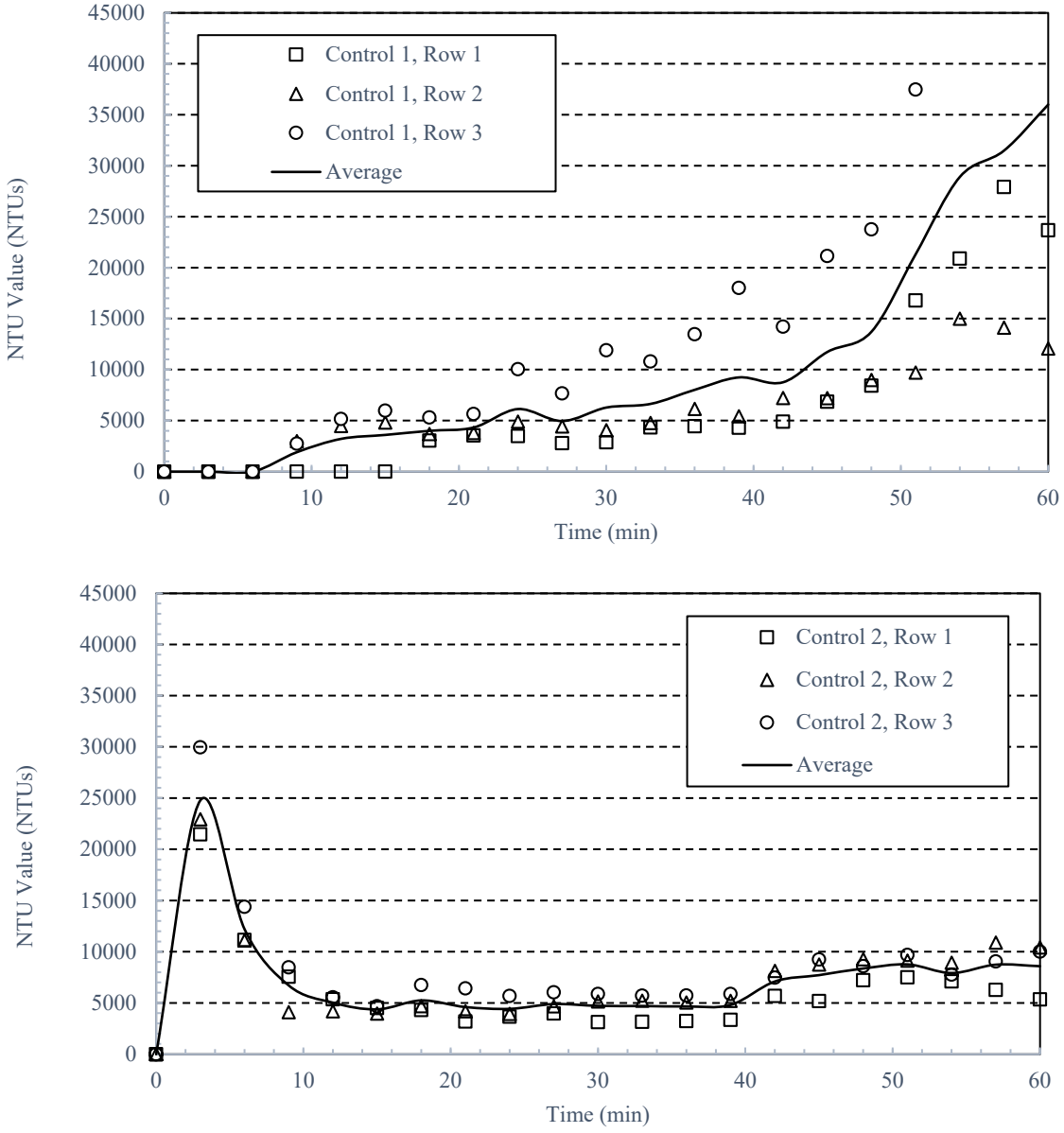

Figure 23: Water Quality for Loess Control 1 (Top) and Control 2 (Bottom)

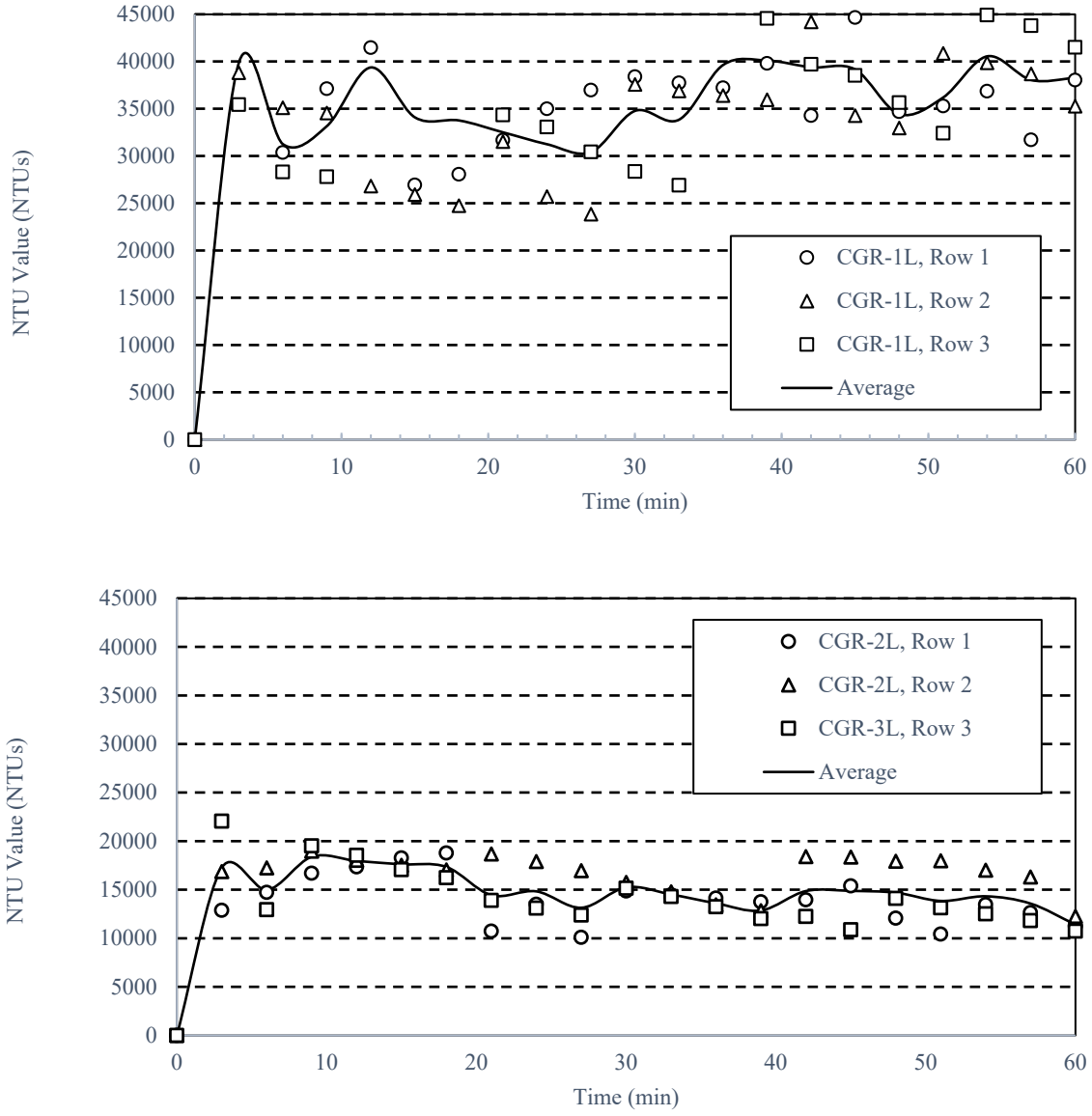

Figure 24: Water Quality for CGR-Amended Loess, CGR-1L (Top) and CGR-2L (Bottom)

For the TSS testing, each bucket of sediment laden runoff water was allowed to settle for a minimum of 24-hours prior to decanting and testing for total solids. For each bucket, the supernatant was vacuumed-off using a 1/4 horsepower pump and an innovative 3D printed "J-shaped" straw designed by graduate student Jaime Schussler at Auburn University. This unique straw allowed the supernatant to be decanted more easily without disturbing the settled fine-sized particles from the rainwater runoff. From the vacuumed supernatant, a 50ml sample was

collected for each bucket tested, oven dried at 110-degrees Celsius, and weighed for sediment particulates. The remaining solids were vacated from each bucket using deionized water (as required) to effectively rinse and capture the fine particles from the sides of the buckets. These solids were then baked and weighed to determine the remaining solids within the original sediment-laden runoff water. An additional degree of granularity was created by separately collecting the rainfall runoff buckets by row and by storm event for each rainfall simulation. TSS were processed in the civil engineering environmental labs at both Iowa State University (ISU) and Michigan State University (MSU) on this project. At ISU Nanopure® water (deionized/DI water) having less than 18.2-megohm ionic purity was used for rinsing to capture the fine particulates from the buckets. At MSU lab-produced deionized/DI rinsing water was used. NTU readings were not taken of the MSU DI water.

Similarities were found between the TSS and turbidity trends in the rainfall simulations for Control-2, CGR-1L, and CGR-2L. For example, Control-2 showed the least amount of soil loss and lowest turbidity values, while CGR-2L fell in the middle and CGR-1L had the highest soil loss and turbidity readings. Control-2 showed a consistent (average) soil loss of 24600-PPM for the first 40-minutes before increasing 60% to an average final peak value of 39500-PPM at the end of the simulation. CGR-2L mirrored the trend for Control-2 except with higher values, averaging 79300-PPM thru the 40-minute mark and then increasing 24% to an average peak value of 98500-PPM at the end of the simulation. In contrast CGR-1L exhibited much more significant soil loss averaging 99600-PPM at 20-minutes and increasing 80% to 179400-PPM at 40-minutes. CGR-1L started to level-off as it approached the end of the simulation (60-minute mark) with a more gradual 10% increase in soil loss through the end of the simulation with an ending peak value of 197500-PPM.

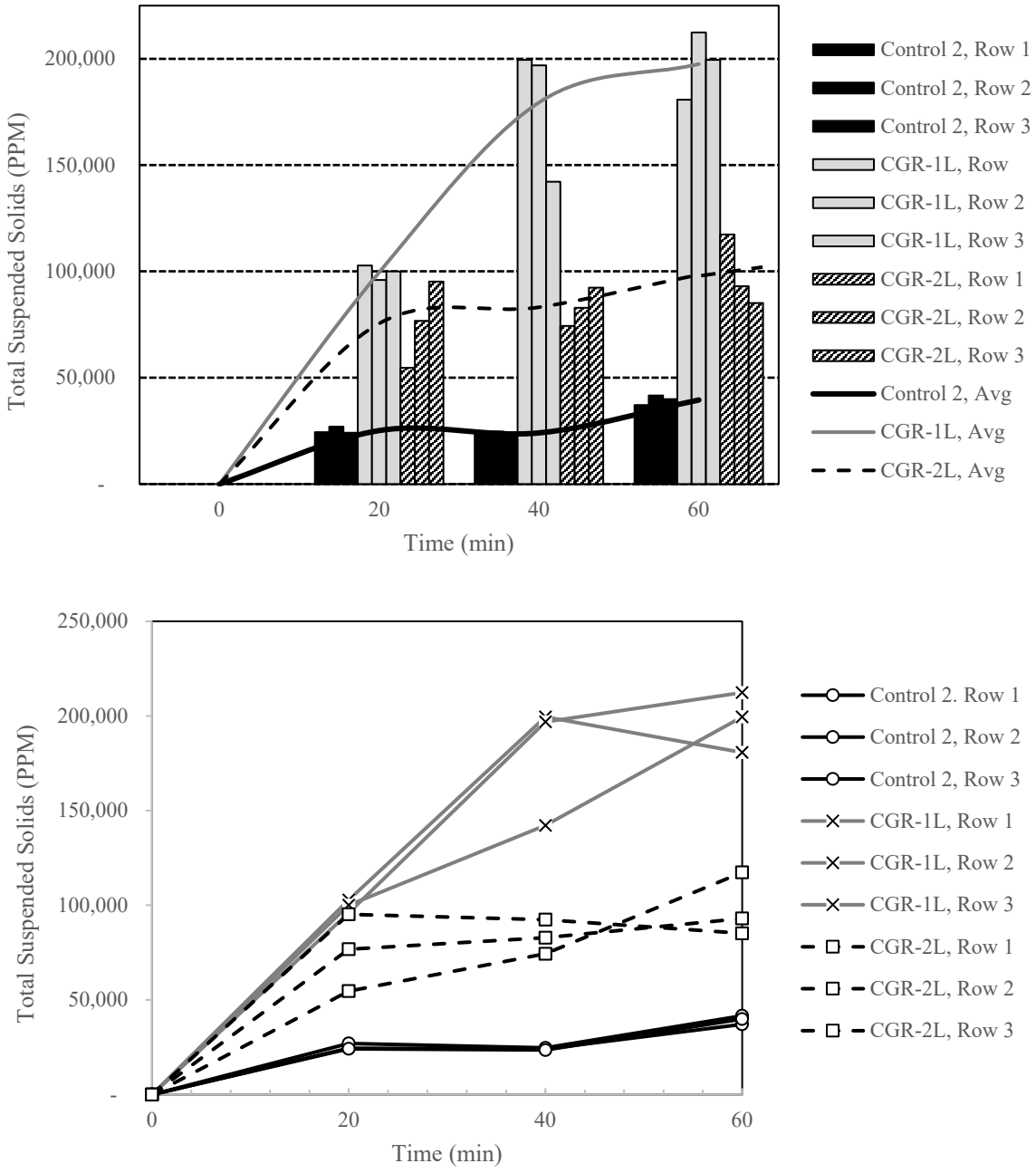

Figure 25: Total Suspended Solids (TSS) Soil Loss Data from Rainfall Simulations

FIGURE 25 shows two plots of the same TSS data. The top graph is a traditional bar graph with trendlines showing the increases in erosion rates with each storm intensity, while the bottom graph shows a spatial graph with pivot points at the transition points between storm events. Both graphs show the magnitude of the significantly higher soil loss for CGR-1L, compared to the

untreated loess and CGR-2L. The reason for the contrasting results between CGR-1 and CGR-2 amended loess is hypothesized to be the result of a greater hydration reaction between the CGR-2 and the loess, however this has not been confirmed through additional testing of the compounds present in both CGRs.

FIGURE 26 shows turbidity results plotted against TSS results for each rainfall simulation. This composite graph clearly shows elevated turbidity levels and increased TSS erosivity trends for CGR-amended soils compared to untreated loess from the rainfall simulations performed. This also indicates that water quality (grab) samples taken over a rainfall event can be a good predictor of TSS (or total soil loss) resulting from the same rainfall event(s).

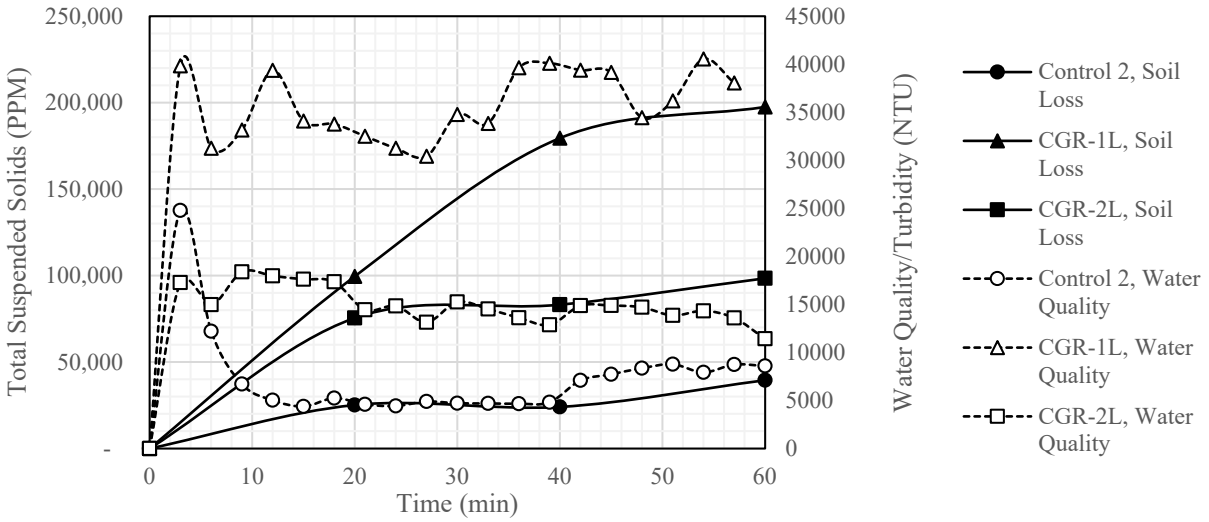

Figure 26: Soil Loss and Water Quality Over Time

For each rainfall simulation, TSS samples were collected and analyzed by row and by rainfall intensity (storm event). In TABLE 10, results were converted to tons/acre of soil loss during each simulation.

Control-1 (loess at 11.5% MC) was also included to show soil losses with the same loess material, but with dryer untreated loess exposed to the same rainfall conditions. With its dryer initial condition, Control-1 (as expected) exhibited a much lower soil loss an average of 0.05-

tons/acre (or 7% of the 0.71-tons/acre soil loss produced by Control-2) during the first 20-minute 2 in./hr. storm. This rapidly changed as Control-1 soil loss jumped to an average of 3.95-tons/acre and 9.97-tons/acre during the next two rainfall intensities, or 250% and 216% of the soil losses by Control-2 at 1.58-tons/acre and 4.62-tons/acre during these final two storms, respectively.

Table 10: Total Suspended Solids (TSS) Collected (Total Soil Loss) in Tons/Acre

Row	Rain Intensity	Control-1	Control-2	CGR-1L	CGR-2L
1	2 in./hr.	0.00	0.66	6.82	1.38
	4 in./hr.	9.82	1.54	14.54	5.60
	6 in./hr.	7.72	4.85	24.27	14.28
2	2 in./hr.	0.08	0.90	5.01	2.30
	4 in./hr.	0.68	1.84	13.04	6.37
	6 in./hr.	3.54	5.04	22.92	10.84
3	2 in./hr.	0.08	0.58	4.41	3.92
	4 in./hr.	1.34	1.35	10.57	9.31
	6 in./hr.	18.65	3.96	19.13	12.33
Avg	2 in./hr.	0.05	0.71	5.41	2.54
	4 in./hr.	3.95	1.58	12.72	7.09
	6 in./hr.	9.97	4.62	22.11	12.48

Soil loss data above are the TSS collected, dried, and weighed for each 20-minute storm event during the 60-minute simulation.

In comparison, CGR-1L and CGR-2L generated significantly more soil loss during each of their rainfall simulations. CGR-2L lost an average of 2.54 T/ac. increasing almost fivefold to 12.48 T/ac. of soil, while CGR-1L approximately doubled the soil loss of CGR-2L with average soil losses starting at 5.41 tons/acre during the second 4 in./hr. storm before exploding to 22.11 T/ac. of soil loss during the last 6 in./hr. rainfall intensity stage of the simulation.

The results in FIGURE 26 and in TABLE 10 show a high amount of soil loss for each soil tested, but the order of magnitude of the CGR-amended soils (CGR-1L and CGR-2L) were significantly higher than the untreated loess.

CHAPTER 3 WIND EROSION STUDY

3.1 Materials

The soils used in the wind erosion portion of this project include the Western Iowa loess also used in the rainfall erosion portion of this dissertation as well as Class A-1 shoulder aggregates from Eastern Iowa. The loess collected came from the "Loess Hills" and the shoulders aggregates came from county roads in both Washington County and Clinton County Iowa. In addition to soils collected, CGRs were collected from active concrete grinding projects located in Eastern, Western, Northern, Central, and Southern Iowa.

3.1.1 Shoulder Materials

For the wind erosion testing portion of this research, a total of five granular shoulder aggregates were collected from unpaved gravel shoulders from five county roads in two counties in Eastern Iowa. Three shoulder aggregates were collected from Washington County, IA (Sites A, B and C) and two from Clinton County, IA (Sites D and E). Site A was collected from County Road G37 (CR G37) while Sites B and C were collected a few miles apart on County Road G26 (CR G26), shown in FIGURE 27. Site D was collected from County Road Y46 (CR Y46) and Site E was collected from County Road Z24 (CR Z24).

Figure 27: Motor Grader and Soil Sampling from CR G37 Located in Washington Co, IA, Photos by Patrick Bollinger

All five sites where soil samples were collected, came from outside unpaved roadway shoulders along from 2 lane undivided PCC concrete county roads with speed limits ranging from 45 to 55 mph. Additionally, all five county road specimens came from aggregate shoulders ranging from 6 feet to 8 feet in widths located next to PCC paved concrete driving lanes. On the outside of each shoulder were vegetated (grass-covered) embankments which dropped-off from the edge of the roadway shoulders at 3:1 slopes, sloped away from the roadway. TABLE 11 lists all 5 roadway shoulder sites sampled.

Table 11: Roadway Shoulder Sites Sampled

Site	County	Town	County Road
Site A	Washington	Washington, IA	18th Street (Route G27)
Site B	Washington	Wellman, IA	190th Street (Route G26)
Site C	Washington	Washington, IA	190th Street (Route G26)
Site D	Clinton	Delmar, IA	185th Street (Route Y46)
Site E	Clinton	DeWitt, IA	330th Avenue (Route Z24)

3.1.2 Shoulder Material Collection

Initially the proposed collection method was to manually shovel the shoulder soil after first loosening the compacted soil with drills and heavy-duty soil auger bits. However due to the winter weather and freezing temperatures, an alternate method of using motorized equipment to scarify the shoulder aggregates was needed. A motor grader was chosen as the most efficient way to blade (loosen) the compacted, frozen shoulder aggregate. At each of the 5 sites, both Washington and Clinton Counties provided a motor grader and motor grader operator to loosen the compacted shoulder soil. This was performed as gingerly as possibly in an effort to minimize crushing or pulverizing the existing aggregate, which was done to reduce any change to the soil particle sizes and gradation of the existing soils. For each sample, the full depth of the compacted shoulder aggregate was loosened, until the underlying subgrade soils were visible. Although the

aggregate depth was anticipated to be 4 inches in depth, the actual depth of the compacted gravel aggregate (above the subgrade) varied from approximately 6 inches to 10 inches in depth. Both Washington County and Clinton County also provided small roadway crews and backfill aggregate to fill the holes created in the shoulders where the soil samples were taken. At each of the five sites visited, (10) 5-gallon buckets were collected ranging in weight from approximately 18 kg (40 lb.) to 25 kg (55 lb.) of soil per bucket. A Caterpillar CAT 140M2 (Washington County) and a Caterpillar CAT 140M3 (Clinton County) all-wheel drive (AWD) motor graders with 12 foot blades were used in each county for loosening the soil. Samples were collected in 2 days from all 5 county roads in December 2019. Collection from Site E is shown in FIGURE 28.

Figure 28: Motor Grader and Soil Sampling from CR Z24 Located in Clinton County, IA, Photos by Patrick Bollinger

3.2 Methods/Testing

The methods and testing for the wind erosion portion of this dissertation involved the collection and preparation of additional shoulder aggregates as well as additional preparation and testing of the loess and CGRs used in the initial rainfall erosion study. Tests for the initial gradation and compaction were required for these additional soils as well as compaction tested of the additional CGR-amended roadway shoulder mixtures.

3.2.1 Specimen Preparation (Homogeneous Mixing) and Moisture Content

To help ensure uniform testing of the shoulder aggregate soils collected from each site, the soils from each site were blended into 5 separate homogeneous batches. This was accomplished by first combining the (10) 5-gallon buckets collected for a given site into a large 150-gallon mixing trough. The entire aggregate sample was then gently mixed for 2-minutes using a Brutus 21665Q 120V 2-speed hand-mixer with 3-flight steel mortar paddle and then gently turned-over (mixed) with spade shovels repeatedly for 5-minutes to thoroughly rotate the soil into a homogeneous soil. The homogeneous soil was then returned to the 10 original buckets for future lab testing and analysis. No water was added or removed during this mixing process. Due to the snow and ice present on the ground when the samples were collected, each of the 5 soils collected were moist during mixing and had sufficient moisture to prevent the loss of fines from airborne dust during mixing.

The in situ moisture content (MC) tested for each of the 5 soils collected ranged from 7.9% to 9.2% for the Washington County soils (Sites A, B, and C) and from 9.7% to 11.8% for the Clinton County soils (Sites D and E). The Clinton County soils had higher initial moisture contents due to a light snowfall the night before the samples were collected. Two buckets from each shoulder sample were oven-dried prior to performing a sieve analysis on each specimen. The oven drying temperature used was 110-degrees Celsius and the drying time varied from 24 hours for Washington County aggregate soils to 48 hours for the slightly more saturated Clinton County soils. After drying, a rubber mallet was gently used to break up clumps of dry soil so that no initial clump was larger than 1-1/2” diameter, larger than a visual observation of the maximum aggregate size for each soil specimen. One bucket of each CGR slurry (CGR 1 thru CGR 5) was also oven-dried for testing. Since over time each sealed bucket of stored CGR had

separated into layers of sand and silt-sized particles with water also separating and rising to the top of the specimen, the CGR required remixing to return it to a viscous liquid (pourable slurry) state prior to any testing. Drying time for each CGRs required 72 hours at 60-degrees Celsius. Lower baking temperatures were used for each CGR to help minimize any change to the chemical composition of the CGR. The Standard Test Methods for Laboratory Determination of Water (Moisture) Content of Soil and Rock by Mass (ASTM D2216-19) was followed for oven drying procedures and moisture content testing.

3.2.2 Sieve Analysis and Soil Classification

On each of the (5) roadway shoulder aggregates (Sites A thru E) a sieve analysis was performed using Standard Test Method for Sieve Analysis of Fine and Coarse Aggregates (ASTM C136/C136M-14). The purpose of this test was to determine the initial gradation (particle size distribution) of each shoulder material as well as the USCS and AASHTO soil classifications. With this information, a compaction standard could then be chosen for each shoulder aggregate material. After a trial sieve test using 1-1/2”, 1” and 3/4” sieve sizes, the nominal maximum aggregate (NMA) was determined as 3/4” for Sites A, B, and C, while the NMA for Sites D and E was 1”. Based on these values, the minimum sieve analysis sample of 5 kg (11lb.) was required for Sites A, B, and C, while 10 kg (22 lb.) was the required minimum sieve sample for Sites D and E. With smaller sample sizes required for sieving Sites A through C, Site A was selected for initial sieving trials to test the accuracy of the sieve shakers and sieve equipment available at MSU.

Two different Gilson sieve shakers were available in the civil engineering labs at Michigan State University, one with 8” diameter round sieves (hereafter Gilson 8”D) and one with 14”x14” square sieves (hereafter Gilson 14x14). After homogeneous mixing and oven-drying, the weight

of the oven dried soil in each bucket of Site A shoulder aggregate dried weighed slightly more over 20 kg. With only 5 kg (or approximately one fourth of the homogeneous oven dried sample) required for the sieve analysis of the Site A soil, and in an effort to conserve soil, a Gilson soil splitter was then used in an attempt to uniformly divide (split or quarter) one bucket of Site A shoulder material. After splitting the material in accordance with ASTM C702, 2 sieve tests were performed using the Gilson 8”D on half the split soil sample, while the Gilson 14x14 shaker was used on the other half of the split sample. Additionally, a second full 5-gallon bucket of Site A soil was sieved in a single batch using the larger Gilson 14x14 shaker to compare with the results of the smaller samples split and sieved. Results found that the smaller Gilson 8”D shaker produced slightly more accurate results (measured in terms of loss of fines) but was limited to smaller batch sizes per sieve test. In one case, two sieve tests were needed to sieve a single 5 kg sample in accordance with ASTM C136. In contrast, the larger Gilson 14x14 shaker processed larger batch sizes per sieve test, but the loss of fines (for particles passing #4 sieves) was greater with the Gilson 14x14 shaker.

The Gilson 14x14 was limited to 5 sieves sizes plus 1 solid pan for each sieve sequence. This meant that although larger samples could be sieved with the Gilson 14x14, a transfer of fines passing #4 (4.76 mm) sieve into a separate container was required before running a sample through a second sequence of finer sieves to process the soil samples down to a #200 (0.074 mm) sieve. Since the loss of fines (specifically soil particles smaller than a #4 sieve) influences the soil particle distribution and possibly affect the USCS and AASHTO soil classifications, care was taken during the transfer of soil to minimize the loss of fines during this exchange. The loss of fines for the smaller 5 kg samples using the Gilson 8”D shaker ranged from 0.12% to 0.45%. With the larger 20 kg samples using the Gilson 14x14, the loss of fines had a range of 1.55% to

5.00%. The sieve sizes used for both the Gilson 8”D and the Gilson 14x14 included 1", 3/4", 1/2", 3/8", #4, #8, #16, #50, #100, #200, and a pan. Additionally, a sieve analysis was performed on the same material after drying the same Site A material collected after running a Standard Proctor compaction tests on the same soil as well. These results were graphed in FIGURE 29. A difference between the gradation curves for the same Site A material was found for each of the like material tested. The primary difference in the curves was visible as expected for material below the #4 (4.75mm) sieve, at the transition between course and fine grain material. This is attributed to the loss of fines experienced during testing. Although the mechanical sieve shakers were responsible for dusting and the loss of fines during sieving, soil splitting is believed to have contributed an initial slightly uneven distribution of fines in the reduced (5 kg) soil samples compared to the full (20 kg) samples.

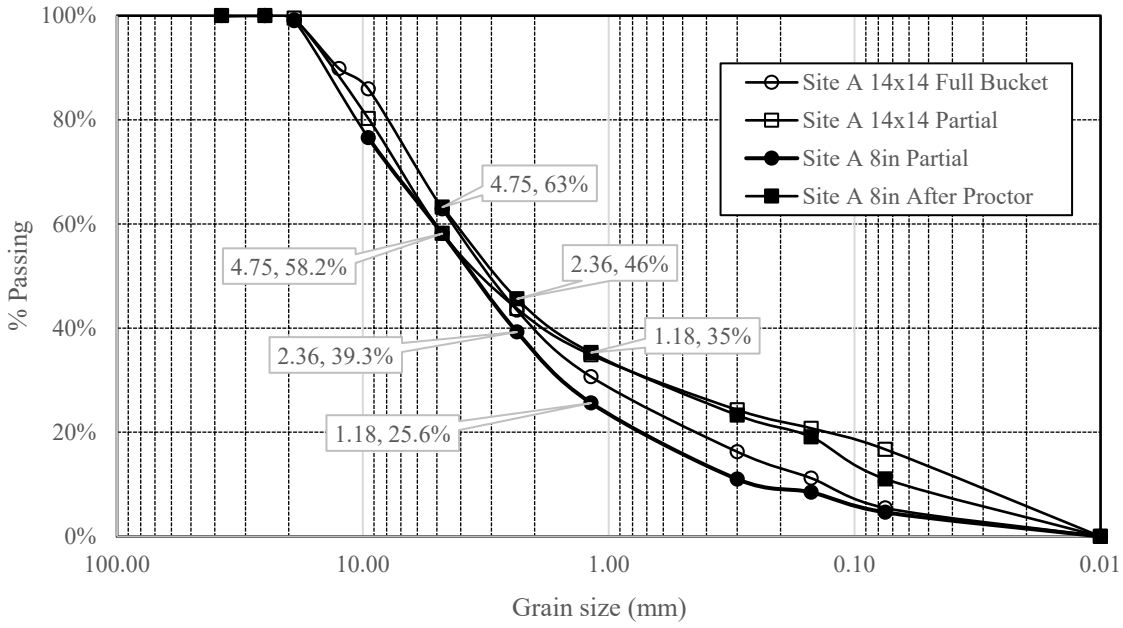

Figure 29: Sieve Analysis Equipment Test Trials with Site A Soil

The Standard Method of Test for Sieve Analysis of Fine and Coarse Aggregates (AASTHO T27) was used to validate the sieve tests performed on the shoulder aggregates. AASHTO T27 limits

soil loss (loss of fines) to less than 0.03% during sieving operations to validate a successful sieve test. Under AASHTO T27, only 1 of the 2 Gilson 8”D sieve tests passed this sieve test validation guideline. However, since the purpose of this sieve analysis for the wind erosion portion of this research was simply to provide a broad (general) soil classification of each shoulder aggregate, even with the slightly higher loss in fines, the Gilson 14x14 shaker was preferred to process larger batches and limit excess handling of the samples. Additionally, it was determined that the use of the Gilson 8”D and the Gilson 14x14 shakers did not significantly change the gradation curves nor did they change the overall AASTHO and USCS soil classifications for the initial Site A soil tested. As a result, the Gilson 14x14 shaker was selected for sieve analysis for the balance of soils for Sites B thru Site E. Adjustments were made to the Gilson 14x14 after the first series of Site A sieve tests, and the loss of fines was reduced to a range of 0.92% to 2.12% for Sites B and C and a range of 0.95% to 1.04% for Sites D and E.

Iowa DOT has a range for acceptable Class A-1 roadway aggregates. Upper and lower limits of this gradation range is based on standard sieve sizes listed for "Granular Surface & Shoulder" material in the Aggregate Gradation table (English units) located under Section 4109.02 of the current Iowa DOT Standard Specification for Highway and Bridge Construction [111,112]. These sieve sizes include 1-1/2", 1", 3/4", 1/2", 3/8", #4, #8, #30, #50, #100, #200, and a pan. This range for Iowa DOT acceptable granular material is shown in the shaded region on FIGURE 30.

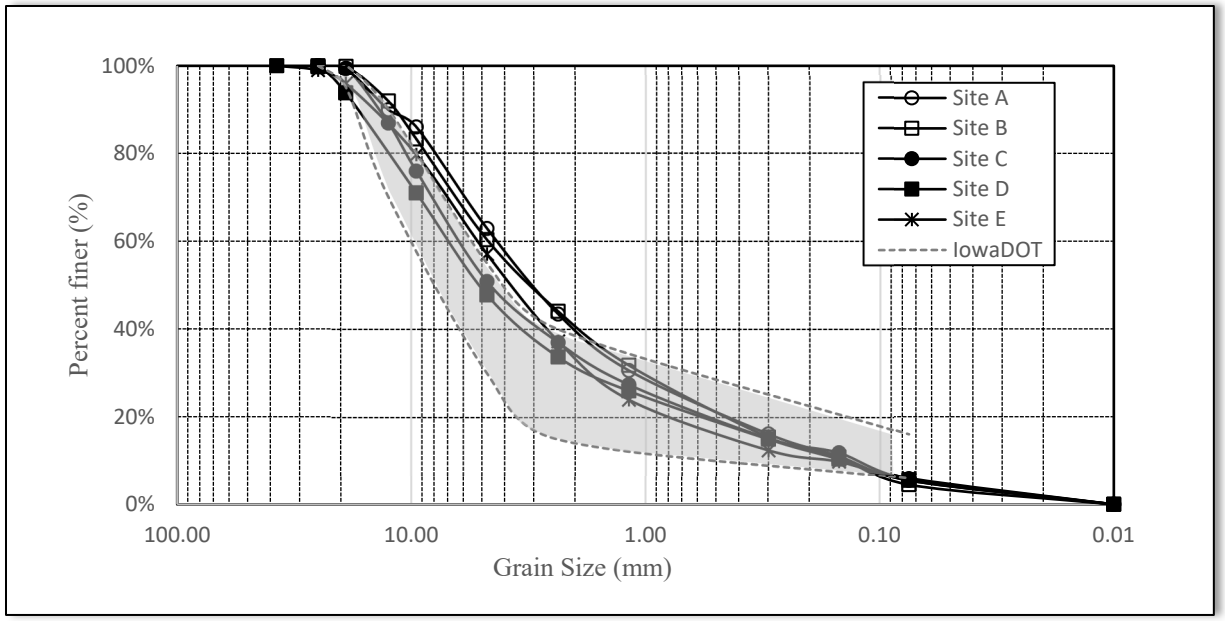

Figure 30: Sieve Analysis Comparison Between 5 Aggregate Shoulder Soils

The soil AASHTO soil classifications for all 5 county specimens were very similar Class A-1-a and Class A-1-b mixes, while the USCS soil classifications contained slight variations between the Washington County soils and the Clinton County soils as well. AASHTO Class A-1-a soils generally represent well-graded soils with gravel, coarse sand, and fine sand. In comparison, soils with A-1-b AASHTO classification contain more sand compared to A-1-a soils which contain more gravel. With respect to the USCS classification, slight differences in gravel to sand ratios for each soil, produced both well graded and poorly graded gravels or sands with silt shown in TABLE 12.

Table 12: Roadway Shoulder Site Soil Classifications

Site	Course Factor	AASHTO	USCS	USCS Full Soil Description
Site A	0.39	Class A-1-b	(SW-SM)g	Well-graded sand with silt and gravel
Site B	0.42	Class A-1-b	(SW-SM)g	Well-graded sand with silt and gravel
Site C	0.52	Class A-1-a	(GW-GM)g	Well-graded gravel with silt and sand
Site D	0.55	Class A-1-a	(GW-GM)g	Poorly graded gravel with silt and sand
Site E	0.46	Class A-1-b	(SP-SM)g	Poorly graded sand with silt and gravel

Previously, the collection of each of the 5 shoulder soils was discussed with the use of a motor grader to loosen the soil. It was hypothesized that the use of a motor grader to loosen the soil would not detrimentally change the gradation of the shoulder soils from their in situ state. To confirm this hypothesis, a sieve analysis was also performed on soils after performing Standard Proctor compaction tests on each soil. Post-Standard Proctor gradation tests revealed only minor changes to initial aggregate soil particle distribution and results did not change the initial AASHTO or USCS soil classifications for each soil. Each post-compaction gradation curve also fell within the Iowa DOT range for Class-A granular shoulder material. For each initial shoulder aggregate collected, soil gradations were very close and within the acceptable range for Iowa DOT Class-A shoulder material with upper and lower limits shown in the shaded region in FIGURE 30.

3.2.3 Soil Mixtures and CGR Dosages

Previously discussed, the choice of a 20% CGR dosage (to 80% soil ratio by weight) was discussed and selected for the rainfall erosion study. To compliment this rainfall erosion testing of 20% CGR amended Western Iowa Loess, the same soil mixtures were included for wind erosion testing. These soil mixtures included a Loess control (with no CGR), 20% CGR-1/80% loess, and 20% CGR-2/80% loess. With respect to CGR-amended shoulder aggregates, soil mixtures with Site A and Site E mixed with 20% and 40% dosages of CGR 4 and CGR 5 were selected for wind erosion testing. Site A and Site E were selected as they represented one soil from Washington County and one soil from Clinton County. CGR 4 and CGR 5 were selected as both of these CGRs were produced and collected from “mainline” CGR projects. The unique difference between CGR 4 and CGR 5 is in their PCC roadway mix design aggregates. The concrete mix design for CGR 4 contained a limestone aggregate while the concrete mix design

for CGR 5 contained a rose quartzite aggregate. With limited data on the mix design for CGR 4, this study is only able to cite the difference in gravels used in these 2 mix designs. CGR 5 was also collected from a newly poured PCC roadway while CGR 4 was collected from a PCC roadway that had cured approximately 18-months from the time of the diamond grinding. Since the 5 CGRs collected at the beginning of the Phase 1 rainfall study had been stored for an extended period of time, each CGR bucket required remixing to get the separated CGRs solids back into a slurry state for mixing with various shoulder aggregates.

Figure 31: Consolidation of CGR Slurry After Storage for Extended Period of Time, Photos by Patrick Bollinger

FIGURE 31 shows the settled/consolidated state of a typical bucket of stored CGR. After breaking up the compacted cylinder of CGR with a garden hoe, a small amount of mixing water (kept from the original CGR discharge for each CGR) was added to the loosened solids to recreate the CGR slurries. However, after trial and error it was found that breaking-up and oven-drying the CGR solids was an easier solution. The CGRs solids once broken-up, were baked at 60-degrees Celsius to minimize any chemical changes to the slurries. Once dried, the CGRs were then gently crushed with rubber mallets to break up any remaining clumps and clods, The dry CGR was then ready to mix with the desired shoulder soils at the required 20% or 40% dosage,

which in turn were hand-mixed (with mixing water added in to match OMC) to produce the homogenous CGR-amended soils ready for compaction and testing.

3.2.4 Standard Proctor (ASTM D698)

All soil specimens were compacted with standard compaction energy. The Standard Test Method for Laboratory Compaction Characteristics of Soil Using Standard Effort (ASTM D698-12e2) was used for compaction. Using this standard, the optimum moisture content (OMC) and max dry unit density (MDD) of both the control (untreated) soil specimen and the CGR-amended soil mixtures were found. Based on the results from sieve analysis and gradation, Method A was chosen for Site A thru Site E shoulder aggregates. This was based on less than 25% (by mass) of material having been retained on a #4 sieve (4.755 mm) sieve for each soil. The OMCs for the Washington County soils (Sites A, B, and C) was 9.4%, 9.6%, and 8.5% respectively, while the OMCs for the Clinton County soils (Site D and E) were approximately 2% lower at 7.3% and 7.6% respectively. However, having similar compositions of limestone-based gravel, sand, and silt, the MDDs were similar, ranging from 130.5 psf to 135.1 psf for each of the 5 soils tested from both counties. The MDD for Site A soil (132.2 psf) and Site E soil (132.3 psf) were the most comparable soils from each county. These similar MDDS was another reason for the selection of Site A and Site E soils for wind erosion testing. Proctor curves for the 13 shoulder soils and CGR-amended soil mixtures are shown in FIGURE 32. Although the OMCs were 2% less for the Clinton County control (untreated soils) compared to the Washington County soils, after blending with CGR-4 and CGR-5 on both 20% and 40% CGR dosages, the trends in increasing OMCs were very similar for the CGR-amended soils for both counties, also shown in FIGURE 32.

Evaluating these curves further revealed a linear correlation with high degree of confidences with the addition of CGR to Site A and to Site E soils by comparing the OMC points for each Proctor curve with increasing dosages of CGR (0%, 20%, and 40%). This linear regression trendline was continuous with the transition from CGR-4 to CGR-5 amendments, with consistently higher moisture contents and lower MDDs with CGR-5 amended soils compared to CGR-4 amended soils). FIGURE 33 shows these trends with Site A soils on the left-hand graph and Site E soils in the right-hand graph below.

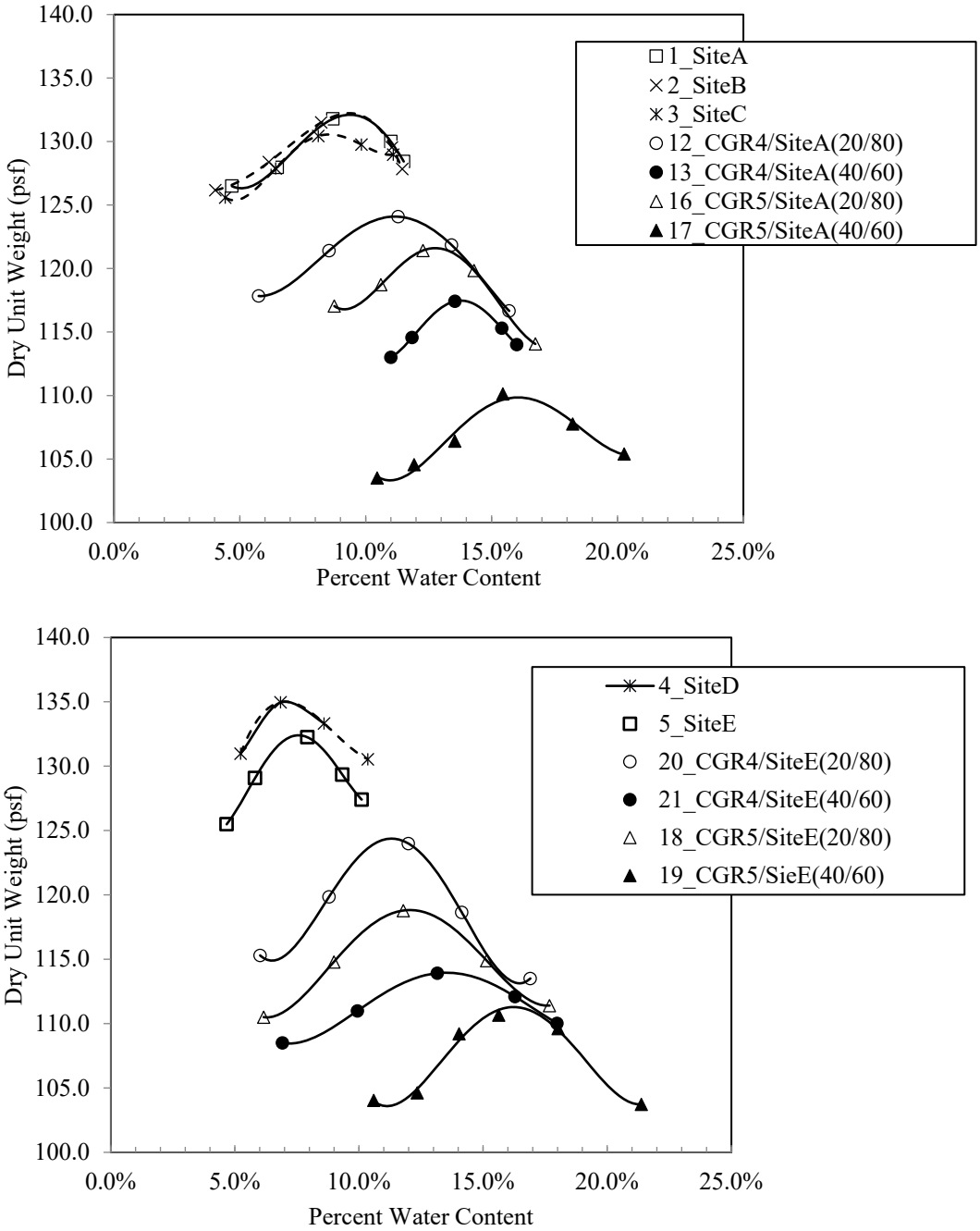

Figure 32: Std. Proctor (By County), Washington Co (Top), Clinton Co (Bottom)

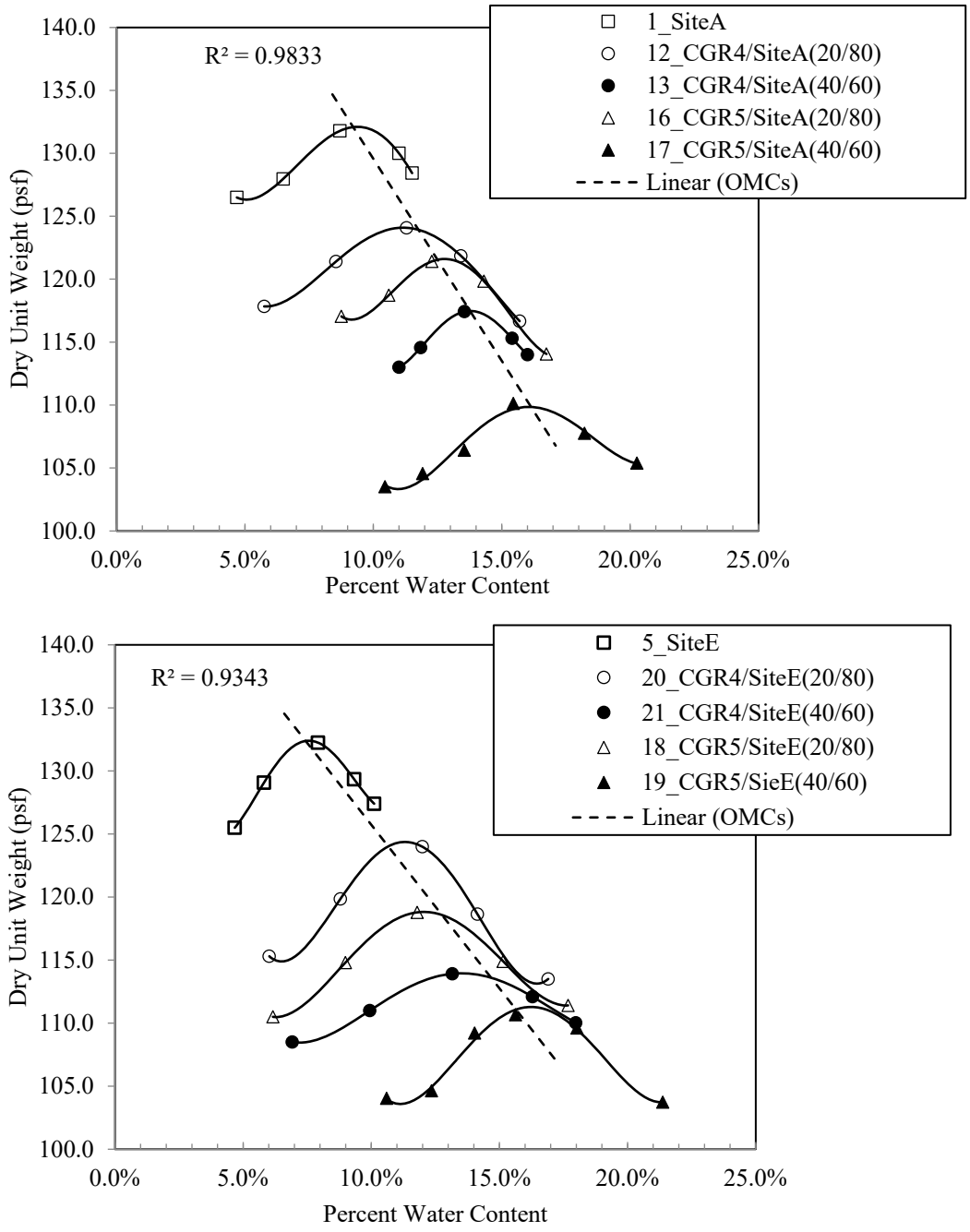

Figure 33: Std. Proctor Trends (By County), Washington Co (Top), Clinton Co (Bottom)

3.3 Compaction

The Uniform Tamping Apparatus (UTA) designed and built for the rainfall portion of this research was adapted and reused for the wind erosion portion of this study. The decision to use

the UTA again was both to standardize and simplify the compaction of the wind erosion soil forms. Like the rainfall compacted soil forms, compaction trials were performed with 150 (gravity) drops x 4-drop locations (or 600-total drops) of the 13.05 lb.-ft. tamper built into the UTA (FIGURE 34). This tamper was raised and then dropped (not thrust down) for each tamp (or drop). The density of the soil was calculated based on the weight and volume of the rigid soil pans. Results from 2 initial compaction trials using Site C soil showed 95% compaction was achieved with 150 (gravity) drops. Therefore, the number of drops was reduced to 125 (gravity) drops x 4-drop locations (or 500-total drops), and two successive UTA test compaction trials were run. Results determined that 90% compaction (+/- 0.5%) was achieved at this tamping rate.

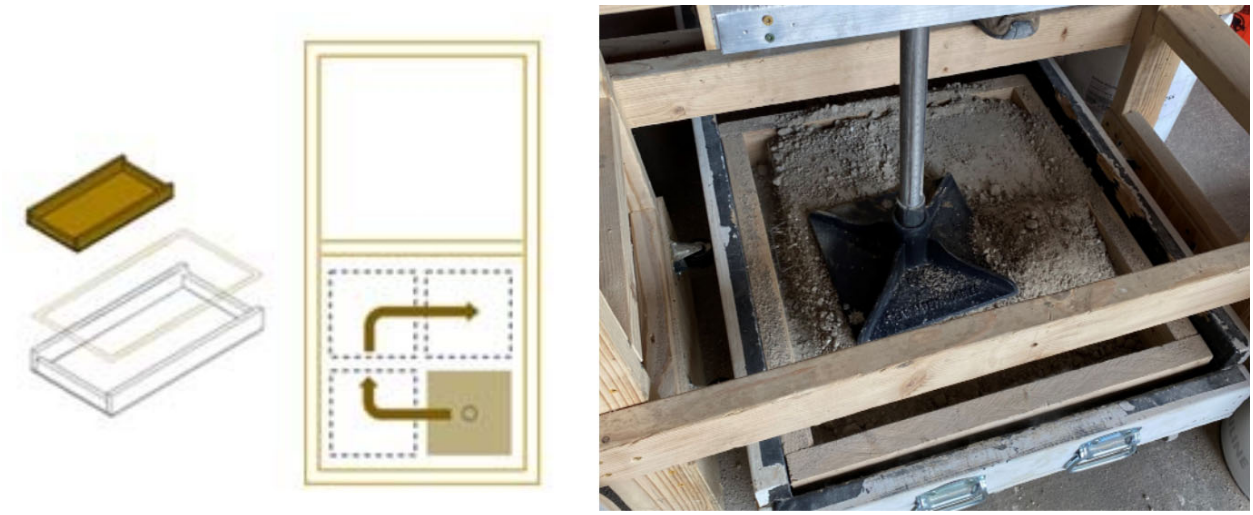

Figure 34: Tamping Pattern and Setup Using UTA for Smaller Wind Erosion Soil Forms, Photo and sketch by Patrick Bollinger

3.4 Wind Erosion Simulation

With respect to the wind erosion portion of this study, the design and construction of a device to wind test compacted soil specimens was required. No standards were found for this work. As a result, equipment, calibration methods, and processes were developed to accomplish this work.

3.4.1 Wind Erosion Test Apparatus (WETA)

The primary goal of the lab-based wind erosion test in this study was to simulate soil wind erosion caused by turbulent air flow (or wind whip) generated by large trucks passing an unpaved gravel roadway shoulder at a high rate of speed. Fugitive dust is a problem for all gravel roads and was one of the primary motivations for the wind erosion testing in this study. The overall design objective for these lab-based simulations was to determine if CGR-amended Class-A shoulder aggregates as well as CGR-amended Western Iowa Loess would be more resistant to wind erosion compared to untreated shoulder soils. The three primary types of wind erosion produced in this lab-based tests are surface creep, saltation, and suspension.

At the Civil Infrastructure Lab (CIL) at Michigan State University (MSU) a wind erosion study was developed and performed during the Summer semester 2020. For this study, a table-mounted wind erosion test apparatus (WETA) was designed and built. This apparatus included a wooden platform complete with a removeable, recessed soil form with the top surface of the soil form designed flush with the surface of the adjacent platform. This setup mimicked the appearance of a flat roadway shoulder adjacent to a hard-surfaced driving lane. For the soil being tested, an 18” x 18” x 3” deep metal soil form (2.25 sf surface area) was selected for multiple reasons. First, the rigidity of a metal soil form allowed compacted soil specimens to remain intact during the multiple soil form removal and weighing sequences required during each erosion test trial. The 3” soil form depth was chosen as it allowed for better compaction compared to more shallow soil forms. Finally, test trials using baking flour and fine grained silica sand both produced the most desirable wind disturbances over an area surface area of less than 24” x 24” with the available blower (wind source). A photo of the removable recessed pan (left) and photo of the final WETA layout (right) are included in FIGURE 35.

Figure 35: Wind Erosion Test Apparatus (WETA) During Fabrication and Final Construction, Photos by Patrick Bollinger

The wind source used for these lab-based wind erosion tests was a Facso SuperCat Model 1200XL 120V 2-speed portable blower with a single inlet, forward-curved, motorized impeller that produced a maximum 35-mph wind (1120 CFM) across the targeted area. This maximum wind speed was best achieved by keeping the 18”x 18” soil form within 42” from the outlet of the blower. Using the blower alone (with no obstacles introduced into the air flow) produced a ‘generally’ uniform air flow. However, for the wind erosion testing in this study, a turbulent air flow was required. Moreover, a multi-directional, repeatable, swirling (or whipping) wind event was essential.

In evaluating the type of obstacle to place in front of the blower, experiments first with simple rectangular obstacles like those used as bluff objects by Dr. Murakami with the University of Tokyo was tried [113]. This produced a rolling flow field over the bluff object, but it reduced the airflow too much to produce noticeable erosion. Next the idea of using obstacles with rounded-fronts used by Dr. Hargitai of Eötvös Loránd University was tried. This produced a desirable dual vertical vortex wind flow, but the inward motion of the vortexes deposited eroded soil behind the rounded obstacle similar to the Lee sand dunes described in Dr. Hargitai’s research

[114]. Finally, attention was turned to fluid mechanics models that produced vortexes. The von *Kármán* Vortex Street classic fluid mechanics model, which includes a swirling wind pattern produced a desirable series of repeating vortices, was considered next. This naturally occurring phenomenon occurs as a result of winds being diverted around a blunt, high-profile object [115,116]. Von *Kármán* Vortex Street vortices were captured with cloud formations rotating around the 6800 foot high island of Tristan da Cunha located in the South Atlantic Ocean by NASA and is shown on the left in FIGURE 36 [115]. After experimenting with 1, 2, and 3 bluff object Von *Kármán* configurations, a single cylindrical object was selected for this study to produce the desired, repeating, swirling von *Kármán* Vortex Street wind event over the targeted soil form surface area.

Still images of the flow lines from 2 fluid mechanics models of the von *Kármán* Vortex Street, one pulled from Biju Patnaik University of Technology in India, were scaled in AutoCAD to match the 12” horizontal face of the Fasco blower [117,118]. From here, the diameter and distance of the blunt object to insert into the windscreen was determined. The bluff object selected and placed into the blower windstream consisted of (2) 4 inch diameter concrete cylinders stacked on top of each other. These cylinders were placed with the vertical tangent line located 12” from the face of the blower and 12” from the front of the recessed soil form. The total distance to the leading edge of the recessed, soil form was 24” from front of the face of the blower shown on the right image in FIGURE 36.

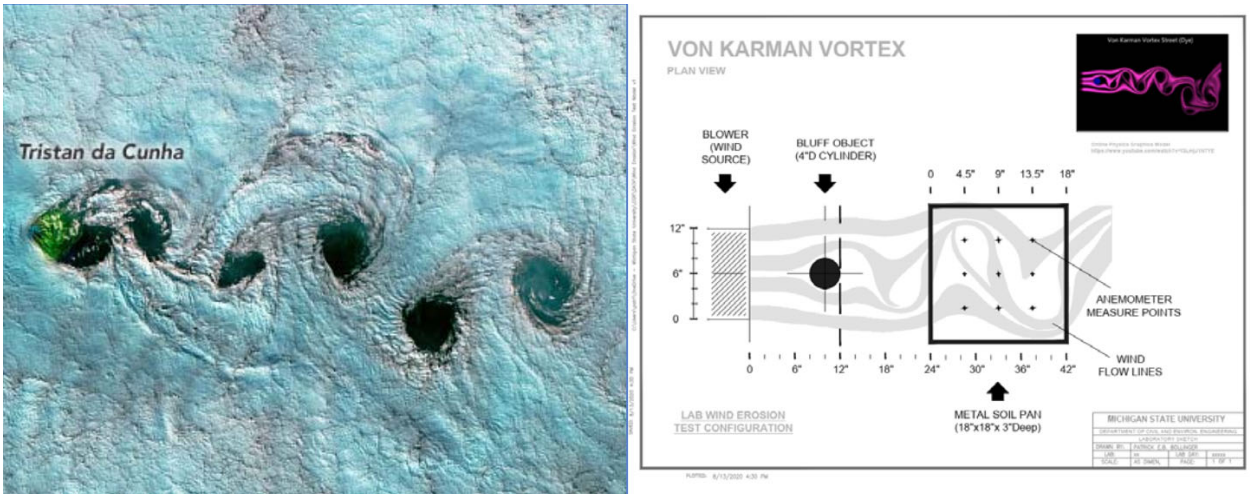

Figure 36: Von Karman Vortex Street [115] and CAD Scaled Version for WETA Layout by Patrick Bollinger

3.4.2 Smoke Test and Anemometer Test Results

Validation of the creation of the von *Kármán* Vortex Street wind event was roughly confirmed using a smoke test and anemometer readings over a 4.5” grid marked on the surface of a rigid cover placed over the recessed soil form. A light smoke was produced using aerosol cans of a photography fog/haze product called Atmosphere Aerosol and velocity readings were taken with a hand-held Davis Instruments Turbo Meter anemometer. Although basic and rudimentary, both of these tests confirmed that the classic von *Kármán* Vortex Street swirling wind patterns were produced with the WETA apparatus described above. Photos showing these tests are included in APENDIX A.

3.4.3 Wind Erosion Test Procedure

The test procedures for the wind erosion testing involved compaction of soil forms, covering, and curing of the compacted soil, and then testing of the cured soil forms. For compaction, the UTA was adapted for use of the smaller 18”x 18” meta soil forms. The area within the 2-ft x 8-ft soil formed was reduced using 2x lumber for these tests. This allowed the smaller 18” x 18” soil form to nest nicely inside the larger wooden rainfall soil forms for compaction.

Figure 37: Steps During Compaction of Soil Forms using UTA, Photos by Patrick Bollinger

Photos of a typical CGR-amended soil mixtures and setup of the modified-UTA compaction layout are shown in FIGURE 37. After tamping compaction using the UTA, a perforated piece of rigid angle iron was used to screed the top surface of the compacted soils forms flush with the top edge of the soil forms. This is shown in FIGURE 38.

Figure 38: Preparation and Screeding of Compacted Soil Form, Photos by Patrick Bollinger

The screeded soil forms were then gently tamped with a rubber mallet and wooden block to compact the loose soil disturbed from screeding. Each compacted soil form was weighed and covered with shrink wrap and placed in a cool section of the CIL lab and allowed to cure for 7-days. This part of the sample preparation process is shown in FIGURE 39. Soil loss due to

saltation from wind erosion was measured for each of the wind erosion tests performed. After compacting each soil form at OMC and allowing each sample to cure for 7-days, each compacted soil form was subjected to a 3-phase wind erosion test.

Figure 39: : Weighing and Curing of (Sealed) Compaction Soil Forms, Photos by Patrick Bollinger

The wind erosion test procedure using the WETA consisted of a 30-minute wind event (Phase 1), followed by 1 hour of air drying in the sun (Phase 2), and concluded with a 30-minute final wind test (Phase 3). The soil from each soil forms was sampled immediately after conclusion of the Phase 3 wind test.

Figure 40: Views of WETA and Compacted Soil Form During Wind Erosion Test, Photos by Patrick Bollinger

Because the air-drying during Phase 2 resulted primarily in moisture loss (not saltation and loss of solids), the loss in weight of the soil form during Phase 2 was recorded but was omitted from soil erosion (soil loss) totals. FIGURE 40 shows 2 photos taken during a typical wind erosion test.

The weight of the soil pan was taken and recorded before and after each of the 3 testing phases. Weight was measured in kg for each compacted soil form (kg/sf) and then converted to tons/roadway mile (tons/mile). One roadway mile with (2) 6 ft wide unpaved gravels roads figured for the conversion to a standard roadway unit of measure. Although it was not possible with the wind erosion setup to physically capture the loss fines, a photo of the type of soil eroded is shown in FIGURE 41.

Figure 41: Soil Loss Due to Wind Erosion from Compacted Soil Form, Photos by Patrick Bollinger

The formula used in the soil loss conversion are shown in FIGURE 42. These calculations include the minor weight loss due to moisture as well as soil loss due to erosion (saltation) off the top surface of the compacted soil forms.

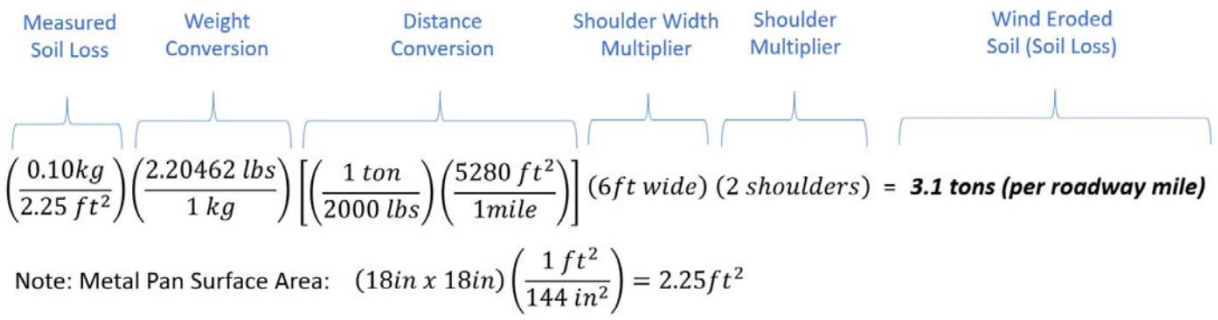

Figure 42: Annotated Conversion Formulas for Wind Eroded Soil (Soil Loss)

After completion of the wind erosion trial, soil from each wind eroded compacted soil form was sampled for moisture content. Soil samples were taken from the top surface of the soil form as well as the interior of the compacted soil with 1 sample taken from each quadrant of the soil form. The purpose for this sampling was to measures any changes in the moisture content as a result of the wind erosion testing. Results showed that an average moisture loss from the top surface of the tested soil forms for the Site A and Site E trials of 4.8% (with a maximum of 6.5% lost and a minimum of 2.4% lost). With respect to samples taken from the middle of the tested soil forms for these same trials, an average of -0.5% change in moisture content from the compacted soil (with a maximum of 1.3% lost and a minimum of -1.8% change from the initial targeted OMC compacted moisture content).

3.5 Results

For this study, 20 wind erosion trials were performed, with 16 base trials consisting of (3) primary soil sets (Washington County soils, Clinton County soils, and Western Iowa loess soils). The final 4 trials consisted of 1 confirmation retesting of the Site A Control soil, 1 test of an uncompacted (loose) Site B Control soil, and 2 trials with oven dried Site C control soils (1 oven dried for 24-hours and 1 oven dried for 48-hours after compaction). All of the trials, with the exception of the Site B uncompacted (loose) test trial, were compacted at OMC. The 10 CGR-amended soil trials were covered and cured for 7-days after compaction, prior to testing.

The results for all 20 wind erosion trials are included in the graph in FIGURE 43. The soil loss for Phase 1 (bottom section of each bar) and the soil loss for Phase 2 (top section of each bar) were recorded for each trial. The results from Phase 1 and Phase 2 each produced approximately 50% of the total soil loss in each trial with the exception of the Site B Control, which exhibited greater erosion during Phase 2 after drying for an hour in the sun. For all of the soil blends tested, the (untreated) Site A Control soil resulted in the highest erosion rate at 8.07 tons/roadway mile.

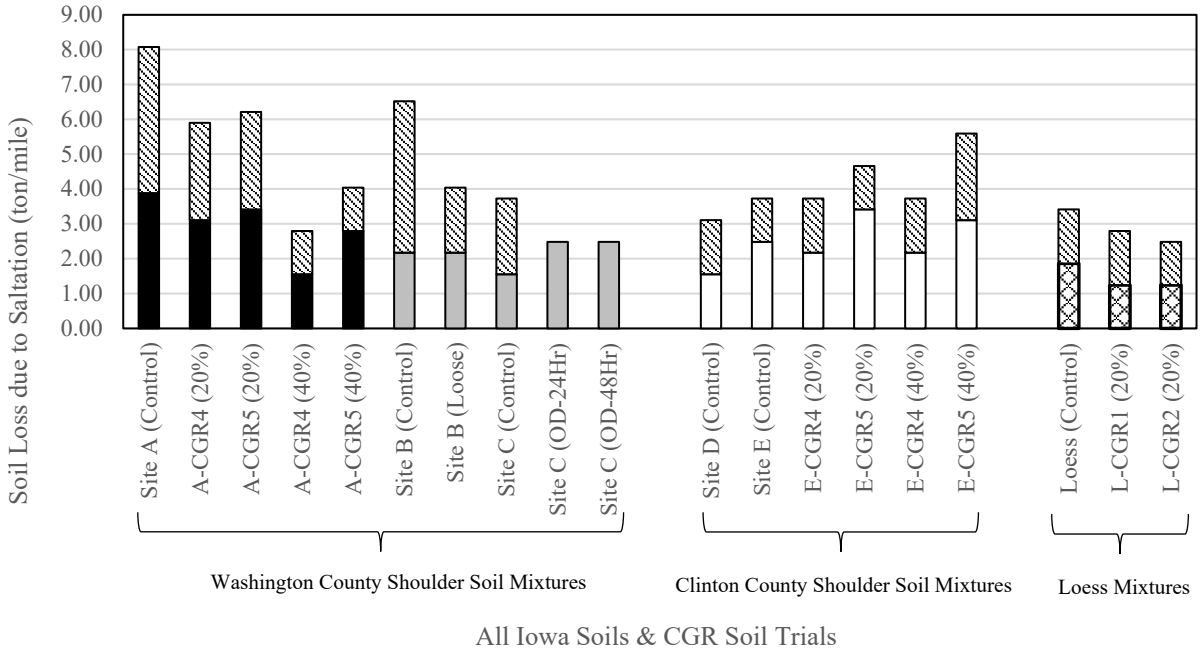

Figure 43: Wind Erosion Soil Loss for All Trials

Trials for the 3 primary soil sets tested were separated and graphed separately and are shown in a side-by-side comparison in FIGURE 44. With respect to the Washington County Soils (left graph, Site A soils), the 4 CGR-amended soils resulted in reduced erosion when blended with the Site A control soil. On average wind erosion decreased 2.17 tons/mile (-25%) and 5.28 tons/mile (-58%) with 20% and 40% CGR dosages, respectively, compared to the untreated control.

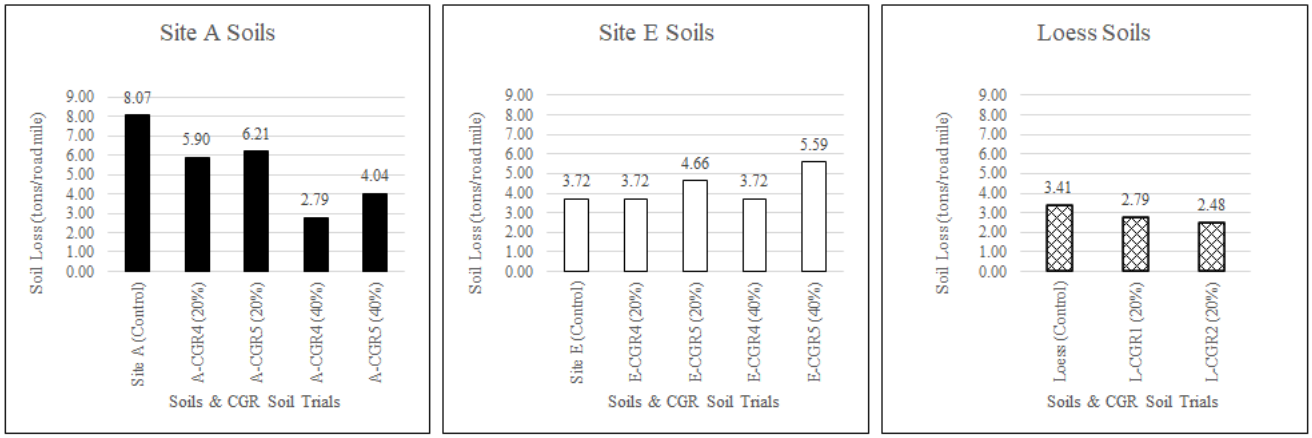

Figure 44: Wind Erosion Soil Loss Results (by Soil Set)

Conversely, the Clinton County soils (center graph, Site E soils), the CGR-amended soils showed mixed results. For CGR-4 amended soils (at both 20% and 40% dosages) soil loss was negligible. For CGR-5 amended soils, Site E eroded 0.93 tons/mile (25%) more and 1.86 tons/mile (50%) more with 20% and 40% CGR dosages, respectively compared to the untreated control.

Lastly, for the Western Iowa Loess soil mixtures (right graph), like Site A soils, there was improvement for CGR-amended loess, compared to the untreated control. Results showed that when amended with 20% CGR dosages, wind erosion decreased 0.63 tons/mile (-18%) and 0.93 tons/mile (-27%) compared to the untreated control soil.

FIGURE 45 shows a comparison of Site A and Site E soils with the same 2 CGR amendments (CGR-4 and CGR-5) at 20% and 40% dosages. Results show that Site A soils improved (stabilized) with an increase in CGR dosage, while Site E worsened (eroded more) with increased erosion.

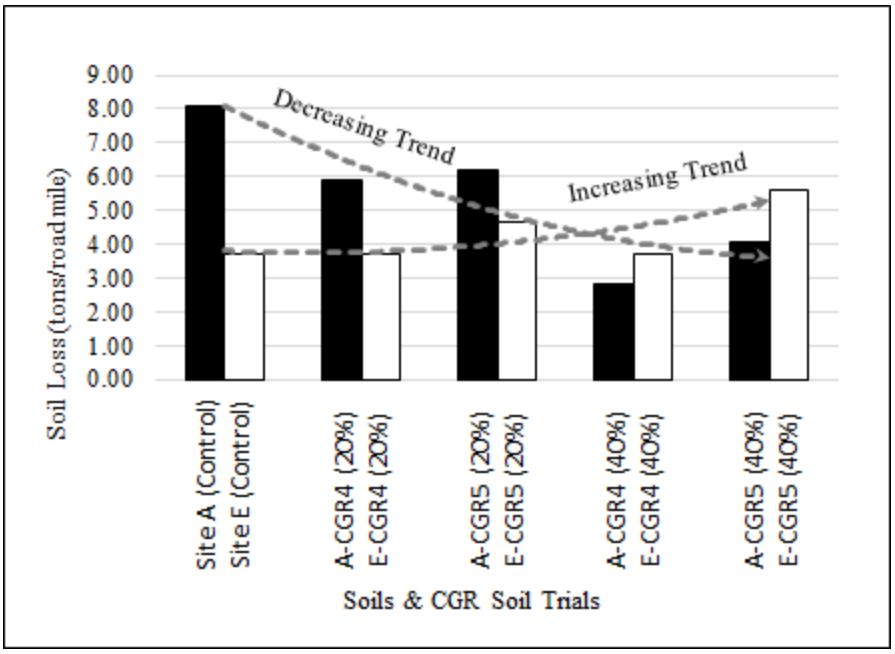

Figure 45: Wind Erosion Soil Loss Results, Site A and Site E Trends

The reason for the unusual results found with Site E soils, could be due to the greater amount of in situ soil collected for this compacted Class-A roadway base. When the Washington County soils (Sites A, B, and C) were collected, the ground was hard and frozen. As a result, the motor grader was only able to loosen the top aggregate, with very little of the underlying in situ soil (subgrade below the Class-A shoulder aggregate) collected. However, when the Clinton County soils were collected (Sites D and E), a wet snow had fallen the night before, resulting in softer, more saturated shoulder soils. As a result, the blade of the motor grader penetrated through the compacted aggregate for the Clinton County soils, slicing into the softer in situ soils beneath. This greater penetration of the blade led to the collection of more subgrade soils along with the 2 aggregate subbases compared to the first three Washington County shoulder soils collected. The trials with the control soils behave differently than expected. These control trials are shown in FIGURE 46. The Washington County soils all appeared to be from similar Class A-1 shoulder material, especially with Site B and Site C sampled from the sample roadway shoulder a mile

from each other. However, results showed significant degrees of soil erosion ranging from 3.72 to 8.07 tons/roadway mile. The Clinton County soils also appeared to be from similar Class A-1 shoulder material although sampled from differently county roads. These two sites (Site D and Site E) shared comparable wind erosion at 3.10 and 3.72 tons/roadway mile.

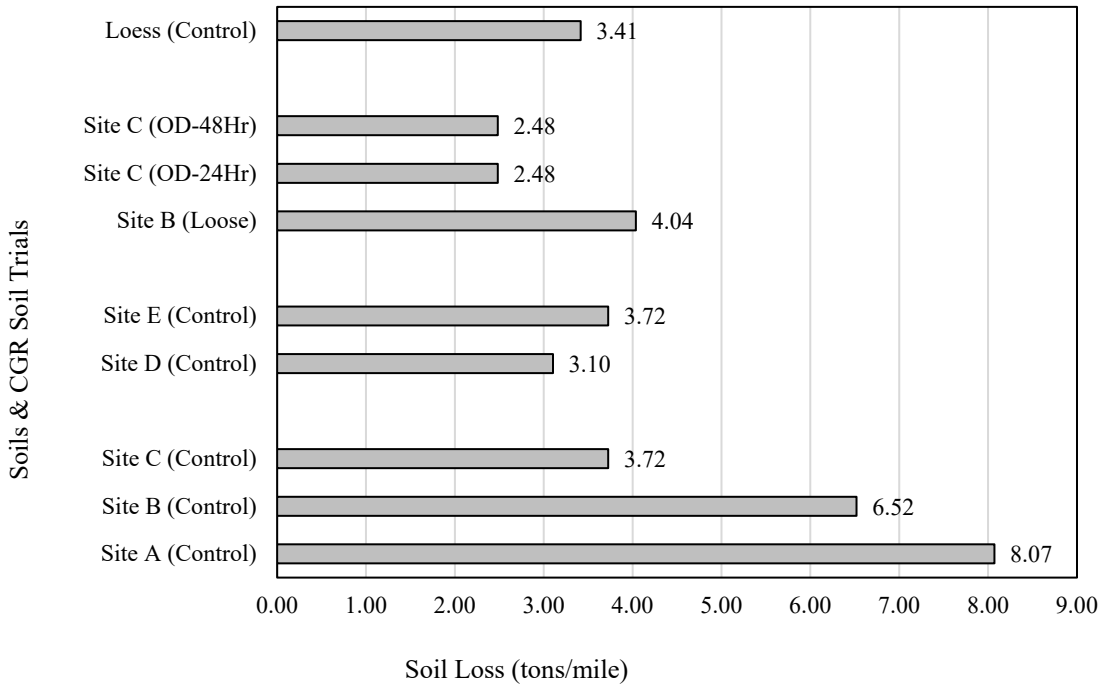

Figure 46: Wind Erosion Soil Loss Results Untreated Soils

With respect to the Site B control from Washington County, an unusual result was found between the 2 test performed on this soil. The loose specimen eroded 38% less than the control compacted at OMC. It is believed that this may have occurred because with compaction, the larger gravels and soil particles may shift down closer to the bottom of the soil form, leaving more fine particles at the top of the compacted soil form. If this was true, then more fines would be available to erode with the compacted sample compared to the loose, uncompacted Site B control soil.

Site C had 3 different wind erosion trials, with each control soil compacted at OMC. The main control was tested immediately after compaction, while the other 2 Site C controls were oven dried at 110 degrees Celsius for 24-hours and the other for 48-hours after the Phase 1 wind erosion test, prior to the Phase 2 wind erosion test. The reason for this oven drying was to simulate compacted roadway shoulders baking in the hot summer sun. Results showed that the oven dried soils did not experience any soil erosion during Phase 2. This resulted in 33% less wind erosion compared to the standards Site C control compacted and immediately tested. This variation on the resting/drying time between the Phase 1 and Phase 2 wind erosion tests was an early version of the wind erosion test procedure. Since oven drying eliminated the wind erosion during the second Phase 2 wind erosion test, a 1 hour rest cycle was used instead, since oven drying seemed to provide stabilization to the Site C control soils tested.

CHAPTER 4 DISCUSSION

4.1 Rain Erosion Discussion

The water quality of the grab samples degraded much more over time for CGR-amended soils, consistently ranging from 1.8 to 4.7 times greater (worse) than the untreated loess throughout these simulations. This is evidenced by studying the average turbidity values for CGR-2L (11,400 NTUs) and CGR-1L (38,400 NTUs), which outpaced average values measured for the untreated loess Control-2 (8,200 NTUs) even with the final average turbidity reading (8,600 NTUs) for the loess at the end of the simulation. Overall, compared to Control-2, TSS soil loss during each simulation ranged from 2.2 times worse with Control-1 to 2.7 and 4.8 times worse with CGR-2L and CGR-1L, respectively. These results showed that although soil erosion was greater for loess compacted on the dry side of optimum compared to loess compacted at OMC, CGR-amended loess faired much worse compared to either untreated loess controls. For example, at the end of the simulation, CGR-1L lost a staggering 49.56 MT/ha (22.11 tons/acre) compared to the untreated loess in Control-2 at 10.35 MT/ha (4.62 tons/acre).

Yang et al. [23] hypothesized that the hydration reaction of the CaO within a typical CGR amendment would positively affect the cohesion and strength of the soil particles based on testing with a clayey sand and a sandy silt; however, results were opposite to these suppositions with the loess and CGRs tested in this study. The decreased cohesion (which resulted in greater erosion in this rainfall study) was attributed to the addition of the fine-grained CGR particles mixed into the already fine-grained silt-sized loess soil particles. This lower cohesion/increased erosion could also be due to the limited 24-hour cure time allowed for the CGR-amended soils, which limited the time available for hydration reactions for the CaO contained within the CGR slurries. Furthermore, differences between the compounds contained within the CGRs used in

this study compared to the 2016 CGR used in the Yang et al. study [23] could also explain the lack of cohesion between the CGR and the loess tested in this study. Additional testing of the loess and CGR cured 7-days would more conclusively determine the impact of amending loess with CGR. Testing for the percentage of CaO compound in the 5 CGRs used in this study would also add clarity to the mechanism behind the increased erosion exhibited by the CGR-amended loess in this rainfall study. Additional research to explore and characterize the mechanisms behind the erosivity of CGR-amended loess due to rain is needed.

4.2 Wind Erosion Discussion

With respect to the wind erosion study, CGR testing was performed on the same loess soil mixtures tested in the initial rain erosion study. However, research in the wind erosion portion of this study was extended to include 5 Class A-1 roadway shoulder aggregates collected from 2 counties in Eastern Iowa, and CGR dosages were doubled to include both 20% and 40% CGR dosages for the shoulder aggregates tested. The curing time for CGR-amended soils was also extended to 7-days (in lieu of the limited 24-hour curing time during the rainfall erosion study) prior to wind erosion testing.

A sieve analysis was performed on all 5 Class A-1 roadway shoulder aggregates, and results showed that the shoulder soils sampled fell within the gradation limits established by Iowa DOT for these aggregate materials. Wind results, however, had mixed results. For the Washington County soils tested (Site A and Site A CGR-amended soils), erosion was reduced with the addition of CGR, and wind erosion lessened to a greater degree with the increase in CGR dosage from 20% to 40% CGR. This confirmed the hypothesis for this study, with the reduction in soil loss attributed to possible hydration reactions resulting in better cohesion in the CGR-amended

soils compared to untreated soils. The theory was also validated with the CGR-amended Western Iowa loess, which also decreased in soil loss due to wind erosion with the addition of 20% CGR. However, for the Clinton County soils (Site E and Site E CGR amended soils), the addition of CGR-4 resulted in no appreciable changes in wind erosion, while the addition of CGR-5 to the Site E control resulted in greater wind erosion as well as an increase in soil loss with increasing dosages of CGR (from 20% to 40% CGR-5). One reason for this disparity could be due to the differences in the concrete mix designs for CGR-4 and CGR-5. CGR-4 had a limestone aggregate, while CGR-5 had a rose quartzite aggregate, which is more inert and less reactive during the curing process. Another reason for the reversing trends with the Clinton County soils could be due to more subgrade soil being captured when the shoulder soils were sampled. The portion of underlying subgrade soils collected with the aggregate shoulder samples for Site D and Site E from Clinton County appeared to have more organic material present in the samples. This was not confirmed through any lab testing but was noticed both in the texture of the samples as well as the strong organic smell of these two soils during drying. It was also observed that mold grew in one partial bucket of Site D and one partial bucket of Site E soil purposely left open to the air for a few weeks. These buckets were discarded, but these results confirmed suspicions that these two soils contained organic material.

4.3 Effects of CGR on pH

It is expected that CGR (residue produced from diamond grinding PCC) would share similar elevated pH values to that of hardened PCC. The increase in pH during the hydration process of fresh PCC is attributed to the release of Ca^{2+} and OH^- ions from several contributing compounds which each include calcium oxide (CaO). Portland cement initially contains a high percentage of CaO at 60%-67% [39] while CGR produced from roadway diamond grinding has a

lower but broad range of CaO content, ranging from 17% [23] to as high as 31% [24]. Although the CaO content was not tested for the 5 CGRs used in this study, tests for pH were performed. The average pH for the 5 CGRs collected for this project was 11.50, with a low pH of 11.13 and a high pH of 11.83. The average pH for the 20% CGR-amended loess was 10.43, with a low pH of 9.59 and a high pH of 10.95. Measurements of pH were also taken during the rainfall simulations. The initial pH for the simulation water was 8.01, while the stormwater runoff of the untreated loess had a slightly increased pH of 8.19 (compared to an initial pH for the untreated loess of 7.10). This slight increase in the pH of the untreated loess is attributed to the pH of the recirculated simulation water used in this study. The average pH for the stormwater runoff of the 20% CGR-amended loess mixes was 11.01, with a low pH of 10.22 and a high pH of 11.68. This showed that the average pH for the stormwater runoff from the CGR-amended loess soil forms after the rainfall simulations was close to the initial average pH of the CGR-amended soils prior to the rainfall simulations (discounting the slight increase in pH due to the simulation water).

4.4 Effects of CGR on Compaction Characteristics with Loess

The CGR-amended soils tested in this study were expected to result in drier soils and possibly stiffer soils due to water used up in the pozzolanic reaction of the CaO in the CGR during hydration. Amending 20% CGR with the fine grained loess in this study resulted in only slight changes in OMC and MDD. The untreated loess had an initial OMC of 16.8% and a MDD of 105.6-pcf. The 2 different 20% CGR-amended loess mixtures had a comparable average OMC of 16.6% and an average MDD 106.2 for the 20% CGR-amended loess soils tested.

4.5 Effects of CGR on Compaction Characteristics with Shoulder Materials

In comparison to CGR-amended loess, mixing 20% and 40% CGR with the 5 different Class 1-A roadway shoulder aggregates produced more substantial changes in OMC and MDD. Untreated

Washington County soils had an average of 9.2% OMC and an average MDD of 131.7 psf, while untreated Clinton County soils had an average of 7.5% OMC and an average MDD of 133.7 psf. Despite the approximate 2% difference between the average OMCs for the soils from these two counties, after blending these untreated aggregates with 20% CGR, the average OMC increased to 11.9% with an average decreased MDD of 122.2 psf across all five 20% CGR-treated shoulder soils. With 40% CGR, OMCs further increased to an average of 14.9%, while MDDs further decreased to an average of 113.2 psf across all 5 40% CGR-treated shoulder soils. Note, the maximum moisture content was the highest for 40% CGR 5 treated soils, averaging 16.1% OMC with the lowest average MDD of 110.7 psf. This difference is attributed to the CGR 5, which was collected from a newer concrete road. It is hypothesized that the CaO content in CGR 5 was higher than the other CGRs collected, as the road was only recently completed at the time of grinding, producing CGR with a higher hydration potential.

In general, CGR had a much broader drying affect to the Class 1-A granular shoulder aggregates in comparison to CGR-amended loess. This is attributed to greater air voids in the coarse grained shoulder aggregates which allowed more water to infiltrate the soil blended with the fine grained CGR material, compared to the already fine grained silty loess. The coarse grained shoulder aggregates from Clinton County, although not formally tested for organic and clay content, exhibited a bit more initial cohesion compared to the Washington County soils. When handling and manipulating the untreated moist soils from Clinton County, these soils held together slightly better than the aggregate from Washington County when a small portion of the soil was rolled into a ball. However, the Clinton County soil did not hold together when trying to further roll the soil balls into cylinders. By comparison, the Washington County soils did not hold together when pressed by hand into balls.

CHAPTER 5 CONCLUSIONS

Utilizing waste materials to help stabilize problematic soils is a creative and sustainable idea. One abundant waste material is CGR slurry, which is produced in large quantities on concrete diamond grinding (roadway) projects in the United States. In lieu of recycling, the two primary means of disposal are discharge of the CGR slurry directly onto adjacent roadway shoulders or collection and transport to local sedimentation pits or local landfills. It seems unusual to still see CGR discarded, since CGR is merely concrete fines with a high lime content, while it is also classified as a non-hazardous waste product by EPA standards (provided the pH is less than 12.0). CGR has been collected and tested in numerous studies and its mineral composition and chemical properties are well known. More importantly, several major studies have concluded that CGR does not have long term effects on soil chemistry, soil infiltration, vegetation growth, or any detrimental effects on fish and the environment [14,21,22,25,31,33,34]; however, the recycling uses for CGR still remain largely unexplored. In this research, two distinct erosion studies, using wind and rain, were performed to observe and determine the effect of CGR-amended soil on erosion. Supporting lab tests performed on both untreated (control) soils as well as CGR-amended soils included sieve analysis (gradation), moisture content, Standard Proctor, pH, turbidity, and the measurement of eroded soil loss. The findings from both the rain and wind erosion studies completed are as follows:

- The pH for the untreated loess was 7.10. A close range of pH was found for the 5 CGRs collected, with a low pH of 11.13 and high pH of 11.83. Similarly, the average pH for the 20% CGR-amended loess ranged from a low of pH of 9.59 to a high pH of 10.95.
- The initial pH of the rainfall simulation water was 8.01, which is presumed responsible for the slight increase in the stormwater runoff from the untreated loess of 8.19. The

average pH for the stormwater runoff from the 20% CGR-amended loess ranged from a low pH of 10.22 to a high pH of 11.68 across the 6 CGR-amended soil forms tested.

- The water quality of the 20% CGR-amended loess was much poorer compared to the untreated loess grab samples collected. The average turbidity values ranged from as low as 1.8 to as high as 4.7 times higher (worse) across all 120 water quality grab samples collected from the 20% CGR-amended loess rainfall simulations. This translates to an average of 410% poorer water quality from the grab samples collected from the CGR-amended loess trials compared to samples collected from the untreated loess. The water quality was the poorest during the middle third of the test (during the 4 in./hr. storm) for all trials of 20% CGR-amended loess. During this storm, the water quality averaged 530% worse for CGR-amended soils tested.
- With respect to the rain-eroded soil collected and weighed after the rainfall simulations, the 20% CGR-amended loess eroded substantially more than the untreated loess during the 60-minute rainfall trials. Soil loss (erosivity) measurements showed an average soil loss of 520% for CGR-amended soil compared to the untreated loess soil. This translates to an average of 17.30 tons/acre for CGR-amended soil compared to 4.62 tons/acre for the untreated loess control. Soil loss increased from the 2 in./hr. storm to the 4 in./hr. storm but decreased from the 4 in./hr. to 6 in./hr. storm.
- Loess compacted on the dry side of optimum (-5.3% OMC) rain eroded 216% more than loess compacted at OMC (or 9.97 tons/acre of soil loss for soil compacted on the dry side of optimum compared to 4.62 tons/acre of soil compacted at OMC).
- With respect to wind erosion results, for all of the soil blends tested, the untreated Site A Control soil resulted in the highest erosion rate at 8.07 tons/roadway mile. However,

wind erosion results of similar untreated soils from Washington County (Site B and Site C) the wind erosion rates were substantially less at 3.72 and 6.52 tons/roadway mile, respectively.

- Amending Washington County shoulder aggregate with CGR decreased the wind erosivity of the soil. Wind erosion decreased 25% and 58% for CGR amended shoulder aggregates (with 20% and 40% CGR), respectively, compared to untreated soils. Conversely, amending Clinton County shoulder aggregate with CGR increased the wind erosivity of the soil. Wind erosion increased 25% and 50% for CGR amended shoulder aggregates (with 20% and 40% CGR), respectively, compared to untreated soils.
- Adding 20% CGR to Western Iowa loess only slightly reduced the wind erosivity of the soil. Additionally, the wind erosion rate of untreated loess mirrored the wind erosion rates of Class 1-A untreated shoulder aggregates from Clinton County.

CHAPTER 6 RECOMMENDATIONS & LIMITATIONS

6.1 Recommendations

The goal of any geotechnical research study is to maximize the number of soils and soil mixtures being tested in order to maximize the data for analysis. Recommendations for future rain erosion tests should include the testing of additional Iowan soils (e.g., glacial till and alluvium) with 20% CGR dosages (as well as other CGR dosages). This would more conclusively determine whether the rain erodibility trends found would continue for CGR-amended soils. With respect to the rainfall simulator, investment into enhancements to the existing simulator (e.g., increase the number of nozzles from 9 to 12 nozzles) would increase the rainfall footprint within the simulator. Additionally, changing the style of simulator from a Purdue-type simulator to a simulator style that produces uniform 3mm gravity-driven raindrops could produce raindrops of more uniform size and distribution within the rainfall simulation room.

Although redundancy is good for test trials, with respect to future rainfall testing, the testing of a single test form of a particular soil blend (in lieu of testing 3 soil forms per rainfall trial) would allow more soils and more soil blends to be initially tested. This would also significantly save on the extra compaction effort required to produce 3 soil forms with the same soil for each test. Regarding the compaction of the soil forms, changing from a single lift to 3 lifts of 1-1/2” soil using the UTA compaction equipment, could dramatically reduce the number of compaction tamps required per soil form, which in turn would put less wear and tear on the UTA. Lifting of the 350 lb. compacted soil forms required the brute strength of 3 men. Installing a wall mounted arm and winch to lift and set the compacted soil forms, would provide a safer and more efficient way to lift the soil forms on the racks for testing.

Another recommendation for future testing is to adjust specimen curing time. The limited 24-hour curing time chosen for the rainfall erosion study (which was chosen due to time constraints) reduced the reaction time for the CGR to gain stability and strength with the CGR-amended loess soils tested. A 7-day cure time following compaction is recommended for future trials. Loess was selected for this study because of its fine particle size, low plasticity, abundance in Iowa, and due to the poor drainage and strength characteristics (generally) associated with silts and loams, which in turn makes it a problematic soil for use in roadside embankments. However, utilizing the same Iowa soils used in previous CGR studies would allow for more direct correlation of the results with these other studies. Complimenting these additional soils with extended curing times could lead to promising uses for CGR as a soil stabilizing amendment.

With respect to the duration of each rainfall simulation, extending each simulation beyond the 60 minute limit would be helpful in determining if any leveling-off trends would continue or change for some soil types. Having the flexibility and extra equipment to collect additional samples is recommended. Finally, rainfall simulations using other sustainable soil amendments such as corncob ash, rice-husk ash, and bamboo ash (and/or CGR amended soils with these materials) could be performed to determine if the pozzolanic characteristics in these materials might serve as a catalyst toward improving the cohesive properties of loess and other Iowan soils.

Recommendations for future wind erosion testing with CGR amended soils would include the testing of the remaining 3 soils (Sites B, C, and D) with CGR, as well as testing the Western Iowa loess with the 40% CGR dosage. This would better confirm the wind erosion behavior of the soils collected for each county road sampled. Extending testing to additional Iowan soils (e.g., glacial till and alluvium) to wind erosion testing with both 20% and 40% CGR dosages could more definitely determine wind erosion trends between different types of soils.

With respect to future research recommendations, increasing the velocity of the wind source to more closely match the posted speed limits (45 and 55 mph) found on these roads would increase the degree of wind erosion produced with each soil mixture sampled. Additionally, if a lateral (perpendicular) secondary wind source were also added to the test, this could further produce the desired swirling 'wind whip' air flow that was the targeted wind effect for this study. Finally, as in the recommendations made for future rainfall studies, wind erosion testing using other sustainable soil amendments such as corncob ash, rice-husk ash, and bamboo ash (and/or CGR amended soils blended with these materials) could create future recycling uses for these waste materials while improving the cohesive characteristics of loess and cohesionless Class A-1 roadway aggregates.

6.2 Limitations

Limitations on this project included both material and time constraints on this project. Materials used in the rain erosion study included the testing of one soil type (Western Iowa loess). Rainfall testing also only include a single dosage of CGR (20%) with only 2 of the 5 CGRs collected. On the rainfall erosion study, testing of the Western Iowa loess was limited to the same single dosage of CGR (20%) also with 2 of the 5 CGRs collected. The wind erosion study did extend testing to 5 shoulder aggregate soils, but testing was narrowed down due to time constraints to 2 soils (Site A and Site E) with using 2 dosages (20% and 40%) with 2 of the 5 CGRs (CGR 4 and CGR 5). The 2020-2021 Pandemic severely limited access to lab facilities for the safety of student and faculty on this project as well. Biases on the project was in the selection of Western Iowa loess for the initial testing. Other Iowa soils would have been good candidates for testing on this project, but the choice to use loess for testing was favored due to its abundance and ease in collection for this project.

APPENDIX

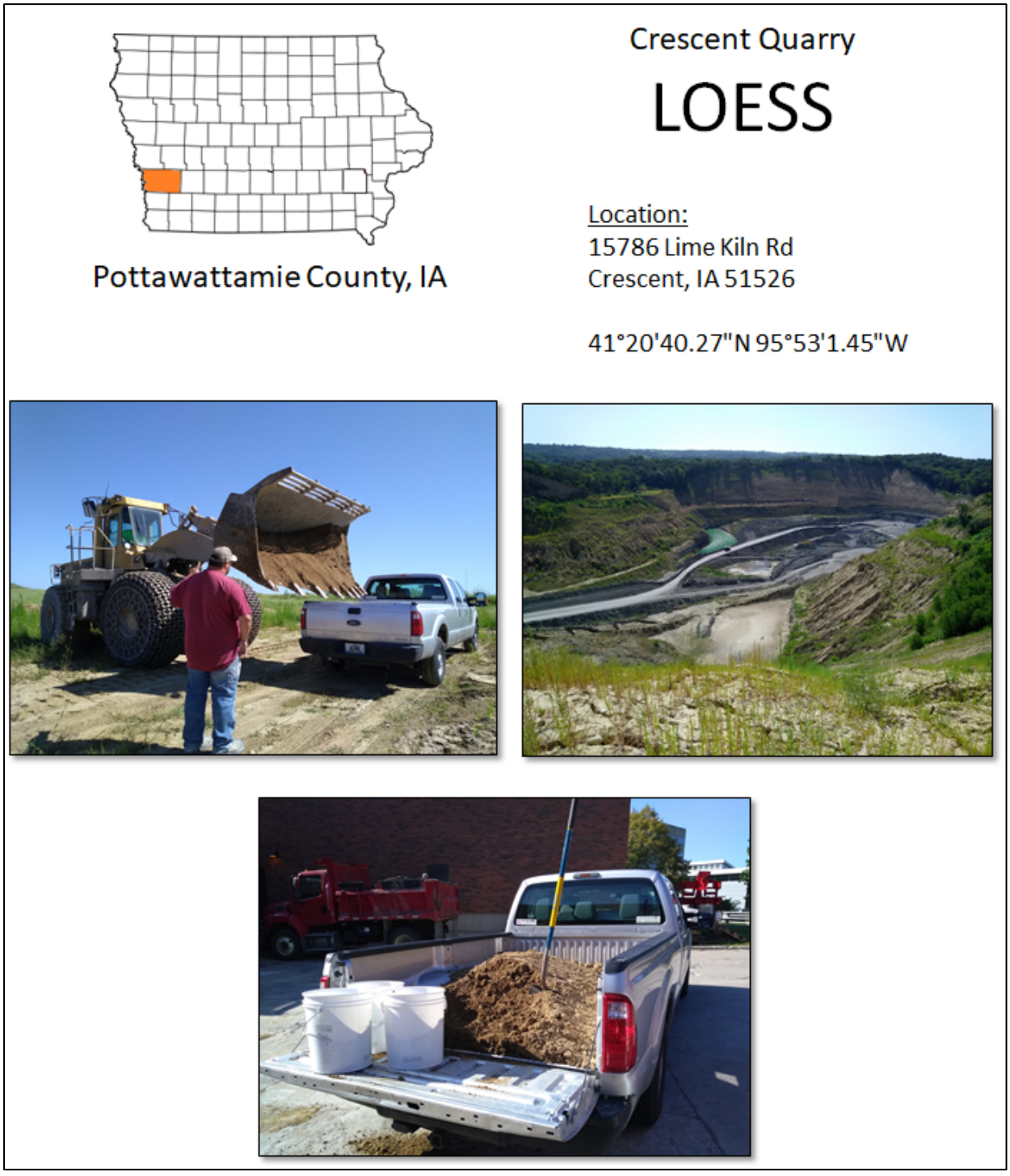

Figure 47: Location of the Second Batch of Loess Soil Collected, Photos by Patrick Bollinger

State of Iowa.

Enlargement: Washington County, IA (left) and Clinton County, IA(right)

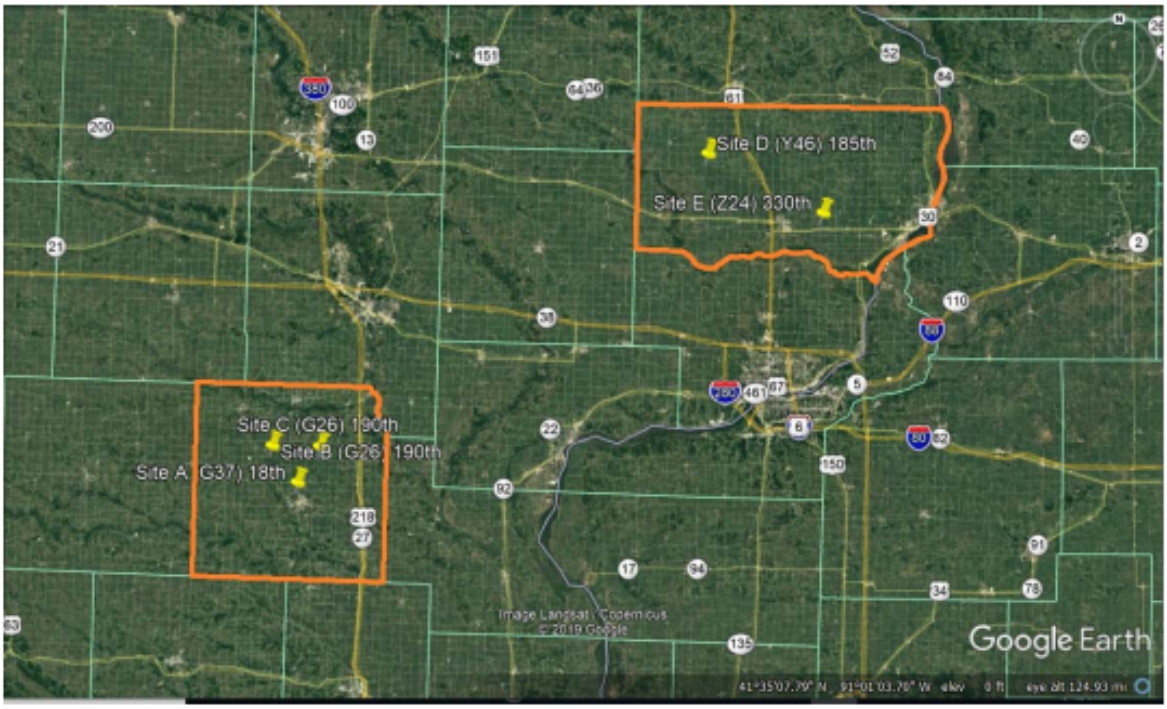

Figure 48: Google Earth Map Location of Five Roadway Shoulder Soils Collected

Figure 49: Location in Washington County, IA Site Where Shoulder Material was Collected, Photos by Patrick Bollinger

Figure 50: Location in Washington County, IA Site Where Shoulder Material was Collected, Photos by Patrick Bollinger

Figure 51: Location in Clinton County, IA Site Where Shoulder Material was Collected, Photos by Patrick Bollinger

Figure 52: Location in Clinton County, IA Site Where Shoulder Material was Collected, Photos by Patrick Bollinger

Figure 53: Loess Hills National Scenic Byway Spine and Excursion Loops [125]

Figure 54: First 3 of 5 CGRs Collected, Photos by Patrick Bollinger

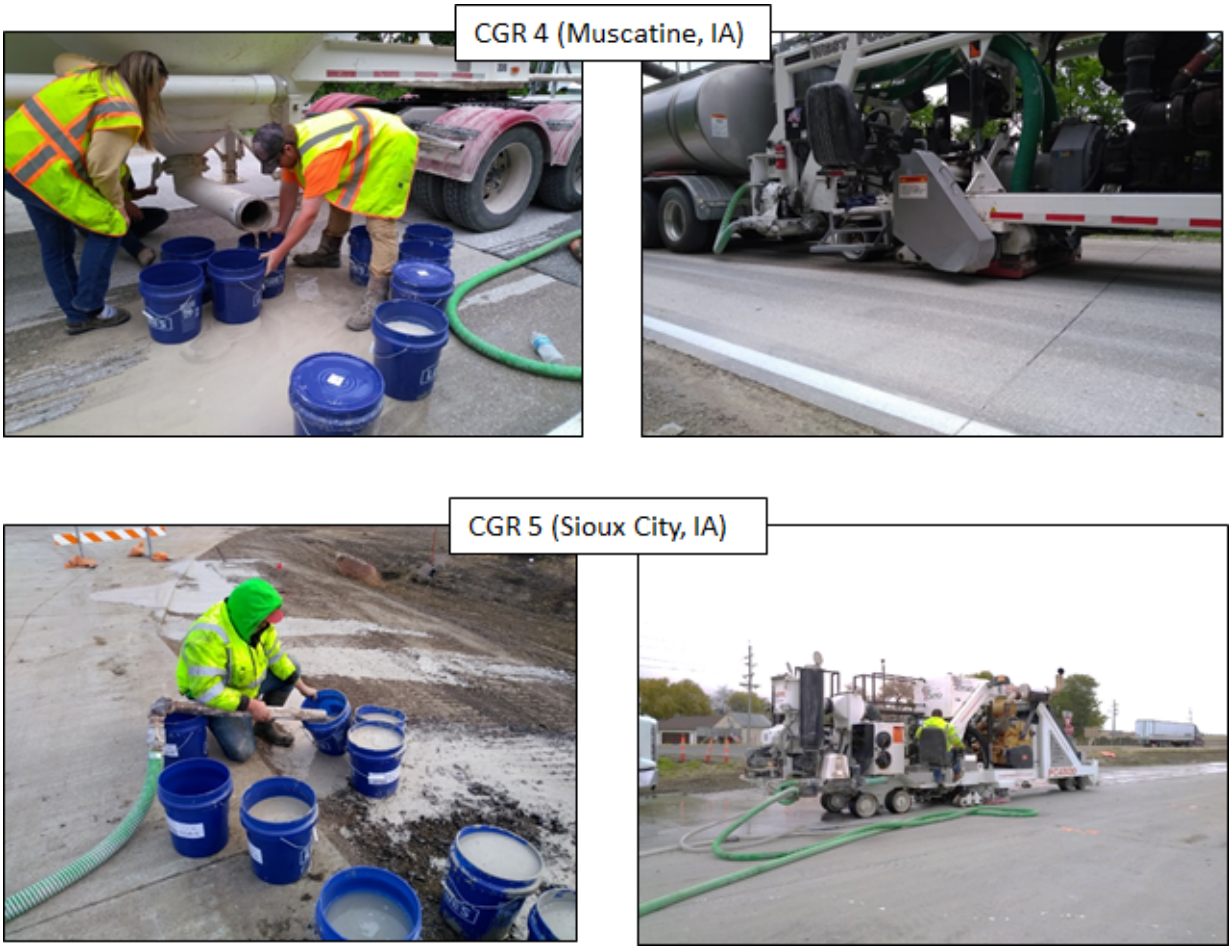

Figure 55: Last 2 of 5 CGRs Collected, Photos by Patrick Bollinger

Figure 56: Early Construction of Soil Forms, Photos by Patrick Bollinger

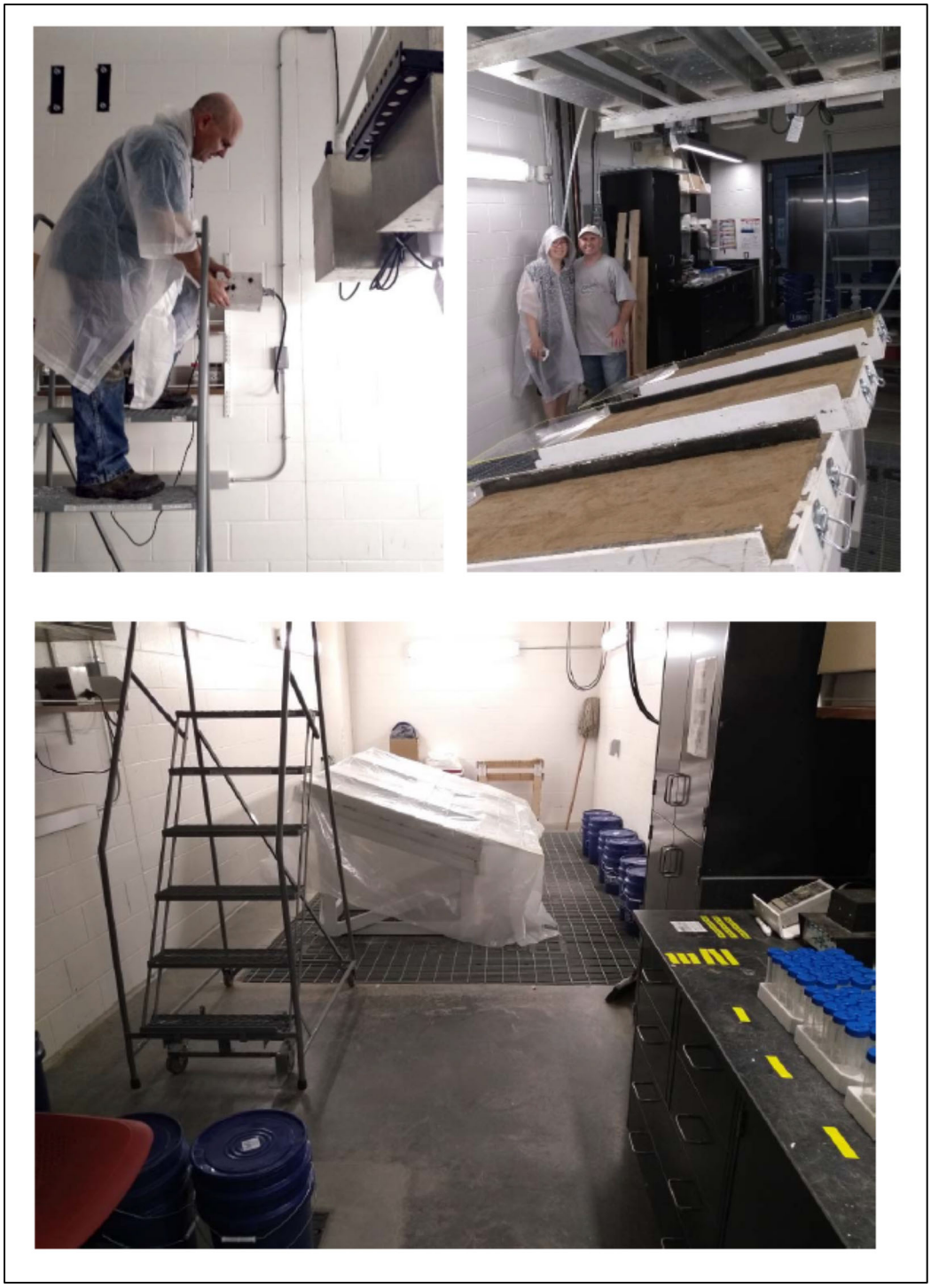

Figure 57: Rainfall Simulator at Iowa State University, Photos by Patrick Bollinger

Figure 58: VeeJet Model 80100 Nozzles in Rainfall Simulator at Iowa State University, Photos by Patrick Bollinger

Figure 59: Assembled Rainfall Wooden Rack, Soil, Form, and Metal Funnel, Photos by Patrick Bollinger

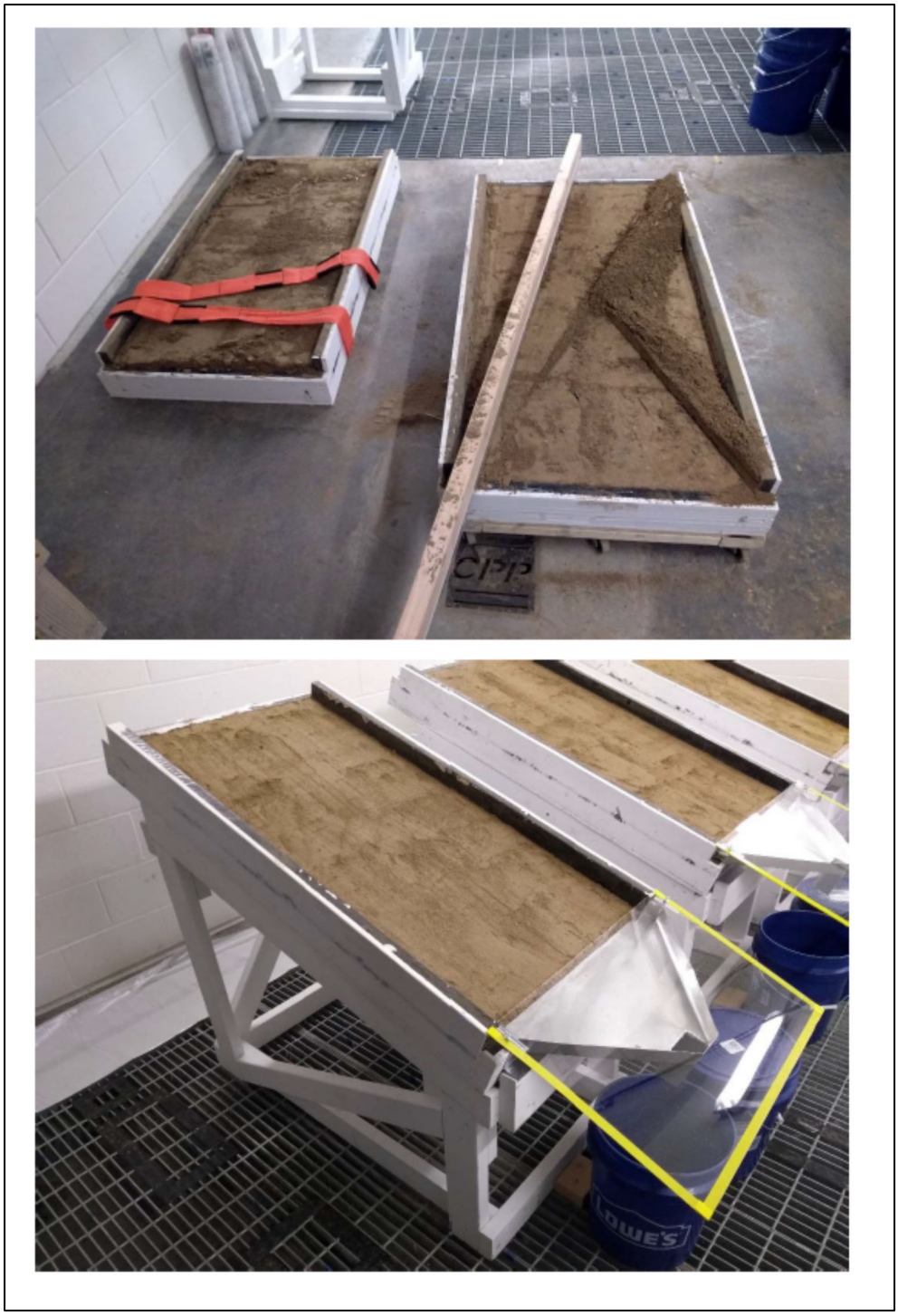

Figure 60: Screeding Process and Typical Compacted Soil Forms, Photos by Patrick Bollinger

Figure 61: Soil Forms Showing Soil Erosion After Rainfall Simulation, Photos by Patrick Bollinger

Figure 62: Saturated Soil After Simulation and Typical Soil Thickness, Photos by Patrick Bollinger

Figure 63: Gilson Sieve Shakers at Michigan State University, Photos by Patrick Bollinger

Figure 64: Gilson 14x14 Sieve Shaker and Sieves at Michigan State University, Photos by Patrick Bollinger

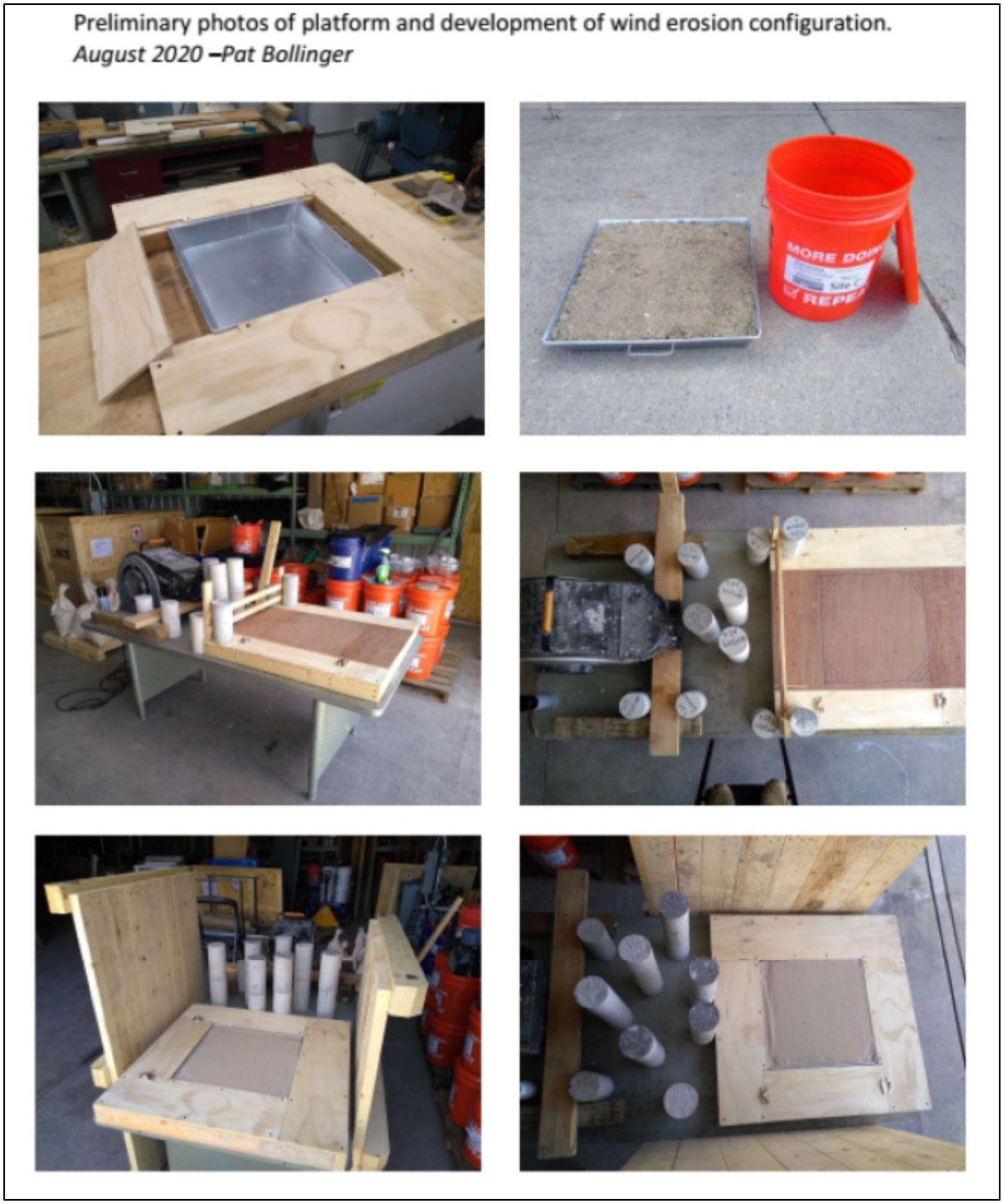

Figure 65: Early Design Photos of Wind Erosion Testing Apparatus (WETA), Photos by Patrick Bollinger

Smoke test over wind erosion soil form (top) and anemometer (bottom).

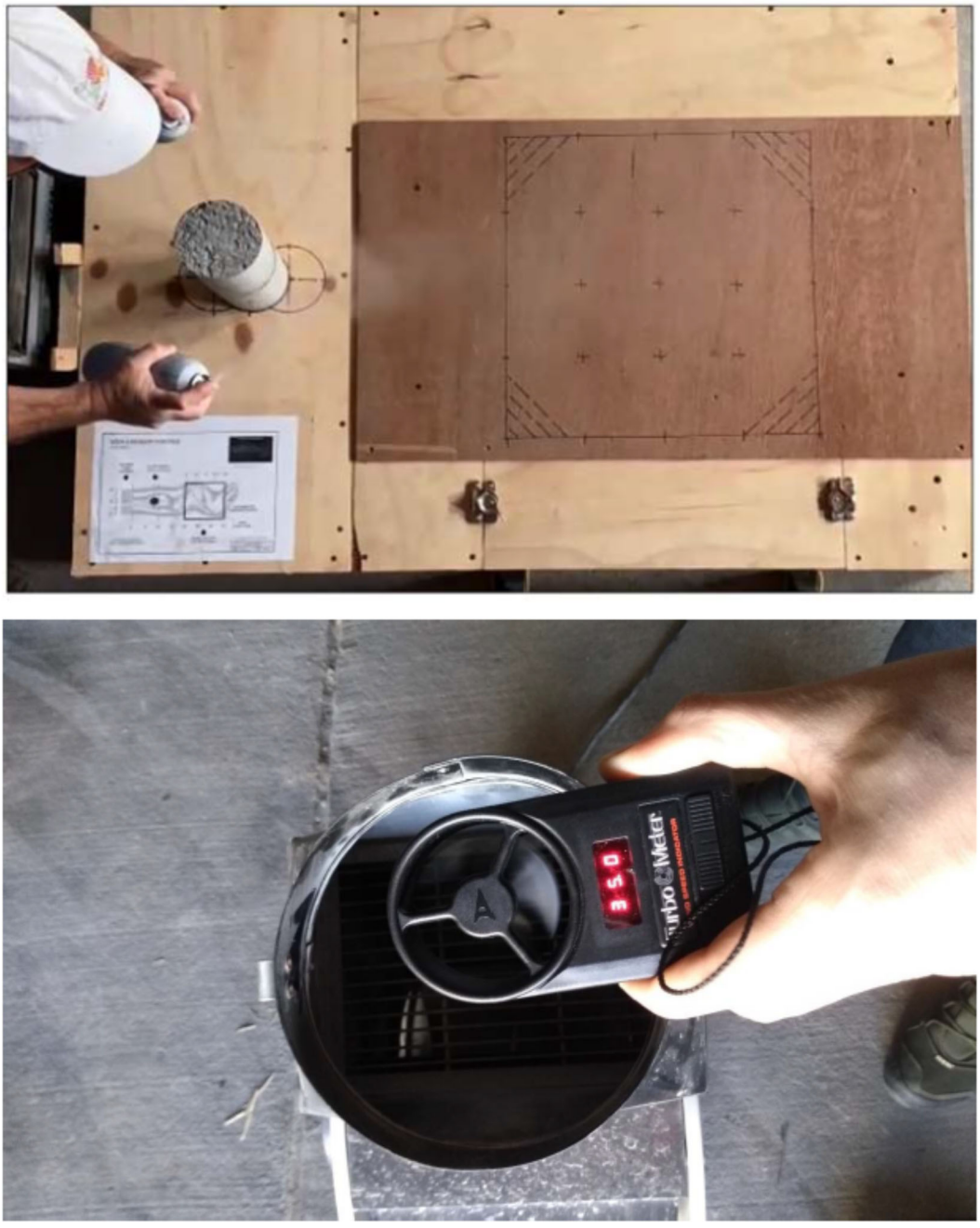

Figure 66: Test/Calibration of Wind Erosion Source and Air Flow, Photos by Patrick Bollinger

SAMPLE PROBLEM

CGR "Collection EFF" Contractor Example:

Project Example

A contractor has a new roadway CPR project and estimates that the project is going to take 3-weeks using a small DP 1500 grinder running an average of 6-hours a day with a supporting water truck supplying water to cool the grinder blades at a rate of 8-gallons a minute. If the contractor is allowed to dispose of the CGR discharge water at a nearby sedimentation pit, but is required to return to the site 1 week after the job is complete to load and dispose of the CGR solids produced on the project, how many gallons of CGR solids will the contractor need to haul to a landfill?

Solution

a) Calculating CGR Discharge volume:

(3-weeks)(5-days/week)(6-hours/day)(60-min/hour)(8-gallon/min) = 43,200-gallons

Referencing back to the dissertation table, this project most closely resembles the CGR-2 in Des Moines, IA shown in TABLE 1 and TABLE 2. On this project, full-lane bump grinding was required on a project that could not discharge at the site. Ready-mix trucks were required to collect the CGR discharge and haul it offsite. The Collection EFF for this project from TABLE 5 was 50%. Therefore, approximately 43,200-gallons/2, or 21,600-gallons of CGR solids will need to be collected after the job and taken to a landfill. TABLE 4 shows that the moist CGR cakes for CGR-2 had a moist unit weight of 133.5 pcf.

b) Calculating amount of CGR solids :

(21,600-gallons)(1-cubic foot/7.48-gallons)(133.5-lbs/cubic foot)(1-ton/2000lbs) = 192-tons.

If a local landfill charges $45/ton for construction debris, the contractor can expect to have a landfill dumping fee of $8,640 from a job of this size.

Figure 67: Sample CGR Collection Design Problem Created by Patrick Bollinger

REFERENCES

REFERENCES

[1] L.M. Snell and B.G. Snell, "*Oldest Concrete Street in the United States*," Concrete International, vol. 24, no. 3, pp. 72-74, 2002.

[2] T.J. Pasko, Jr., "*Concrete Pavements - Past Present and Future*," FHWA Public Roads Magazine, vol. 62, no. 1, July/August 1998. [Online]. Available: https://www.fhwa.dot.gov/publications/publicroads/98julaug/concrete.cfm.

[3] American Society of Civil Engineers, "*First Concrete Pavement*," ASCE.org. https://www.asce.org/project/first-concrete-pavement/ (accessed Mar. 1, 2021).

[4] Portland Cement Association (PCA), "*Highways - History of Concrete Highways*," CEMENT.org. https://www.cement.org/cement-concrete/paving/concrete-paving-types/highways#:~:text=The%20first%20concrete%20highway%20constructed,pave%202%2C348%20miles%20of%20roadway (accessed Mar. 1, 2021).

[5] C. McLaren, "*Arkansas Highway history and Architecture, 1910-1965*," Arkansas Historic Preservation Program, Little Rock, AR, 1999.

[6] Bureau of Transportation Statistics, "*National Transportation Statistics - Public Road and Street Mileage in the United States by Type of Surface*" (2019). Distributed by U.S. Department of Transportation. https://www.bts.gov/content/public-road-and-street-mileage-united-states-type-surfacea.

[7] Federal Highway Administration, "*Highway Statistics 2019: Highway Infrastructure: National Tables: Public road length by type of surface and ownership/functional system: HM-12,*" (2020). Distributed by U.S. Department of Transportation. https://www.fhwa.dot.gov/policyinformation/statistics/2019/pdf/hm12.pdf.

[8] K.W. Gee, "*Technical Advisory T 5040.36 Surface Texture for Asphalt and Concrete Pavements*," Federal Highway Administration, Washington, D.C., 2005, Accessed March 1, 2021 [Online]. Available: https://www.fhwa.dot.gov/pavement/concrete/diamond.pdf.

[9] R.O. Rasmussen, S. Garber, R. Sohaney, P. Wiegand, D. Harrington, "*Tech Brief: What Makes a Quieter Concrete Pavement: Concrete Pavement Surface Characteristics Program*," National Concrete Pavement Technology Center, Ames, IA, 2010.

[10] R.O. Rasmussen, P.D. Wiegand, G.J. Fick, D.S. Harrington, "*How to Reduce Tire-Pavement Noise: Better Practices for Constructing and Texturing Concrete Pavement Surfaces*," National Concrete Pavement Technology Center, Ames, IA, Tech Rep. DTFH61-06-H-00011, 2012.

[11] M.B. Snyder, "*Tech Brief: Concrete Pavement Texturing*," Washington, D.C., Rep. FHWA-HIF-17-011, 2019.

[12] B. Hibbs and R. Larson, "*Tire Pavement Noise and Safety Performance: PCC Surface Texture Technical Working Group*," Federal Highway Administration, Washington, DC, Tech Rep. FHWA-SA-96-068, 1996.

[13] S. Rao, H.T. Yu, L. Khazanovich, M. Darter, and J. Mack, "*Longevity of Diamond-Ground Concrete Pavements*," Transportation Research Board, Washington D.C., 1999.

[14] M. Mamo, D. McCallister, W. Schacht, "*Evaluation of Concrete Grinding Residue (CGR) Slurry Application on Vegetation and Soil Responses along Nebraska State Hwy 31*," Tech Rep. NDOR SPR-P1(13) M335, 2015.

[15] International Grinding and Grooving Association, "*IGGA History*," IGGA.net. Available: https://www.igga.net/history/ (accessed Feb. 2019).

[16] P. Kenter, "*Diamond grinding can go a long way for road lifespan*," Daily Commercial News by Construct Connect, Feb. 24, 2012. {Online]. Available: https://canada.constructconnect.com/dcn/news/infrastructure/2012/02/diamond-grinding-can-go-a-long-way-for-road-lifespan-dcn048926w.

[17] AC Business Media, LLC., "*Canada's Sixth Busiest Airport Becomes Country's First Major Airport to Groove Runway Pavement*," Dec. 16, 2013. [Online]. Available: https://www.forconstructionpros.com/business/article/11223195/canadas-sixth-busiest-airport-becomes-countrys-first-major-airport-to-groove-runway-pavement.

[18] The British Cementitious Paving Association, "*Road: Roads get grinding and grooving*," BritPaveNews, vol. 21, pg. 4, 2020.

[19] J. Willis, "*Surface Grinding Concrete Pavements*," The British Cementitious Paving Association, 12th Intl. Symposium on Concrete Roads 2014 in Prague, Czech Republic," 2014, pp. 1-8.

[20] International Grooving and Grinding Association, "*Diamond Grinding Slurry Handling Best Management Practices*," 2013. [Online]. Available: https://www.igga.net/resources/diamond-grinding-slurry-handling-best-management-practices/.

[21] H. Ceylan, Y. Zhang, B. Cetin, S. Kim, B. Yang, C. Luo, R. Horton, K. Gopalakrishnan, "*MnDOT Concrete Grinding Residue: Its Effect on Roadside Vegetation and Soil Properties*," Iowa State Univ., Ames, IA, Rep. MN/RC 2019-06, 2019.

[22] C. Luo, "*The effects of road surface concrete grinding residue (CGR) on selected soil properties and plant growth*" (2019). PhD Dissertation. Dept. of Agronomy, Iowa State Univ., Ames, 2019. [Online]. Available: https://lib.dr.iastate.edu/etd/17046.

[23] B. Yang, Y. Zhang, B. Cetin, and H. Ceylan, "*Concrete Grinding Residue: Management Practices and Reuse for Soil Stabilization*," Transport. Res. Record: J of the Transport. Res. Board, vol. 2673, no. 11, pp. 748–763, Jun 2019, doi: 10.1177/0361198119854292.

[24] M. Kluge, N. Gupta, B. Watts, P. A. Chadik, C. Ferraro, T. G. Townsend, "*Characterisation and management of concrete grinding residuals*," Waste Mgmt. and Res. vol. 36, no. 2, pp. 149–158, Dec 2017, doi: 10.1177/0734242X17744040.

[25] C. Luo, Z. Wang, F. Kordbacheh, Y. Zhang, B. Yang, S. Kim, B. Cetin, H. Ceylan, R. Horton, "*The Influence of Concrete Grinding Residue on Soil Physical Properties and Plant Growth*," J. Env. Quality, vol. 48, no. 6, pp. 1842-1848, Nov 2019, doi: 10.2134/jeq2019.06.0229.

[26] K. Dispenza, "*Research studies show potential environmental benefits of concrete grinding residue: Is Slurry an Ugly Word?*," Roads and Bridges Media, Feb. 2020. [Online]. Available: https://www.roadsbridges.com/research-studies-show-potential-environmental-benefits-concrete-grinding-residue.

[27] U.S. Environmental Protection Agency (EPA), "*40 CFR, Chapter 1, Subchapter 1, Part 261, Subpart C: Characteristics of Hazardous Waste*," https://www.ecfr.gov/cgi-bin/text-idx?node=sp40.28.261.c (Accessed May 10, 2019).

[28] S. Goodwin and M. Roshek, "*Recycling Project: Concrete Grinding Residue*," Transp. Res. Rec. J. of the Transp. Res. Board, vol. 1345, pp. 101–105. 1992. [Online]. Available: http://onlinepubs.trb.org/Onlinepubs/trr/1992/1345/1345-013.pdf.

[29] Transportation Research Board (TRB), National Research Council, "*NCHRP Synthesis 204: Portland Cement Concrete Resurfacing*," National Academy Press, Washington, D.C., 1994. [Online]. Available: http://onlinepubs.trb.org/Onlinepubs/nchrp/nchrp_syn_204.pdf.

[30] Neal, B. F., and J. H. Woodstrom, "*Rehabilitation of Faulted Pavements by Grinding*," California Department of Transportation (CALTRANS), Sacramento, CA, USA, Rep. CA-DOT-TL-5167-4-76-18, 1976.

[31] Holmes and Narver Inc., "*Concrete Grinding Residue Characterization. Final Report. Caltrans District 11, Task Order No. 8*" California Department of Transportation (CALTRANS), Sacramento, CA, USA, 1997. [Online]. Available: https://www.igga.net/wp-content/uploads/2018/08/Concrete_Grinding_Residue_Characterization_1997.pdf.

[32] D. Yonge and H. Shanmugam, "*Assessment and Mitigation of Potential Environmental Impacts of Portland Cement Concrete Highway Grindings*," Washington State Transportation Center (TRAC), Pullman, WA, Rep. WA-RD 628.1 T1804-10, 2005.

[33] DeSutter, T., L. Prunty, and J. Bell, "*Concrete Grinding Residue Characterization and Influence on Infiltration*," J. of Envir. Quality, vol. 40, no. 1, pp. 242–247, 2011.

[34] B. Yang, B. Cetin, Y. Zhang, C. Luo, H. Ceylan, R. Horton, S. Kim, M. Mahedi, "*Effects of concrete grinding residue (CGR) on selected sandy loam properties*," J. Clean Prod., vol. 240, no. 118057, Dec 2019, doi: 10.1016/j.jclepro.2019.118057.

[35] DeSutter, T., P. Goosen-Alix, L. Prunty, P. J. White, and F. Casey, "*Smooth Brome (Bromus Inermis Leyss) and Soil Chemical Response to Concrete Grinding Residue Application*," Water, Air, and Soil Pol., vol. 222, no. 1, pp. 195–204, 2011.

[36] A. L. Correa, B. Wong, "*Concrete Pavement Rehabilitation – Guide for Diamond Grinding*," Washington, D.C., Rep. FHWA-SRC 1/10-01(5M), 2001, Accessed Jun 16, 2020 [Online]. Available: https://www.fhwa.dot.gov/pavement/concrete/diamond.pdf.

[37] T. G. Townsend, P. Chadik, N. Gupta, M. Kluge, T. Vinson, J. Schert, "*Concrete Debris Assessment for Road Construction Activities*," Gainesville, FL, Tech Rep. FDOT BDV31-977-48, August 2016.

[38] H. Ceylan, K. Gopalakrishnan, S. Kim, R. F. Steffes, "*Evaluating Roadway Subsurface Drainage Practices*," Iowa State Univ., Ames, IA, Rep. InTrans 12-428., May 2013, Accessed Mar 31, 2019. [Online]. Available: https://lib.dr.iastate.edu/intrans_reports/60.

[39] H. S. Coban, "*The use of lime sludge for soil stabilization*," M.S. thesis, Dept. Civil Const. Env. Engin., Iowa State Univ., Ames, 2017.

[40] Sawangsuriya, T. B. Edil, "*Evaluation of Soil Stiffness and Strength for Quality Control of Compacted Earthwork*," Int. J. of Earth Energy and Env. Sci., vol. 10, no. 2, pp. 114-118, 2016.

[41] V. Schaefer, L. Stevens, D. White, H. Ceylan, "*Iowa SUDAS Design Guide for Improved Quality of Roadway Subgrades and Subbases*," Ames, IA, USA, Tech. Rep. IHBR TR-525, 2008.

[42] Christopher, B. R., Schwartz, C. W., and Boudreau, R. L., "*Federal Highway Administration FHWA NHI-05-037 Geotechnical Aspects of Pavements Reference Manual*," 2006, Accessed Jun 23, 2020. [Online]. Available: https://www.fhwa.dot.gov/engineering/geotech/pubs/05037/index.cfm.

[43] P. Kinnell, "*The Effect of Slope Length on Sediment Concentrations Associated with Side-Slope Erosion*," Soil Sci. Soc. of America J., vol. 64, no. 3, pp. 1004-1008, May 2000, doi: 10.2136/sssaj2000.6431004x.

[44] S. R. Benik, B. N. Wilson, D. D. Biesboer, D. Hansen, B. Stenlund, Dwayne, "*Performance of Erosion Control Products on a Highway Embankment*," Trans. ASAE, vol. 46, no. 4, pp. 1113-1119, 2003, doi: 10.13031/2013.13962.

[45] M. D. Ricks, M. A. Horne, B. Faulkner, W. C. Zech, X. Fang, W. N. Donald, M. A. Perez, "*Design of a pressurized rainfall simulator for evaluating performance of erosion control practices*," Water J. (Switzerland), vol. 11, no. 11, pg. 2386. Nov 2019, doi: 10.3390/w11112386.

[46] D.J. White, P. Vennapusa, "*Tech Transfer Summary, Low-Cost Rural Surface Alternatives*," Center for Earthworks Engin. Research, Ames, IA, Tech Rep. IHRB TR-632, 2013.

[47] Design Manual: Deep Mixing for Embankment and Foundation Support (FHWA-HRT-13-046), U.S. Dept of Transportation, Federal Highway Administration. Washington, DC., USA, 2013.

[48] M.A. Kestler, "*Stabilization Selection Guide for Aggregate and Native-Surface Low Volume Roads,"* U.S. Department of Agriculture Forest Service, Mar. 2009. [Online]. Available: https://www.fs.fed.us/t-d/pubs/pdf/hi_res/08771805hi.pdf.

[49] *Geotechnical Aspects of Pavements Reference Manual (NHI-05-037 Chapter 7)*. U.S. Dept. of Transportation, Federal Highway Administration, Washington, D.C., USA, 2006. [Online]. Available: https://www.fhwa.dot.gov/engineering/geotech/pubs/05037/05037.pdf.

[50] M. Brusseau, I. Pepper, C. Gerba, *Environmental and Pollution Science*, 3rd ed., Cambridge, MA: USA: Academic Press, ch. 32, pp. 585-603, 2019.

[51] G.R. Robinson Jr., W.D. Menzie, H. Hyun, "*Recycling of construction debris as aggregate in the Mid-Atlantic Region, USA*," Res. Cons. Recycling, vol. 42, no. 3, pp. 275-294, Oct 2004, doi: 10.1016/j.resconrec.2004.04.006.

[52] B. Cetin, A.H. Aydilek and Y. Guney, "*Stabilization of recycled base materials with high carbon fly ash*," J. Res. Consv. and Recyl., vol. 54, no. 11, pp. 878-892, Sept. 2010. doi: 10.1016/j.resconrec.2010.01.007.

[53] S.N. Jones and B. Cetin, "*Evaluation of waste materials for acid mine drainage remediation*," J. Fuel, vol. 188, pp. 294.309, Ja. 2017, doi: 10.1016/j.fuel.2016.10.018.

[54] C. Li, J. Ashlock, B. Cetin, C. Jahren, "*Feasibility of Granular Road and Shoulder Recycling*," IHRB and Iowa DOT, Ames, IA, Tech Rep. IHRB Project TR-685, Iowa DOT 15-526, 2018.

[55] C. Cline, M. Anshassi, S. Laux, T. G. Townsend, "*Characterizing municipal solid waste component densities for use in landfill air space estimates*," Water Mgmt. Res J. Sust. Circular Econ., vol. 38, no. 6, pp. 673-679, Jan 2020, doi: 10.1177/0734242X19895324.

[56] User guidelines for by product and secondary use materials in pavement construction (FHWA-RD-97-148), U.S. Dept. of Transportation, Federal Highway Administration, Washington, D.C. USA, 2016, Accessed Jan. 10, 2020. [Online]. Available: https://www.fhwa.dot.gov/publications/research/infrastructure/pavements/97148/index.cfm.

[57] Specifications for Highway and Bridge Construction: Division 25 Misc. Construction: Section 2532 Pavement Surface Repair (Diamond Grinding), Iowa Department of Transportation, Ames, IA, USA, 2020, Accessed Mar 12, 2020. [Online]. Available: https://iowadot.gov/erl/index.html

[58] D. Helms, "*Readings in the History of the Soil Conservation Service*," USDA Soil Conservation Service, Washington, D.C., Rep. 625-708/60587. 1992. Accessed Jun 28, 2020. [Online]. Available: https://www.nrcs.usda.gov/wps/portal/nrcs/detail/national/about/history/?cid=stelprdb1043489.

[59] J. A. Lee, T. E. Gill, "*Multiple causes of wind erosion in the Dust Bowl*," Aeolian Res., vol. 19, pp. 15-36, Dec 2015, doi: 10.1016/j.aeolia.2015.09.002.

[60] U.S. Department of Agriculture, "*Hugh Hammond Bennett: Father of Soil Conservation*," NRCS.USDA.gov. 2020, https://www.nrcs.usda.gov/wps/portal/nrcs/detail/national/about/history/?cid=stelprdb1044395 (accessed Sept 19, 2020).

[61] S.M. Argabright, R. G. Cronshey, J. D. Helms, G. A. Pavelis, H. R. Sinclair, "*A Historical Study of Soil Conservation: Northern Mississippi Valley Working Paper No. 10*," USDA Natural Resources Conservation Service, Washington, D.C., 1995. Accessed Mar 29, 2019. [Online]. Available: https://www.nrcs.usda.gov/wps/portal/nrcs/detail/national/technical/nra/rca/?cid=nrcs143_014204.

[62] W. S. Badger, "*Structure of friable Iowa loess*," Ph.D. dissertation, Dept. Civil Engin,, Iowa State Univ., Ames, 1972.

[63] E. A. Bettis III, J. C. Prior, G. R. Hallberg, R. L. Handy, "*Geology of the Loess Hills Region*," Proc. Iowa Acad. Sci., vol. 93, no. 3, pp. 78-85, 1986.

[64] K. Pye, "*The nature origin and accumulation of loess*," Quaternary Sci. Rev., vol. 14, no. 7-8, pp. 653-667, 1995, doi: 10.1016/0277-3791(95)00047-X.

[65] X. Liu, M. Zhang, H. Zhang, Y. Jia, C. Zhu, H. Shan, "*Physical and mechanical properties of loess discharged from the Yellow River into the Bohai Sea China*," Engin Geo. J., vol. 227, pp. 4-11, Sept. 2017, doi: 10.1016/j.enggeo.2017.04.019.

[66] Q. Y. Mu, C. Zhou, C. W. W. Ng, "*Compression and wetting induced volumetric behavior of loess: Macro- and micro-investigations*," Trans. Geotechnics, vol. 23, Jun 2020, doi: 10.1016/j.trgeo.2020.100345.

[67] L. Chen, W. Wei, B. Fu, Y Lu, "*Soil and water conservation on the Loess Plateau in China: Review and perspective*," Prog. in Phys. Geo.: Earth and Env., vol. 31, no. 4, pp. 389-404, 2007, doi: 10.1177/0309133307081290.

[68] X. Wen, L. Zhen, "*Soil erosion control practices in the Chinese Loess Plateau: A systematic review*," Env. Dev. J., vol. 34, Jun 2020, doi: 10.1016/j.envdev.2019.100493.

[69] J. C. Bryce, "*Erosion and Deposition in the Loess-Mantled Great Plains, Medicine Creek Drainage Basin Nebraska*," U.S. Dept. of the Interior, Washington, D.C., Rep. 352-H, 1966. Accessed Jun. 22, 2020. [Online]. Available: https://pubs.usgs.gov/pp/0352h/report.pdf.

[70] U. S. Department of Agriculture, "*Land Resource Regions and Major Land Resource Areas of the United States the Caribbean and the Pacific Basin*," USDA, Washington, D.C. Rep. Handbook 296, 2006.

[71] D. R. Muhs, "*The geochemistry of loess: Asian and North American deposits compared," J. Asian Earth Sci.*, vol. 155, pp. 81-115, Apr. 2018, doi: 10.1016/j.jseaes.2017.10.032.

[72] J. E. Adams, "*A rainfall simulator and the erodibility of some Iowa soils*," Ph.D. dissertation, Dept. Agronomy, Iowa State College, Ames, 1956.

[32] T. E. Fenton, J. D. Highland, J. A. Phillips, "*Highway Guide of Iowa Soil Associations*," Dept. of Agronomy, Iowa State Univ. Extension, Ames, IA, USA, Tech. Rep. PM-389. July 1967.

[74] J. Prior, *Landforms of Iowa*. Iowa City, IA: USA: University of Iowa Press. 1991, pp. 16-19.

[75] B. L. Schmidt, "*Relative erodibility of three loess-derived soils in southwestern Iowa*," Ph.D. dissertation, Dept. Agronomy, Iowa State Univ. of Sci. and Tech., Ames. 1962.

[76] D. L. Karlen, L. A. Kramer, D. E. James, D. D. Buhler, T. B. Moorman, M. R. Burkart, "*Field-scale watershed evaluations on deep-loess soils: I. Topography and agronomic practices*," J. Soil Water Cons., vol. 54, no. 4, pp. 693-703, Oct 1999.

[77] B. L. Wells, T. O. Borich, J. D. Frus, "*Conservation tillage in an Iowa county*," J. of Soil and Water Cons., vol. 38, no. 3, pp. 284-286, May 1983.

[78] L. A. Kramer, M. R. Burkart, D. W. Meek, R. J. Jaquis, D. E. James, "*Field-scale watershed evaluations on deep loess soils: II. Hydrologic responses to different agricultural land management systems*," J. of Soil and Water Conservation. vol. 54, no. 4, pp. 705-710, 1999.

[79] J.E. Gilley, J.W. Doran and B. Eghball, "*Tillage and fallow effects on selected soil quality characteristics of former conservation reserve program sites*," J. Soil and Water Cons., vol. 56, no. 2, pp. 126-132, April 2001.

[80] D. Page-Dumroese, R. Miller, J. Mital, P. McDaniel, D. Miller, "*Volcanic-ash-derived forest soils of the inland Northwest: Properties and implications for management and restoration*," USDA Forest Service Rocky Mountain Research Station, Fort Collins, CO, Rep. Proc. RMRS-P-44, 2005, Accessed July 31, 2020. [Online]. Available: https://www.fs.usda.gov/treesearch/pubs/26202.

[81] L. D. Cast, T. J. Casias, R. A. Baumgarten, "*Bureau Case History of Loess Cut Slopes in Nebraska*," US DOI, Geotechnical Services Branch, Denver, CO, Rep. GR-88-3, Sept 1988, Accessed Jun 14, 2020. [Online]. Available: https://www.usbr.gov/tsc/techreferences/research/GR-88-3.pdf

[82] C. R. Song, Y-R. Kim, H. Bahmyari, L. Bitar, S. Amelian, "*Nebraska Specific Slope Design Manual*," Lincoln, NE, Rep. NDOT SPR-1(17) M061, NTC 26-1121-4036-001, 2018.

[83] D. Gehr, "*Gov. Kim Reynolds issues disaster proclamation after flood barrier is breached in western Iowa*," Des Moines Register, Sept. 19, 2019. [Online]. Available: https://www.desmoinesregister.com/story/news/2019/09/18/iowa-flood-2019-levee-break-council-bluffs-pottawattamie-county-missouri-river-evacuate-i-29-sioux/2366535001/.

[84] National Agronomy Manual (190–V–NAM), 4th ed, U.S. Department of Agriculture, Washington D.C., USA, 2011.

[85] National Geographic. "*Erosion*," Resource Library Encyclopedia. NationalGeographic.org. https://www.nationalgeographic.org/encyclopedia/erosion/ (accessed Sept 19, 2020).

[86] Ohio State University Extension and College of Food, Ag. and Env. Sci., "*AgBMPs: Inter-rill and rill erosion*," AgBMPS.OSU.edu. https://agbmps.osu.edu/scenario/inter-rill-and-rill-erosion (Dec 12, 2020).

[87] Q. Zhang, Z. Wang, Q. Guo, N. Tian, N. Shen, B. Wu, J. Liu, "*Plot-based experimental study of raindrop detachment, interrill wash and erosion-limiting degree on a clayey loessal soil*," J. Hydrology, vol. 575, pp. 1280-1287, Aug 2019, doi: 10.1016/j.jhydrol.2019.06.004.

[88] K.R. Olson, L.D. Norton, T. E. Fenton, R. Lal, "*Quantification of soil loss from eroded soil phases*," J. of Soil and Water Cons., vol. 49., no. 6, pp. 591-596, Nov 1994.

[89] R. Cruse, D. Flanagan, J. Frankenberger, B. Gelder, D. Herzmann, D. James, W. Krajewski, M. Kraszewski, J. Laflen, J. Opsomer, D. Todey, "*Daily estimates of rainfall, water runoff, and soil erosion in Iowa*," J. Soil and Water Cons., vol. 61, no. 4, pp. 191-199, July 2006.

[90] P. B. Berendzen, R. M. Cruse, L. L. Jackson, R. Mulqueen, C. F. Mutel, D. Osterberg, N. P. Rogovska, J. L. Schnoor, D. Swenson, E. S. Takle, P. S. Thorne, "*Climate Change Impacts on Iowa, 2010*" Iowa State Univ. Leopold Center Pubs and Papers. Ames, IA, Rep. 74. Accessed Jan 7, 2021. [Online] Available: http://lib.dr.iastate.edu/leopold_pubspapers/74.

[91] Iowa Statewide Urban Design and Specifications (SUDAS), Iowa Department of Transportation. Ames, IA, USA, 2017.

[92] U.S. Department of Agriculture, "*2017 National Resources Inventory: Iowa Soil Erosion*," NRCS.USDA.gov., 2020, https://www.nrcs.usda.gov/Internet/NRCS_RCA/reports/nri_eros_ia.html (accessed Sept 19, 2020).

[93] S.M. Argabright, "*Evolution in use and development of the wind erosion equation*," J. Soil and Water Cons., vol. 46, no. 2, pp. 104-105, Mar 1991.

[94] N. P. Woodruff, F. H. Siddoway, "*A Wind Erosion Equation*," Soil Science Soc. of America Proc., vol. 29, pp. 602-608. 1965.

[95] E. G. Smith, E. George, B. C. English, "*Determining Wind Erosion in the Great Plains*," Dept. of Agronomy, Iowa State Univ., Ames, IA, Rep. Series 82-WP-3, May 1982. Accessed Jun 12, 2020. [Online]. Available: http://lib.dr.iastate.edu/card_workingpapers/7.

[96] U.S. Department of Agriculture, "*NRCS Wind Erosion Prediction System (WEPS) Information*," USDA NRCS, 2020, Accessed July 1, 2020. [Online]. Available: https://www.nrcs.usda.gov/wps/portal/nrcs/detail/national/technical/tools/weps/?cid=nrcs144p2_080196.

[97] W. S. Chepil, "*Soil Conditions That Influence Wind Erosion*," USDA Economic Research Service, Washington, D.C., 1958, Accessed Jun 14, 2020. [Online]. Available: https://ageconsearch.umn.edu/record/157333.

[98] J. Knappett, R.F. Craig, "Basic characteristics of soil," in *Craig's Soil Mechanics, 8th ed*., Abingdon: UK: CRC Spon Press, 2012, pp. 3-5, ch. 1, pp. 13-19.

[99] *Gravel Roads Construction and Maintenance Guide*, K. Skorseth, A. A. Selim, and South Dakota Local Transportation Assistance Program, Brookings, SD, USA, 2000.

[100] *Gravel Roads Construction and Maintenance Guide*, U.S. Dept. of Transportation, Federal Highway Administration, Washington, D.C., USA, 2015.

[101] A. L. Shoemaker, "*Evaluation of Anionic Polyacrylamide as an Erosion Control Measure Using Intermediate-Scale Experimental Procedures*," M.S. thesis, Dept. Civil Env. Engin., Auburn Univ., Auburn, AL, 2009.

[102] W. T. Wilson, "*Evaluation of Hydromulches as an Erosion Control Measure Using Intermediate-Scale Experiments*," M.S. thesis, Dept. Civil Env. Engin., Auburn univ., Auburn, AL, 2010.

[103] Miner, N. (2019). *Structural racking for use rainfall simulator* [Unpublished image].

[104] M. Mahedi, B. Cetin, A. Y. Dayioglu, "*Leaching behavior of aluminum, copper, iron and zinc from cement activated fly ash and slag stabilized soils*," Waste Mgmt. vol. 95, pp. 334-355. Jun 2019, doi: 10.1016/j.wasman.2019.06.018.

[105] *Specifications for Highway and Bridge Construction: Division 21 Earthwork, Subgrades, and Subbases: Section 2107 Embankments*, Iowa Department of Transportation, Ames, IA, 2020, USA, Accessed Mar 12, 2020. [Online]. Available: https://iowadot.gov/erl/index.html

[106] L. D. Meyer, "*An investigation of methods for simulating rainfall on standard runoff plots and a study of the drop size, velocity, and kinetic energy of selected spray nozzles*," USDA-ARS Special Report, vol. 81, pp. 1-86, 1958.

[107] A. A. Nasritdinov, "*Using rainfall simulation and tracer anions to study the effects of soil bulk density and soil moisture on nitrate leaching characteristics*," M.S. thesis, Dept. of Ag. Engin. (Ag. Struct. and Envir. Sys. Engin.), Iowa State Univ., Ames, 2003.

[108] J. Zhou, "*Using rainfall simulation, TDR, and tracer anions to determine effects of soil properties on nitrate leaching*," Ph.D. dissertation, Dept. Ag. Engin. (Ag. Struct. and Envir. Sys. Engin.), Iowa State Univ., Ames, 2004.

[109] American Meteorological Society (AMS), "*Raindrop*," Glossary of Meteorology. AMETSOC.org. https://glossary.ametsoc.org/wiki/Raindrop (accessed Jan. 26, 2021).

[110] U.S. Environmental Protection Agency (EPA), "*Secondary Drinking Water Standards: Guidance for Nuisance Chemicals*," https://www.epa.gov/sdwa/secondary-drinking-water-standards-guidance-nuisance-chemicals (Accessed May 10, 2019).

[111] *Specifications for Highway and Bridge Construction: Division 41 Construction Materials: Section 4109 Aggregate Gradations*, Iowa Department of Transportation, Ames, IA, 2020, USA, Accessed Mar 12, 2020. [Online]. Available: https://iowadot.gov/erl/index.html

[112] *Specifications for Highway and Bridge Construction: Division 41 Construction Materials: Section 4120 Granular Surfacing and Granular Shoulder Aggregate*, Iowa Department of Transportation, Ames, IA, 2020, USA, Accessed Mar 12, 2020. [Online]. Available: https://iowadot.gov/erl/index.html

[113] S. Murakami, "*Comparison of various turbulence models applied to a bluff body*," J. of Wind Eng. and Ind. Aer., vol. 46–47, pp. 21-36, 1993, doi: 10.1016/0167-6105(93)90112-2.

[114] H. Hargitai, "*Obstacle Dunes and Obstacle Marks*," Ency. of Planetary Landforms, April 2014, doi: 10.1007/978-1-4614-9213-9_246-1.

[115] K. Hansen, "*Two Views of Von Karman Vortices*," EarthObservatory.NASA.gov, 2017, https://earthobservatory.nasa.gov/images/90734/two-views-of-von-karman-vortices (accessed Aug. 3, 2020).

[116] J. Schmaltz, "*Going with the Flow*," EarthObservatory.NASA.gov., 2017, https://earthobservatory.nasa.gov/images/88005/going-with-the-flow (accessed Aug. 3, 2020).

[117] P. Ghosh, "*Performing CFD Analysis Over a 2D Cylinder to Visualize Von Karman Vortex Shedding Using ANSYS Fluent*," M.S. cert., Skill-Lync.com, Chennai, India, 2020. Accessed Aug. 15, 2020. [Online]. Available: https://skill-lync.com/projects/performing-cfd-analysis-over-a-2d-cylinder-to-visualize-von-karman-vortex-shedding-using-ansys-fluent.

[118] Physics Graphics, Ukraine, *Von Karman Vortex Street* (March 21, 2016). Accessed: Aug 3, 2020. [Online Video]. Available: https://youtu.be/f3LmjJ1N7YE.

[120 Iowa State Univ (2019). "*Iowa Smart Agriculture- Soil Conservation Viewed Through a Crystal Ball*," Available https://youtu.be/eSpXNIv3-uY.

[121] R. Perkins, B. Hansen, B. Wilson and J. Gulliver, "*Development and Evaluation of Effective Turbidity Monitoring Methods for Construction Projects*," Univ. of Minnesota, St. Paul, MN, Rep. MN/RC 2014-24, 2014.

[122] W. H. Wischmeier, D . D . Smith, "*Predicting rainfall erosion losses - A guide to conservation planning AH-537*," Washington D.C., 1978.

[123] W. S. Chepil, N. P. Woodruff, F. H. Siddoway, "*How to control soil blowing*," USDA, Washington, D.C., 1961.

[124] P., Vennapusa, D.J. White, D.K. Miller, "*Western Iowa Missouri River Flooding—Geo-Infrastructure Damage Assessment, Repair, and Mitigation Strategies,*" Center for Earthworks Engin. Research, Ames, IA, Tech Rep. IHRB TR-638, 2013.

[125] America's Byways, "*Loess Hills National Scenic Byway Spine and Excursion Loops*," 2013, https://www.legis.iowa.gov/docs/SC_MaterialsDist/2013/SDAJB004.PDF (accessed Apr. 24, 2020).

Std *Standard Method of Test for Sieve Analysis of Fine and Coarse Aggregates*, AASHTO T27, American Association of State Highway and Transportation Officials, Washington DC, 2020.

Std *Standard Test Method for Sieve Analysis of Fine and Coarse Aggregates*, ASTM C136 / C136M-19, ASTM International, West Conshohocken, PA, 2019.

Std *Standard Practice for Reducing Samples of Aggregate to Testing Size*, ASTM C702 / C702M-18, ASTM International, West Conshohocken, PA, 2018.

Std *Standard Test Methods for pH of Water*, ASTM D1293-18, ASTM International, West Conshohocken, PA, 2018.

Std *Standard Test Methods for Laboratory Determination of Water (Moisture) Content of Soil and Rock by Mass*, ASTM D2216-19, ASTM International, West Conshohocken, PA, 2019.

Std *Standard Test Methods for Determining Sediment Concentration in Water Samples*, ASTM D3977-97(2019), ASTM International, West Conshohocken, PA, 2019.

Std *Standard Test Methods for pH of Soils*, ASTM D4972-19, ASTM International, West Conshohocken, PA, 2019.

Std *Standard Test Method for Determination of Rolled Erosion Control Product (RECP) Performance in Protecting Hillslopes from Rainfall-Induced Erosion*, ASTM D6459-15, ASTM International, West Conshohocken, PA, 2015.

Std *Standard Test Methods for Laboratory Compaction Characteristics of Soil Using Standard Effort*, ASTM D698-12e2, ASTM International, West Conshohocken, PA, 2012.

Std *Standard Test Method for Determination of Turbidity Above 1 Turbidity Unit (TU) in Static Mode*, ASTM D7315-17, ASTM International, West Conshohocken, PA, 2017.